Methanation of Synthesis Gas

Published on June 1, 1975 on http://pubs.acs.org | doi: 10.1021/ba-1975-0146.fw001

Methanation of Synthesis Gas

Len Seglin, EDITOR

Bechtel Associates

A symposium sponsored by
the Division of Fuel Chemistry
at the 168th Meeting of the
American Chemical Society,
Atlantic City, N.J.,
Sept. 9, 1974.

ADVANCES IN CHEMISTRY SERIES **146**

AMERICAN CHEMICAL SOCIETY
WASHINGTON, D. C. 1975

Library of Congress CIP Data

Methanation of synthesis gas.

(Advances in chemistry series; 146 ISSN 0065-2393)

Includes bibliographical references and index.

1. Methanation—Congresses. 2. Synthesis gas—Congresses.

I. Seglin, Len. II. American Chemical Society. Division of Fuel Chemistry. III. Series.

QD1.A355 no. 146 [TP156.M45] 540'.8s
ISBN 0-8412-0244-3 [665'.77] 75-33967
ADCSAJ 146 1-177 (1975)

Advances in Chemistry Series

Robert F. Gould, *Editor*

FOREWORD

ADVANCES IN CHEMISTRY SERIES was founded in 1949 by the American Chemical Society as an outlet for symposia and collections of data in special areas of topical interest that could not be accommodated in the Society's journals. It provides a medium for symposia that would otherwise be fragmented, their papers distributed among several journals or not published at all. Papers are refereed critically according to ACS editorial standards and receive the careful attention and processing characteristic of ACS publications. Papers published in ADVANCES IN CHEMISTRY SERIES are original contributions not published elsewhere in whole or major part and include reports of research as well as reviews since symposia may embrace both types of presentation.

PREFACE

This volume brings together papers which were presented at the Methanation Symposium of the Division of Fuel Chemistry as part of a meeting celebrating the 50th anniversary of that Division. These papers deal with various aspects of Methanation—a field which has grown in less than a decade from an interesting but idle laboratory activity to one of almost feverish industrial interest. It is hoped that this collective work will meet partially the need for fundamental and applied information to satisfy the requirements for this burgeoning field.

What has happened in less than a decade to promote methanation to its existing station? We in the United States are beginning to realize or do now realize that we are running out of natural gas (*sic* methane)—a commodity which we had in abundance but which in less than the age of the Division of Fuel Chemistry, we managed to deplete faster than is possible by nature to replace or by humans to find.

That's the situation now. We are meeting most of these needs today by drawing rapidly on our bank account. Tomorrow that will not be possible. Viable alternates must be found now, or else our energy-based society will find itself strained beyond repair. One of the most logical alternates is to convert coal, our largest fossil fuel resource, to gas and oil. Technology exists today for doing that, albeit possibly not in the most economic or elegant way. New and better ways are being developed, and some of these in due time will make their contribution to meeting our future energy needs.

In all coal gasification processes—yesterday's, today's or tomorrow's—an excessive quantity of carbon monoxide is produced. This must be reduced to near zero in order to meet market requirements—safety, interchangeability with natural gas, and lowest delivered cost to distant markets.

The basic chemistry for removing carbon monoxide by reducing it with hydrogen to methane has long been known, but its application, especially where carbon monoxide is present in large concentrations on the huge scale needed, was not a reality. There were two areas of concern. The first was whether or not the large heat relase which occurs during the carbon oxide–hydrogen reaction could be accommodated in commercial scale reactors. The second was whether or not existing and developing purification processes could reliably and economically remove

catalyst poisons in the incoming gas stream, since very low sulfur tolerance exists in the nickel catalysts which are typically proposed for methanation.

Thus methanation was one of the missing links which needed to be resolved before we could seriously consider coal gasification as a possible solution to our future gas needs. Fortunately, we feel this link is being satisfied as evidenced, for example, by the results of some of the chapters in this volume.

The chapters in this volume treat this developing field of chemical technology in a progressive fashion. The chapter by Seglin *et al.* surveys the overall subject. It discusses, and where necessary, critiques the fundamentals of the methanation field and their application to commercial practice.

The chapter by Gruber deals with thermodynamic equilibrium considerations. It develops a graphical method for presenting these results, and touches on the potentially important problem of carbon-laydown on the catalyst.

The chapter by Hausberger *et al.* deals with catalyst development, and the performance of several new high-nickel catalysts in bench-scale and large pilot tests with high carbon oxide concentrations. Kinetics of the reaction over these catalysts are developed.

The chapter by Bridger and Woodward deals with methanation as a means for removing carbon oxides from ammonia synthesis gas. This technology, together with earlier pioneer work by Dent and co-workers (*1*), are the forerunners of all modern methanation developments. The chapter deals with catalyst formulation and characterization and with the performance of these catalysts in commercial plants as a function of time on-stream.

The chapter by Haynes *et al.* describes the pilot work using Raney nickel catalysts with gas recycle for reactor temperature control. Gas recycle provides dilution of the carbon oxides in the feed gas to the methanator, hence simulating methanation of dilute CO-containing gases which under adiabatic conditions gives a permissible temperature rise. This and the next two papers basically treat this approach, the hallmark of first-generation methanation processes.

The chapter by Eisenlohr *et al.* deals with the results of large scale pilot operations using a newly developed high-nickel catalyst with hot-gas recycle for temperature control. This and other work, conducted by Lurgi Mineraloeltechnik GmbH. with South African Coal and Oil Limited (SASOL), are the bases of the methanation process which Lurgi is proposing for commercial plants.

The chapter by Bair *et al.* presents the results obtained by IGT

using high-nickel catalyst in multi-stage reactors with cold-gas recycle for temperature control.

The chapter by White *et al.* proposes a different approach to methanator temperature control. Here the temperature rise is controlled by limiting the amount of reaction in each stage, and that is done by introducing steam (a product of the reaction). High initial temperatures are followed by successively lower temperatures entering each reactor in series. This is a second-generation methanation approach which may follow closely on the first-generation approaches typified by the previous three papers.

The chapter by Blum *et al.* covers another candidate second-generation process. This approach uses a large circulating catalyst–liquid slurry stream as the thermal flywheel to control the temperature rise. This is analogous to the H-Oil proces used for hydrotreating oil (2).

The last chapter is a round-table discussion by the speakers at the symposium of questions posed by the attendees on topics relating to the preceding papers or other topics pertinent to the field. This type of forum presented an excellent opportunity for interplay between the two groups, especially as it related to topics not covered in the formal papers.

The editors thank the authors of the papers for their valuable contributions, the reviewers for their interest and helpful suggestions, the American Chemical Society Staff for their editorial effort, and the Society and the Division of Fuel Chemistry for their sponsorship of this work. Lastly, we acknowledge the help of R. Tracy Eddinger, the 1974 Storch Award Recipient, during the course of putting this Symposium together.

Literature Cited

1. Dent, F. J. *et al.*, *Inst. Gas Engr. Trans.* (1945) **95**, 602–709.
2. Keith, P. C. *et al.*, U.S. Patent **2,987,467** (June 6, 1961).

LEN SEGLIN
R. H. MCCLELLAND

Bechtel Associates Professional Corp.
New York, N.Y.
December 1974

Survey of Methanation Chemistry and Processes

L. SEGLIN and R. GEOSITS

Bechtel Associates Professional Corp., 485 Lexington Ave., New York, N. Y. 10017

B. R. FRANKO and G. GRUBER

FMC Corp., P.O. Box 8, Princeton, N. J. 08540

This paper surveys the field of methanation from fundamentals through commercial application. Thermodynamic data are used to predict the effects of temperature, pressure, number of equilibrium reaction stages, and feed composition on methane yield. Mechanisms and proposed kinetic equations are reviewed. These equations cannot prove any one mechanism; however, they give insight on relative catalyst activity and rate-controlling steps. Derivation of kinetic equations from the temperature profile in an adiabatic flow system is illustrated. Various catalysts and their preparation are discussed. Nickel seems best; nickel catalysts apparently have active sites with $\Delta F \cong 3$ *kcal which accounts for observed poisoning by sulfur and steam. Carbon laydown is thermodynamically possible in a methanator, but it can be avoided kinetically by proper catalyst selection. Proposed commercial methanation systems are reviewed.*

The Middle East oil crisis increased natural gas needs, and dwindling gas reserves have intensified the need to use our huge coal reserves for the synthesis of gas, especially methane. Energy requirements will double in the next 10 years and triple before the turn of the century. Use of pipeline gas has been increasing by 6% per year, almost double the overall energy demand. The rate of gas discovery in the United States has not kept pace with use, and the estimated reserves of some 2,500 trillion cubic feet could easily be depleted in 25 years. Liquid natural gas is imported to ease shortages, but it is 5–10 times as expensive as natural gas.

One of the most promising ways of providing a high Btu gas is the hydrogenation of carbon oxides, preferably carbon monoxide, to methane; this process is known as methanation. The importance of research on methanation has been increasing for some time (a) as the need for a high Btu fuel has increased; (b) since low concentrations of undesirable monoxide in hydrogen-rich gases could be removed by methanation (*e.g.*, ammonia production); (c) as the use of methane as a carbon source has increased in the chemical industry (*e.g.*, the syntheses of carbon tetrachloride and carbon bisulfide); and (d) inasmuch as methane formation is undesirable in the hydrogenation of carbon monoxide to alcohols or hydrocarbons.

The synthesis gas for methanation, containing hydrogen and carbon oxides, is produced by gasification of coal by partial oxidation and/or by the reaction with steam.

This paper presents a review of the chemistry of the methanation process, the mechanisms of the key reactions, the kinetics of the reactions over various catalysts, and the application of this background to commercial processes.

Methanation Background

Chemistry and Thermodynamics. The principal reactions which occur in the methanation process are:

$$CO\uparrow + 3H_2\uparrow \rightleftarrows CH_4\uparrow + H_2O\uparrow \quad (1)$$

$$CO\uparrow + H_2O\uparrow \rightleftarrows H_2\uparrow + CO_2\uparrow \quad (2)$$

$$CO_2\uparrow + 4H_2\uparrow \rightleftarrows CH_4\uparrow + 2H_2O\uparrow \quad (3)$$

$$2CO\uparrow \rightleftarrows C\downarrow + CO_2\uparrow \quad (4)$$

At the temperatures used in coal gasification ($\sim 870°C$), methane formation also occurs by hydrogenation of carbon:

$$2H_2\uparrow + C\downarrow \rightleftarrows CH_4\uparrow \quad (5)$$

The first catalytic study of Reaction 1 was published in 1902 by Sabatier and Senderens (*1*) who reported that nickel was an excellent catalyst. Since that time, the active catalysts were identified as the transition elements with unfilled 3*d*, 4*d*, and 5*d* orbitals: iron, cobalt, nickel, ruthenium, rhenium, palladium, osmium, indium, and platinum, as well as some elements that can assume these configurations (*e.g.*, silver). These are discussed later. For practical operation of this process,

it is essential to avoid both Reaction 4 and the reverse of Reaction 5 since carbon formation and laydown would plug the catalyst bed and render it inoperative. These reactions may be avoided by operating the methanation reactors under conditions where carbon is not a stable phase as defined by the thermodynamics of Reactions 4 and 5.

The heats of these reactions (*2, 3*) (Figure 1) indicate that all the reactions are exothermic over the cited range of conditions. For example, the heat liberated under typical reaction conditions for the conversion of CO to methane is 52,730 cal/mole CO; that for carbon dioxide is 43,680 cal/mole. Such high heats of reaction cannot be absorbed by the process stream in an adiabatic reactor unless the CO and/or CO_2 conversion is limited to less than about 2.5 moles/100 moles feed gas. Since

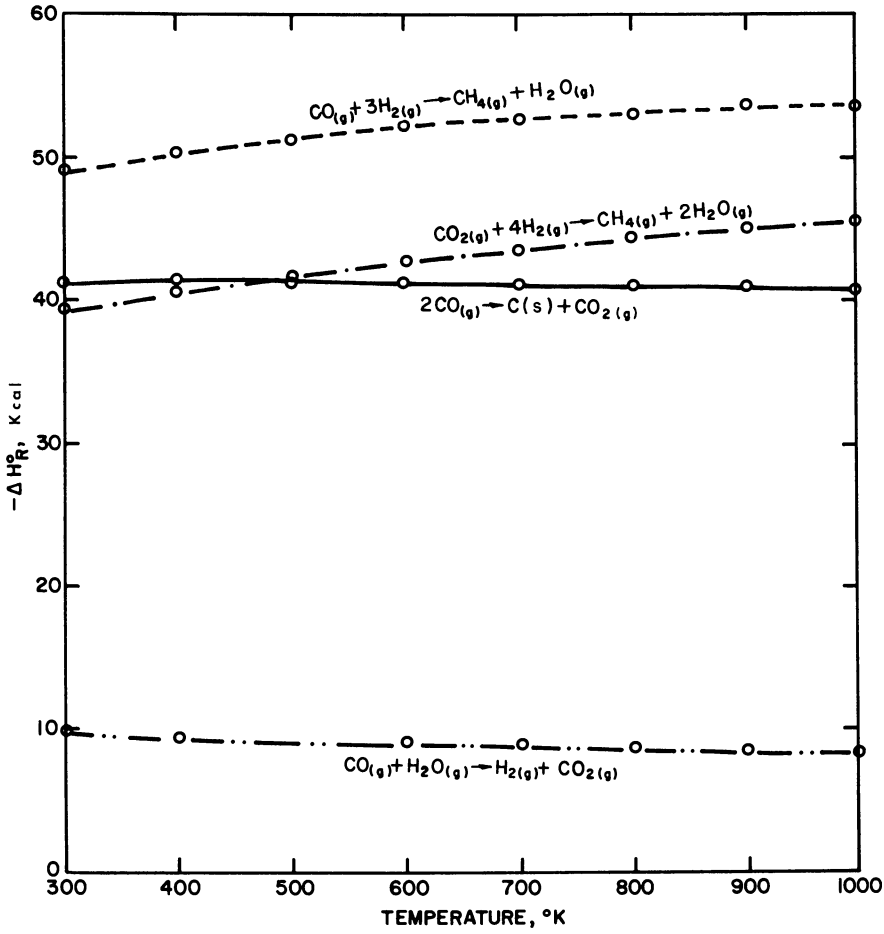

Figure 1. Heat of methanator reactions

product gases from coal gasification processes contain upwards of 20 mole % CO, it was necessary to develop temperature control systems which will permit safe operation of this reaction. These methods are discussed below.

Changes in free energy and the equilibrium constants for Reactions 1, 2, 3, and 4 are quite sensitive to temperature (Figures 2 and 3). These equilibrium constants were used to calculate the composition of the exit gas from the methanator by solving the coupled equilibrium relationships of Reactions 1 and 2 and mass conservation relationships by a Newton–Raphson technique; it was assumed that carbon was not formed. Features of the computer program used were as follows: (a) any pressure and temperature may be specified; (b) an inert gas may be present; (c) after

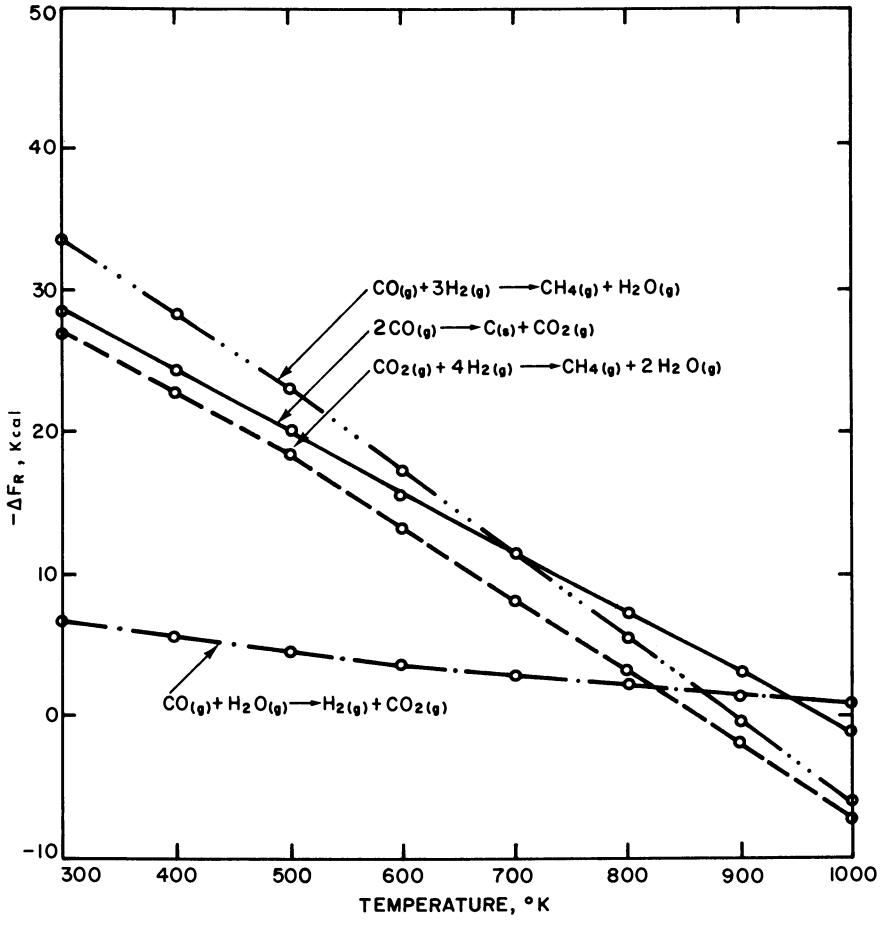

Figure 2. Free energies of methanator reactions

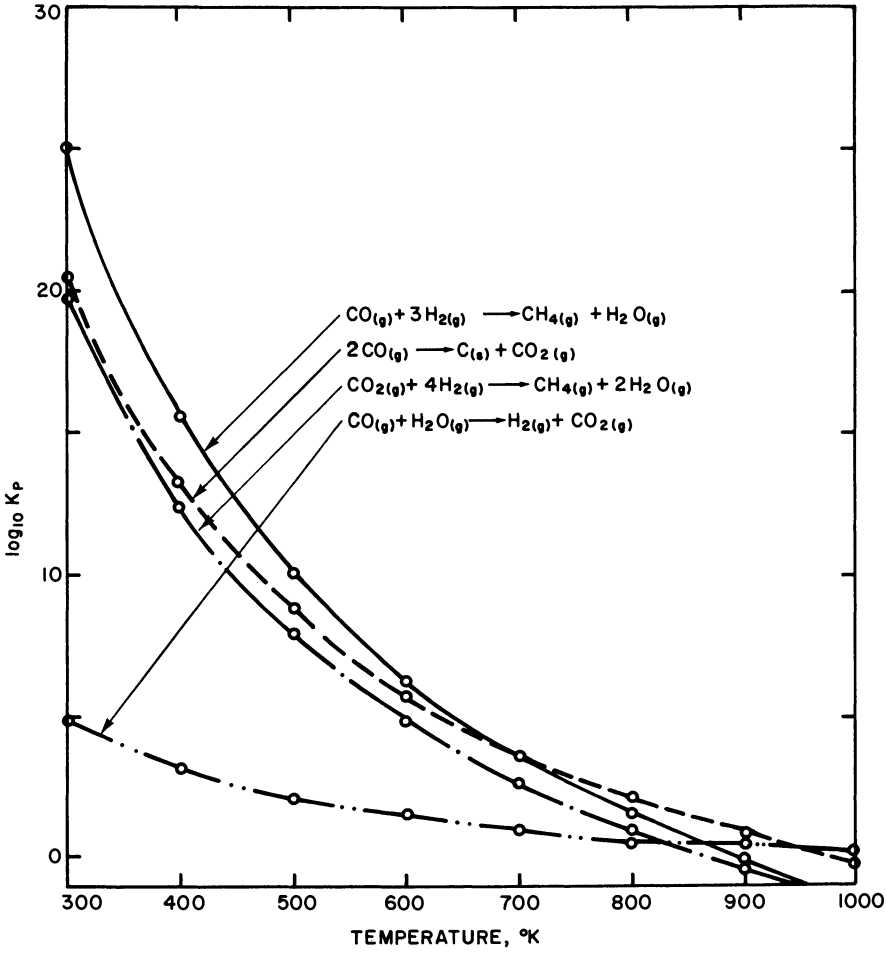

Figure 3. Equilibrium constants of methanator reactions

equilibrium is achieved, the program automatically calculates the next stage of equilibrium after removing water from the previous equilibrium mixture; (d) the starting composition is arbitrary; and (e) since mass is removed from the system in multiple stages, the printout for all species is in units of moles per mole of initial CO, and equilibrium concentrations are given as mole fraction on a water-free basis.

Equilibrium constants as a function of temperature were calculated from

$$\Delta F = -RT\ln K_p \qquad (6)$$

Table I. Constants for Reactions 1 and 2

Reaction	*A*	*B*	*C*	*D*	*E*
1	−34.976	−.00529	13.4	−45986.8	35500
2	30.992	+.00028	−3.0	−11321.2	91500

$$\frac{\Delta F}{T} = A + BT + C\ln T + D/T + E/T^2 \qquad (7)$$

where T is in °K, and the standard state for K_p is 1 atm. The constants used for Reactions 1 and 2 are given in Table I.

Assuming equilibrium, the gas composition of the methanated gases depends on (a) the number of equilibrium methanation stages used where an equilbrium stage is defined as one in which the feed gas is converted to a composition defined by the free energy changes of Reactions 1 and 2 (the feed gas to the stages after the first stage is the gas from the preceding stage with the water removed); (b) the methanation conditions, *i.e.*, temperature and pressure; and (c) the feed gas composition. As the number of equilibrium stages increases, methane content increases, hydrogen concentration decreases, and the heating value of the gas increases (Figure 4). As pressure increases and temperature decreases, methane concentration increases, hydrogen concentration decreases, and the heating value increases (Figure 5). As the H_2:CO ratio in the feed

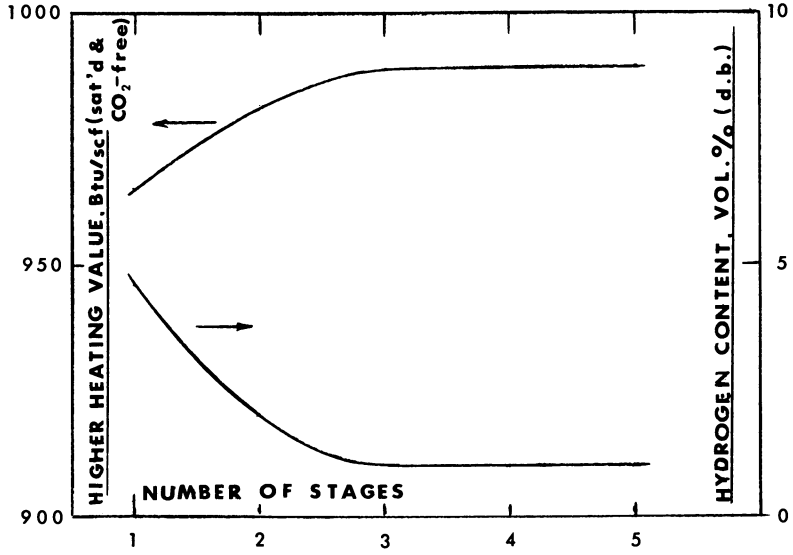

Figure 4. Effect of number of equilibrium stages on heating value and H_2 content of product gas
Conditions: 20 atm, 371°C, and H_2:CO = 3:1

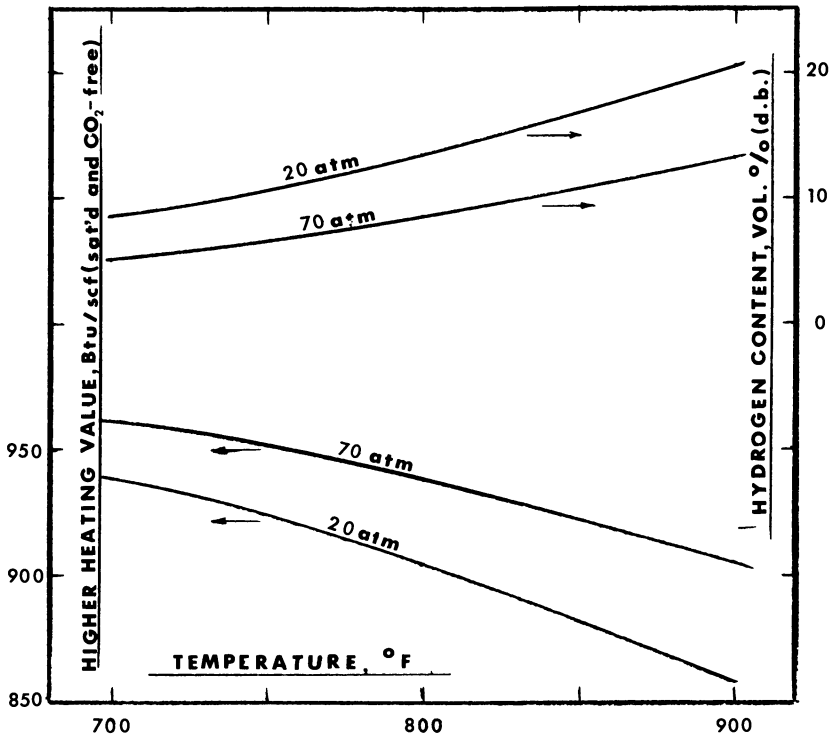

Figure 5. Effect of temperature and pressure on heating value and H_2 content of product gas with 3:1 H_2:CO in feed

increases, and assuming no carbon laydown, methane concentration decreases, hydrogen increases, and the heating value decreases (Figure 6). Equilibrium calculations indicate that carbon (solid) would be a stable phase at low H_2:CO levels, and hence operation at these levels would be undesirable unless catalysts were used to inhibit carbon formation.

Mechanisms. The mechanism of hydrogenation of carbon monoxide to higher hydrocarbons has been studied intensively for some years. Relatively little work, however, was done on the mechanism of the methanation reaction in spite of the fact that this reaction is the simplest of the series. Undoubtedly, this resulted from the greater commercial interest in the higher hydrocarbons, especially during the early development of the Fischer–Tropsch synthesis. This situation will undoubtedly change with the increasing interest in high Btu pipeline gas.

Any mechanistic theory must explain the following:

(a) No methanol is observed. Furthermore, methanol is formed when CO is hydrogenated over copper–zinc oxide, with only one of the two bonds to oxygen being broken.

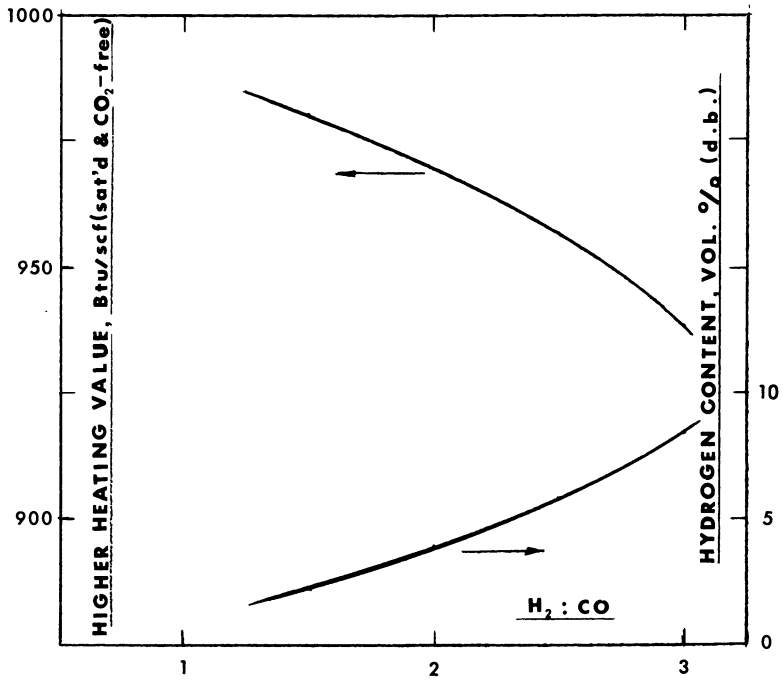

Figure 6. Effect of H_2:CO ratio in feed gas on heating value and H_2 content of product gas at 20 atm and 371°C

(b) No formaldehyde is formed. A formaldehyde intermediate would almost necessitate methanol as an intermediate.

(c) Methylene radicals, CH_2, have been detected.

(d) Metal carbonyls are not present.

(e) The reaction occurs on the surface of the catalyst and not in the gas phase.

(f) There is conflicting evidence about the ratios of $CO:H_2$ sorbed on the surface. However, evidence is good that an equimolar ratio of the gases desorbs irrespective of the ratio of the original mixture. This leads to the postulate of some sort of weakly bonded HCOH complex.

Studies of the bonding of carbon monoxide to the metal surfaces produced structures in which the carbon atom is linked to one, two, or three metal atoms. The existence of bonds to two or three atoms (bridged bonds) has been questioned on the basis of theoretical calculations. None of these bondings, however, clarify the mechanism to any extent.

There is also evidence that the adsorbed gases may be charged; this led Vlasenko and Uzefovich to develop a completely ionic mechanism (*4*) in which the bracket, [ ], represents a metallic site:

$$[\,] + e^- + H_2 \rightleftarrows [H_2] \qquad (8a)$$

$$[\,] + CO \rightleftarrows [CO]^+ + e^- \quad (8b)$$

$$[CO]^+ + [H_2]^- \rightleftarrows [HCOH]^+ + e^- \quad (8c)$$

$$[HCOH]^+ + [H_2]^- \rightleftarrows [CH_2] + H_2O + [\,] \quad (8d)$$

$$[CH_2] + [H_2]^- \rightleftarrows CH_4 + e^- + [\,] \quad (8e)$$

where step 8c is slow.

Even if it is assumed that the reaction is ionic, Occam's Razor would lead to the conclusion that the system is too complex and that the effort to keep it ionic is too great. It is difficult to undersand why step 8c is slow and why a simple uncharged complex would not be equally reasonable. We prefer a mechanism in which the carbon monoxide molecule is adsorbed parallel to the surface and in which the oxygen orbitals as well as the carbon orbitals of C=O bond electrons interact with the metal. It seems reasonable that hydrogenolysis occurs exclusively only because the oxygen is held in some way while the two bonds are broken and it finally desorbs as water. The most attractive picture would be (a) adsorption of CO and H_2 with both atoms on the surface

C — O

(b) formation of weak bonds to adjacent hydrogen (the complex is planar and is still on the surface)

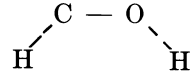

(c) hydrogenolysis or reaction with the absorbed hydrogens on the side opposite to CH_2

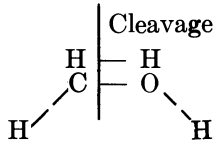

(d) saturation (the methylene group reacts with an other adsorbed hydrogen molecule)

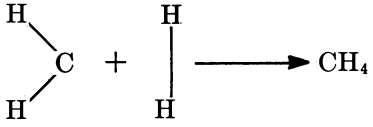

Instinctively it would seem that Step C would be rate controlling and the slowest. In the case of the Fischer–Tropsch reaction, one would postulate that the surface would offer more methylene groups for chain polymerization. This mechanism differs from that of Vlasenko and Uzefovich (*4*) essentially in the concept that the whole molecule interacts with the surface. Furthermore, the HCOH intermediate is wholly horizontal to the surface rather than perpendicular.

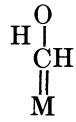

Unfortunately, direct experimental proof of this mechanism is not available. Kinetic data (*see* below) offer none since the interpretation need not be unique—more than one mechanism can serve equally well. In addition, the physical properties of the catalyst are obviously contributing, and, in the extreme, diffusion can be rate-controlling, completely obscuring chemical mechanisms.

Vlasenko and Uzefovich (*4*) also concluded that the most probable mechanism for hydrogenolysis of CO_2 to methane proceeds according to:

$$2[\,] + 2e^- + H_2 \rightarrow 2[H] \quad (9a)$$

$$2[H]^- + CO_2 \rightarrow [HCOOH] + [\,] \quad (9b)$$

$$[HCOOH] \rightarrow [H] + C\begin{matrix}OH\\OH\end{matrix} + 2e^- \quad (9c)$$

$$C\begin{matrix}OH\\OH\end{matrix} + H_2 \rightarrow H{-}C{-}OH + H_2O \quad (9d)$$

$$H{-}C{-}OH + H_2 \rightarrow CH_2 + H_2O \quad (9e)$$

$$CH_2 + H_2 \rightarrow CH_4 \quad (9f)$$

where 9c is the slow step.

According to this scheme, the process is initiated by the activation of only the hydrogen on the catalyst surface, after which the reaction takes place in the gas volume. Mills and Steffgen (*5*) questioned this mechanism and concluded that the mechanism of CO_2 methanation is uncertain and that this would be a fruitful field for investigation.

There have been a number of investigations on the hydrogenation of carbon monoxide and carbon dioxide together, (*6, 7, 8*); it was concluded that CO_2 is not hydrogenated in the presence of carbon monoxide. Such

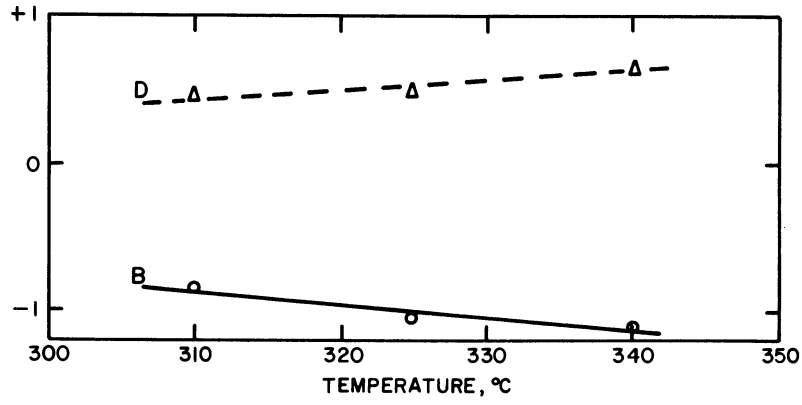

Figure 7. Effect of temperature on methanation reaction constants (10)

$CO + 3H_2 \rightleftarrows CH_4 + H_2O$ *and* $r_{CH_4} = \frac{P_{CO}P_{H_2}^3}{(A + BP_{CO} + DP_{CO_2} + EP_{CH_4})^4}$ *where* $A = 1.26$ *and* $E = -2.57$

a conclusion might be erroneous because it does not take into account that simultaneous with methane formation is the formation of water which reacts with CO to make CO_2 by the water–gas shift reaction. This leads to the observation that the CO_2 concentration, instead of decreasing, may actually increase or at best maintain steady until the carbon monoxide is substantially consumed. Thus, only at low concentrations of CO would CO_2 reduction to methane be observed.

Undoubtedly our understanding of the methanation reaction is unsatisfactory. Fortunately, the application of newer techniques (*9*) of vibrational and electronic spectroscopy to the study of the chemisorbed layer on single crystals will soon lead to greater insights and ultimately to better catalysts and better reactor design and operation.

Kinetics. Extensive studies of the kinetics of methane synthesis were reported by White and co-workers (*10, 11, 12, 13, 14, 15*). They studied the reaction between CO and hydrogen over a reduced nickel catalyst on kieselguhr at 1 atm and 300°–350°C (*10*). They correlated the rate of methane formation by the equation:

$$r = \frac{P_{CO}\ P^3_{H_2}}{(A + BP_{CO} + DP_{CO_2} + EP_{CH_4})^4} \text{ lb moles/hr, lb catalyst} \quad (10)$$

where *A*, *B*, *D*, and *E* are appropriate factors that depend moderately on temperature (Figure 7). Concurrent with the formation of methane from CO and hydrogen by Reaction 1 is the shift reaction between CO and the water formed in the methanation reaction to produce CO_2 and hydrogen by Reaction 2. The rate of CO_2 formation was expressed by the empirical equation:

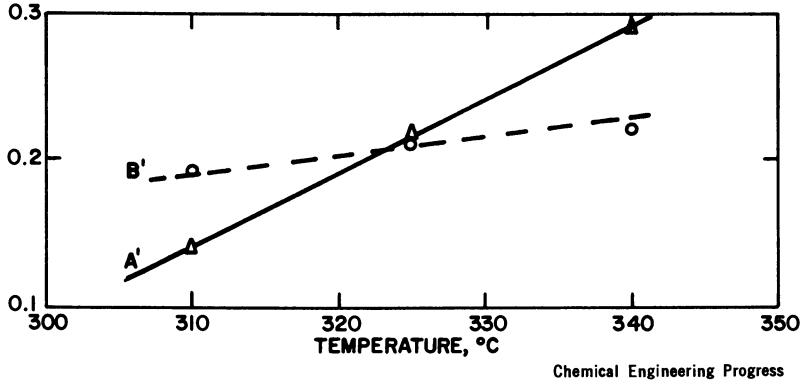

Figure 8. Effect of temperature on CO_2 reaction constants (10)
$CO + H_2O \rightleftarrows CO_2 + H_2$ and $r_{CO_2} = A'(P_{CO_2} - B')$

$$r = A'(P_{CO} - B') \text{ lb moles/hr, lb catalyst} \qquad (11)$$

where A' and B' are appropriate factors whose dependence on temperature is plotted in Figure 8. This relationship for the CO_2 formation rate holds until this rate equals the rate of methane formation; after that the two rates are equal and the methane rate equation (Equation 10) can be used for the CO_2 rate equation (Equation 11).

The kinetic expression was derived by Akers and White (*10*) who assumed that the rate-controlling factor in methane formation was the reaction between the adsorbed reactants to form adsorbed products. However, the observed temperature-dependence of the rate was small, which indicates a low activation energy, and diffusion was probably rate-controlling for the catalyst used.

Obviously, the kinetics developed above apply to the specific catalyst used by those investigators. As the catalyst changes, the values of the factors (A, B, D, E, A', and B') change. Furthermore, investigations at elevated pressures (*12*) indicated that these factors also vary with total pressure.

The synthesis of methane from CO_2 and hydrogen was studied by Binder and White (*11*) over a reduced nickel catalyst (Harshaw Ni-88). The surface reaction between the CO_2 and hydrogen appeared to be rate controlling. The rate of reaction can be correlated by either of the following rather awkward equations:

$$r = \frac{C_1 \left[P_{CO} P_{H_2}^2 - \frac{P_{CH_4} P_{H_2O}^2}{K_1 P_{H_2}^2} \right]}{(P_{H_2}^{1/2} + C_2 P_{CO_2} + C_3)^5} \text{ lb moles/day, lb catalyst} \qquad (12)$$

$$r = \frac{C_1' \left[P_{CO_2} P_{H_2}^4 - \frac{P_{CH_4} P_{H_2O}^2}{K_1} \right]}{(P_{H_2}^{1/2} + C_2' P_{CO_2} + C_3')^9} \text{ lb moles/day, lb catalyst} \qquad (13)$$

where C_1, C_2, C_3, C_1', C_2', C_3', and K_1 are appropriate factors whose dependence on temperature is noted in Table II. The variation of C_1 and C_1' with temperature indicates activation energies of about 30,000 and 16,000 cal/mole respectively. Energies as high as these indicate that, for the catalyst in question, the surface reactions were controlling and not the diffusional steps.

The first equation was derived by assuming that the rate-controlling step is the reaction of one molecule of adsorbed CO_2 with two molecules of dissociated adsorbed hydrogen. The second equation, which correlates almost as well, is based on the assumption that the rate-determining step is the reaction of one molecule of adsorbed CO_2 with two molecules of adsorbed hydrogen. This indicates that, in this particular case, it was not possible to prove reaction mechanisms by the study of kinetic data.

In other instances, reaction kinetic data provide an insight into the rate-controlling steps but not the reaction mechanism; *see*, for example, Hougen and Watson's analysis of the kinetics of the hydrogenation of mixed isooctenes (*16*). Analysis of kinetic data can, however, yield a convenient analytical insight into the relative catalyst activities, and the effects of such factors as catalyst age, temperature, and feed-gas impurities on the catalyst.

The conventional experimental approach to obtaining kinetic data is rather awkward, and it involves varying space velocity as a means for simulating contact, or reaction, time. An alternate approach is to run adiabatic experiments and to obtain catalyst bed temperatures as well

Table II. CO_2 Methanation Reaction Rate Constants at One Atmosphere (*11*)

$$r = \frac{C_1 \left[P_{CO_2} P_{H_2}^2 - \frac{P_{CH_4} P_{H_2O}^2}{K_1 P_{H_2}^2} \right]}{[P_{H_2}^{1/2} + C_2 P_{CO_2} + C_3]^5}$$

$$r = \frac{C_1' \left[P_{CO_2} P_{H_2}^4 - \frac{P_{CH_4} P_{H_2O}^2}{K_1} \right]}{[P_{H_2}^{1/2} + C_2' P_{CO_2} + C_3']^9}$$

	Temperature, °C					
Term	*260*	*288*	*315*	*343*	*371*	*399*
K_1	6.1×10^6	8.3×10^5	1.41×10^5	2.92×10^4	6.3×10^3	1.52×10^3
C_1	57.5	226	772	2540	7060	18800
C_2	0.474	0.444	0.420	0.396	0.379	0.362
C_3	0.005	0.161	0.339	0.570	0.814	1.094
C_1'	88	187	364	697	1210	2070
C_2'	0.232	0.208	0.1885	0.172	0.1585	0.147
C_3'	0.038	0.063	0.093	0.1315	0.168	0.208

as inlet and outlet stream flows and conditions. Then, by straightforward sectional heat balances, the amount of reaction occurring in each section of the catalyst bed and the material balances for each section can be calculated. The derived gas composition profile and contact times can then be combined as suggested by Hougen and Watson (*16*) to give a rate equation and an insight into the rate-controlling steps.

This approach was applied to data obtained by Hausberger, Atwood, and Knight (*17*). Figure 9 shows the basic temperature profile and feed gas data and the derived composition profiles. Application of the Hougen and Watson approach (*16*) and the method of least squares to the calculated profiles in Figure 9 gave the following methane rate equation:

$$r = \left[\exp\left(-\frac{38900}{RT} + 21.97\right)\right] P_{CO}\, P_{H_2}{}^3 \text{ lb mole } CH_4/\text{sec ft}^3 \text{ catalyst} \quad (14)$$

where T is in °K. This equation fits the derived data within ±1% over the entire reactor. The indicated high activation energy, 38.9 kcal, suggests that the surface reaction is the rate-controlling step for this catalyst.

Catalysts. The methanation of CO and CO_2 is catalyzed by metals of Group VIII, by molybdenum (Group VI), and by silver (Group I). These catalysts were identified by Fischer, Tropsch, and Dilthey (*18*) who studied the methanation properties of various metals at temperatures up to 800°C. They found that methanation activity varied with the metal as follows: ruthenium > iridium > rhodium > nickel > cobalt > osmium > platinum > iron > molybdenum > palladium > silver.

Nickel. As a methanation catalyst, nickel is presently preeminent. It is relatively cheap, it is very active, and it is the most selective to methane of all the metals. Its main drawback is that it is easily poisoned by sulfur, a fault common to all the known active methanation catalysts. The nickel content of commercial nickel catalysts is 25–77 wt %. Nickel is dispersed on a high-surface-area, refractory support such as alumina or kieselguhr. Some supports inhibit the formation of carbon by Reaction 4. Chromia-supported nickel has been studied by Czechoslovakian and Russian investigators.

The use of leached nickel–aluminum alloy has been investigated by Gudkov and Chernyshev (*19, 20*), by the Bureau of Mines (*21, 22*), and by the Institute of Gas Technology (IGT) (*23, 24*). The Russian work was done in a fluidized catalyst bed with extremely high space velocities, upwards of 60,000. The Bureau of Mines investigators used their tube wall reactor system in which Ranel nickel alloy is sprayed on the tubes, and aluminum is leached out leaving a highly porous, high-surface-area catalyst directly in contact with the cooled surface; this is the basis of

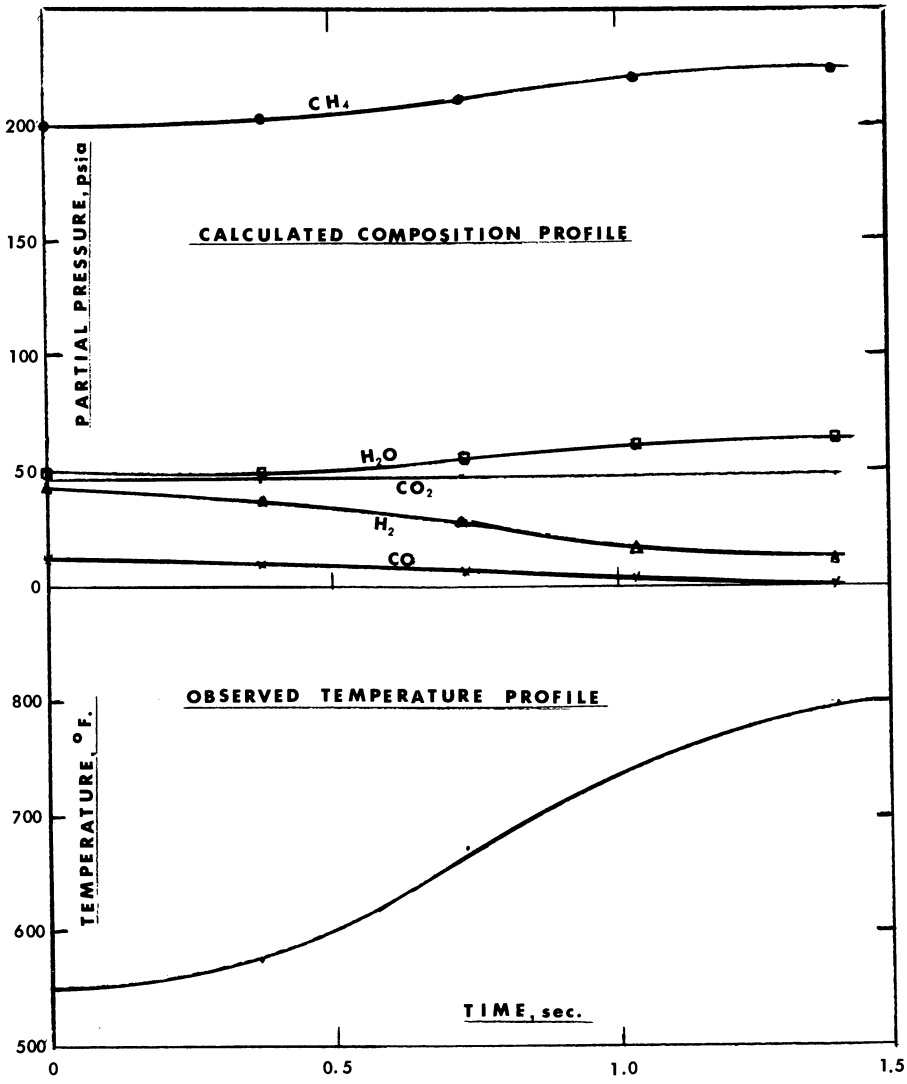

Figure 9. Calculated reaction profile from observed temperature profile

their unique methanation process. IGT reported higher activity for the Raney nickel than for nickel on kieselguhr; however, Raney nickel had a greater tendency to lay down carbon, especially at low hydrogen:CO ratios.

Other methods for producing nickel-supported catalyst have been reported. These include:

(a) Preparation of nickel hydroaluminate ($2NiO \cdot Al_2O_3 \cdot 7H_2O$) which is dehydrated at 500°C in vacuum and hydrogen reduced (25).

(b) Impregnation of alumina with nickel nitrate followed by calcination and reduction; this catalyst had lower activity and stability than a coprecipitated catalyst from nickel nitrate on sodium aluminate (*26*).

(c) Catalyst and Chemicals, Inc. (CCI) patented (*27*) a catalyst produced by mixing nickel oxide with calcium aluminate and alumina hydrate, then pelletizing, calcining, and reducing the mixture to form a highly active methanation catalyst.

OTHER METALS. Ruthenium was studied by the Bureau of Mines (*28*). It is highly active but easily poisoned by sulfur and not particularly selective to methane. Oddly enough, carbon monoxide appears to inhibit the rate of methane formation.

Partially extracted Raney cobalt is very active, but it is easily poisoned by sulfur and tends to lay down carbon more readily than Raney nickel (*21*). Cobalt is less active than nickel and much less selective to methane (*29*).

Iron is reasonably active, but less selective than nickel. It also tends to lay down carbon and to be poisoned by sulfur (*30, 31*).

Molybdenum and tungsten are unique in that they are resistant to sulfur, and, in fact, are commonly sulfided before use. The Bureau of Mines tested a variety of molybdenum catalysts (*32*). They are moderately active but relatively high temperatures are required in order to achieve good conversion, even at low space velocities. Selectivity to methane was 79–94%. Activity is considerably less than that of nickel. Although they are active with sulfur-bearing synthesis gas, the molybdenum and tungsten catalysts are not sufficiently advanced to be considered candidates for commercial use.

CATALYST POISONS. Hausberger, Atwood, and Knight (*33*) reported that nickel catalysts are extremely sensitive to sulfides and chlorides. If all materials which adversely affect the performance of a catalyst were classified as poisons, then carbon laydown and, under extreme conditions, water vapor would be included as nickel methanation catalyst poisons.

Sulfur. It is not readily predictable from existing thermodynamic data that sulfur would be a poison of nickel catalysts. The action of sulfur is undoubtedly through the reaction of hydrogen sulfide with nickel, according to:

$$\mathrm{Ni}\downarrow + \mathrm{H_2S}\uparrow \rightleftarrows \mathrm{NiS}\downarrow + \mathrm{H_2}\uparrow \qquad (15)$$

Hydrogen sulfide is present in the feed gas, or it can be formed by hydrogen reduction of any sulfur-bearing compound over the nickel catalyst.

The equilibrium ratios of hydrogen-to-hydrogen sulfide for the reaction, derived (*34*) from available thermodynamic data (*35*), are plotted in Figure 10 as a function of temperature. When P_{H_2}/P_{H_2S} over the catalyst is less than the equilibrium value, the nickel can be sulfided and hence poisoned. Conversely, when this ratio is greater than the equi-

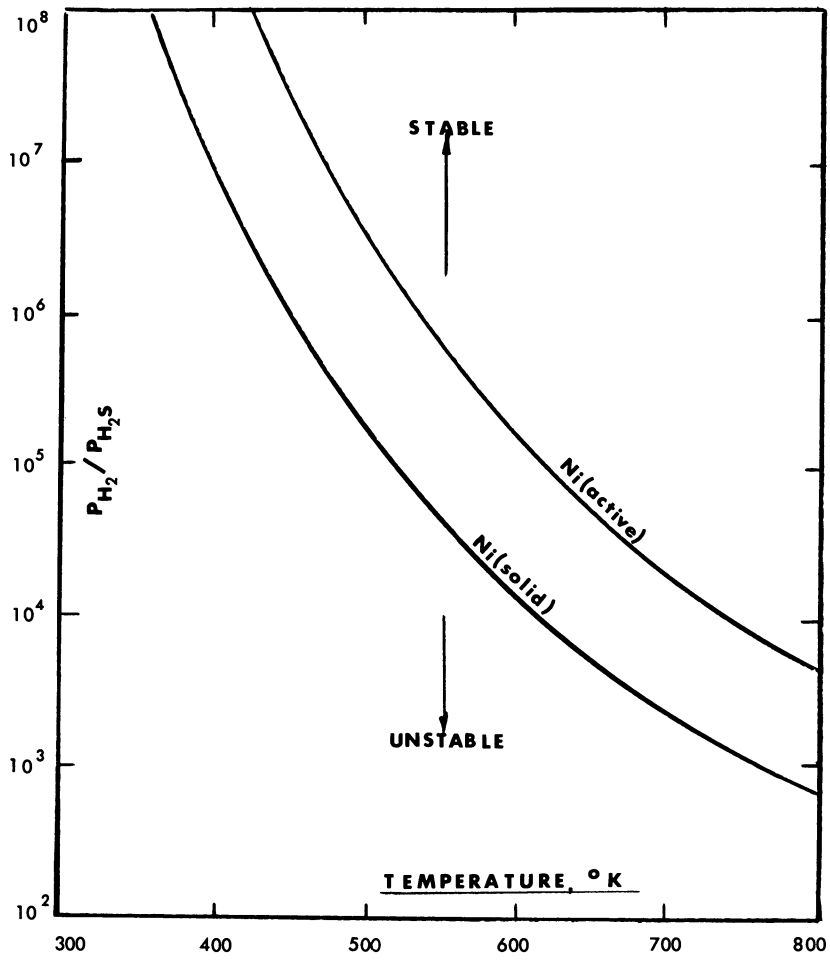

Figure 10. Effect of temperature on stability of nickel in presence of H_2S and H_2. Data from References 34 and 35.

librium value, the nickel sulfide if present would tend to be reduced, or, if not present, it would not be formed, and hence the catalyst would not be poisoned. These thermodynamic data suggest that, under conditions typical of those expected in commercial operation, as much as about 4 ppm H_2S could be tolerated in the feed. Hausberger *et al.* (33) reported that sulfide poisoning occurs at levels as low as 0.3 ppm H_2S. This discrepancy suggests that sulfide poisoning occurs at active centers, and that the nickel in these centers has a greater-than-zero free energy above Ni↓. To make the thermodynamics of Reaction 15 involving active sites agree with sulfide-poisoning experience, it is suggested that

$$Ni\downarrow \rightarrow Ni(active) \tag{16}$$

with $\Delta F \cong 3$ kcal. The estimated equilibrium ratio P_{H_2}/P_{H_2S} over active sites is plotted in Figure 10.

Steam. Steam is a potential poison of nickel catalysts under extremely high steam concentrations and low hydrogen concentrations. This is apparent in Figure 11 where the equilibrium ratio of P_{H_2}/P_{H_2O} over Ni↓ and over Ni(active) is plotted as a function of temperature for the following reactions:

$$Ni\downarrow + H_2O\uparrow \rightleftarrows NiO\downarrow + H_2\uparrow \tag{17}$$

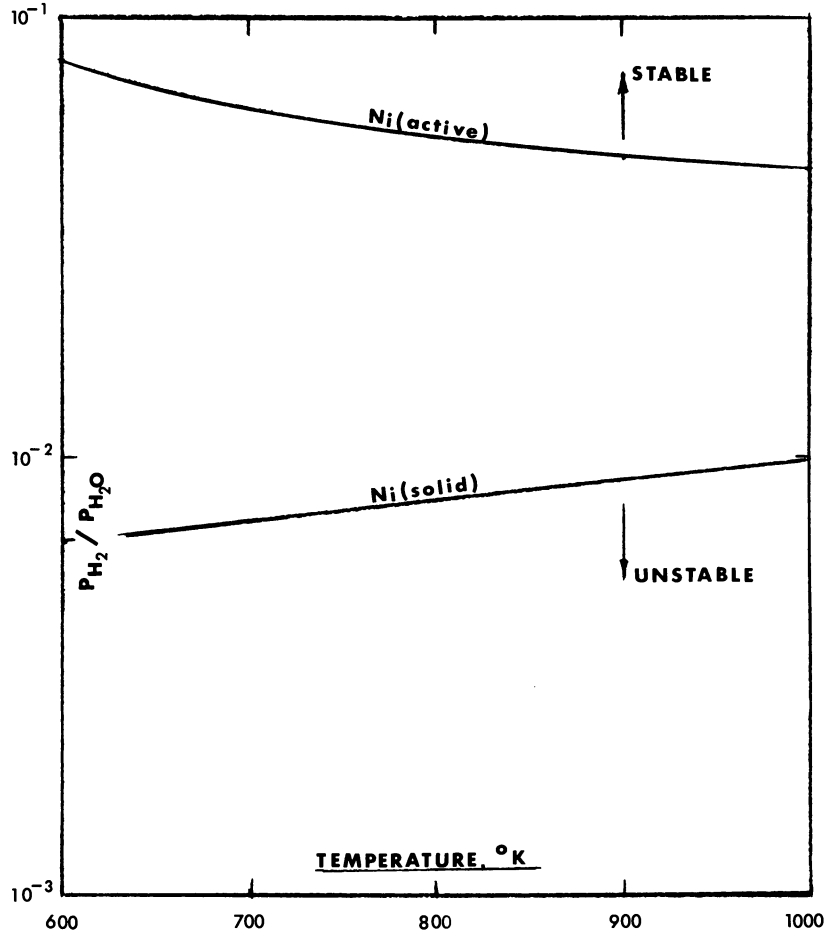

Figure 11. Effect of temperature on stability of nickel in an atmosphere of steam and hydrogen

$$Ni(active) + H_2O \uparrow \rightleftarrows NiO \downarrow + H_2 \uparrow \quad (18)$$

The Ni(active) curve indicates the limiting steam concentrations above which the nickel catalyst may be poisoned by steam (*see* Table III). Thus the limiting concentration of steam at which the nickel catalyst is not yet affected is controlled by the exit conditions where the hydrogen concentration is low. Since the limiting concentration of steam, 35 mole %, is less than that of the reacting gases, 50 mole %, it appears that mixing dry diluting gas with the reacting gas may be beneficial. This has not been demonstrated experimentally.

Carbon Laydown. The potential for carbon laydown is readily estimated from the thermodynamics of Reactions 4 and 5. The areas where carbon laydown, according to these reactions, is thermodynamically possible were developed by Gruber (*36*). It is readily seen that carbon laydown *via* Reaction 4 is thermodynamically favorable at the reactor inlet for practically any commercially conceivable feed gas composition. As noted by Gruber (*36*), carbon laydown is thermodynamically unfavorable at the reactor outlet for practically all commercially conceivable methanator conditions. The methanation reactor will therefore, in practice, have two zones—the first is a finite zone between the inlet and some way down the catalyst bed where carbon laydown is thermodynamically possible, and the second zone is the balance of the reactor.

Carbon laydown cannot be tolerated in a commercial methanation process since it could lead to rapid plugging and shutdown of the catalyst bed. Fortunately there are catalysts which avoid laydown in the first zone (*33, 37*), as opposed to catalysts which do not (*21, 22, 23, 24*).

Methanation Processes

As is indicated in Figure 1, the heat liberated in the conversion of carbon monoxide to methane is 52,730 cal/mole CO under expected reaction conditions. Also, the heat liberated in the conversion of carbon dioxide is 43,680 cal/mole CO_2. Such high heat releases strongly affect the process design of the methanation plant since it is necessary to prevent excessively high temperatures in order to avoid catalyst deactivation and carbon laydown. Several approaches have been proposed.

Table III. Limiting Concentrations of Steam

Location	*T, °C*	*Typical H_2, mole fraction*	*Limiting H_2O, mole fraction*
Reactor inlet	300	0.10	1.14
Reactor outlet	480	0.03	0.354

(a) The equilibrium-limited reactor recycles sufficient product gas to provide added mass to help absorb the heat liberated by the reaction, thereby limiting the temperature rise in the reactor to a safe level. These reactors operate adiabatically, and the temperature rise is controlled by the gas recycle. This approach was studied extensively in the laboratory and on a pilot-scale by IGT (*38*), the British Gas Council (*39*), and the U. S. Bureau of Mines (*31*). An addition, it is the basis for the Continental Oil Co. (CONOCO) methanation program at Westfield, Scotland (*40*), the CCI pilot plant in Louisville (*33*), and the Lurgi–South African Synthetic Oil, Ltd. (SASOL) process development (*37*).

(b) The throughwall-cooled reactor is used by SASOL in their ARGE-designed Fischer–Tropsch plant (*41*) which has the same temperature control problem as methanation. The temperature rise within the bed is controlled by removing the heat of reaction through the walls of a bundle of catalyst-filled tubes. An alternate design, the Tube Wall Reactor, was proposed by the Bureau of Mines (*42, 43, 44*). The catalyst is prepared by flame-spraying a nickel–aluminum alloy onto 2-in. diameter tubes so as to form a bonded layer. The layer is then partially leached with caustic to form a Raney-type catalyst adhering to the tube wall. By having a heat transfer medium, such as boiling Dowtherm or water on one side of the tube, the catalyst temperature can be closely controlled, hopefully. The Synthane pilot plant now under construction will use the tube wall reactor system.

(c) The fluidized catalyst reactor is used by SASOL in their Kellogg-designed Fischer–Tropsch plant (*45*). This design uses a large circulating stream of catalyst as a thermal fly wheel for controlling the temperature rise within the reactor.

(d) The steam-moderated reactor was discussed by White, Roszkowski, and Stanbridge (*46*). It involves the combination of gas shift and methanation with steam used in a multistage reactor system to control the equilibrium composition of the exit gas. The temperature rise is thereby controlled, and the need for a large recycle gas compressor, such as that used in the equilibrium-limited reactor, is eliminated.

(e) The kinetically limited reactor is predicated on the possibility of using very high space velocities (*i.e.*, using small catalyst beds) to produce an effluent gas significantly different from an equilibrium gas as discussed above. Operation is adiabatic. By reducing the approach to equilibrium, one would have a lower degree of conversion and hence a lower heat release and temperature rise. Theortically, it should therefore be possible to control the temperature of each step by intercooling between each stage. The idea is intriguing, but, to our knowledge, no one would consider this approach without considerable development work.

(f) The slurry methanation system was described by Blum, Sherwin, and Frank (*47*). It is based on using a large circulating stream of catalyst in an oil slurry to absorb the heat of reaction. Earlier work on this system was studied intensively for the Fischer–Tropsch process (to make liquids) (*48, 49, 50, 51, 52, 53, 54*).

Equilibrium-Limited Reactor. This system is the basis for most practical, commercial methanation plants. It is safe from the standpoint

of design and operation. It uses sufficient product gas recycle to assure a limited and safe temperature rise, even if equilibrium is attained fully and no heat is removed from the reactor (adiabatic operation).

A schematic flow diagram of this process is presented in Figure 12 which depicts three catalyst beds operating in series. Fresh make-up gas is mixed with total recycle and fed to the first bed. The effluent from the first bed is partially cooled so that when it is combined with another portion of cold make-up, the mixture is at or above the initiating reaction temperature. The mixture is fed to the second bed. This procedure is continued to the third and subsequent beds.

The number of beds in series is an independent variable in the process design of such a system. It can be shown by analysis that the volume of recycle gas decreases almost in proportion to the increase in number of beds. Offsetting the reduction in recycle volume is the pressure drop across the system. Theoretical recycle power requirements then decrease somewhat as the number of beds increases. This is plotted in Figure 13 where it is assumed that (a) the make-up gas contains three moles H_2 to one mole CO; (b) the outlet gas composition corresponds to the equilibrium for Reactions 1, 2, and 3; (c) the recycle gas has the same composition as the outlet gas; (d) inlet and outlet gas temperatures are 260°

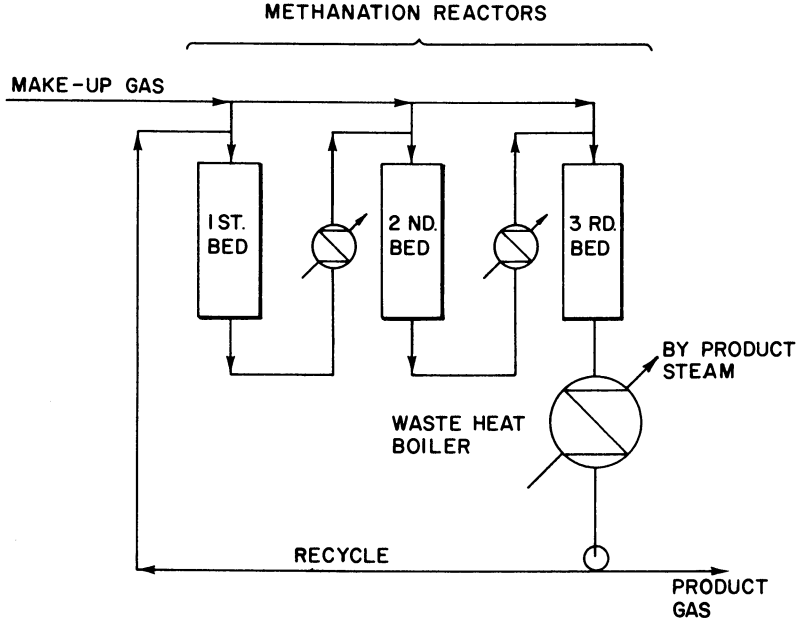

Figure 12. Schematic flow sheet for methanation system using equilibrium-controlled adiabatic reactors

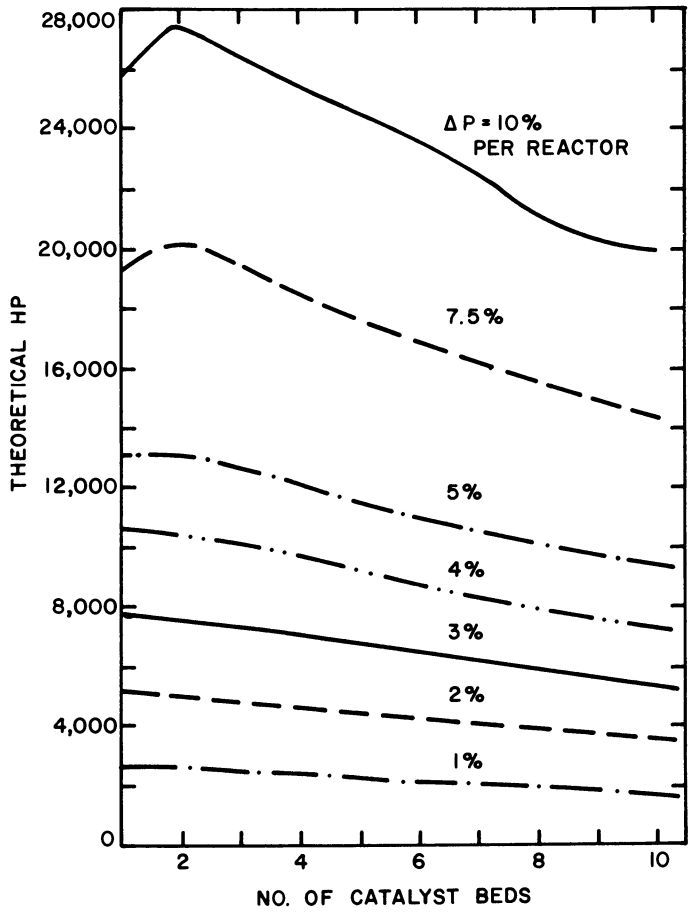

Figure 13. Effect of pressure drop and number of reactors in series on theoretical horsepower for hot gas recycle compressor H_2:CO = 3:1, standard ft³/day = 250,000,000

and 482°C, respectively; and (e) the pressure drop per reactor bed and accessories is as shown in Figure 13.

The total reactor volume required is independent of the number of beds in the series. This is evident because (a) all the beds operate with the same temperature profile and essentially the same pressure, (b) the inlet gas composition is the same for all the beds, and (c) the outlet gas composition is the same for all beds. Hence, the average driving force is the same for all beds, and the catalyst volume is simply related to the total production of methane.

In summary, increasing the number of beds in series for the system shown in Figure 12 decreases the volume of recycle somewhat more than proportionately to the number of beds, decreases the recycle compressor power requirements somewhat, and has no effect on the catalyst volume. On balance, it would appear that the capital savings achieved by increasing the number of beds will be minimal.

There are other options in the design of this system besides the variation in bed number. One of the most important is whether wet or dry gas is recycled. The above discussion assumed wet gas. This method has the following advantages over dry gas recycle (proposed by CONOCO and IGT): (a) carbon is less likely to form; (b) less heat exchange equipment is required for cooling the recycle to condense water and for reheating to achieve reaction-initiation temperatures; and (c) more by-product steam is recovered from the heat liberated by the methanation reaction. The most serious disadvantage of the wet gas recycle is the need for compressing hotter gases (at about 200°C) which entails greater mechanical problems and larger power requirements than when cooler gases are handled.

Throughwall-Cooled Reactor. This approach was used by SASOL in one of their Fischer–Tropsch plants which has been in successful operation for about 20 years. Figure 14 shows the elements of this design. The SASOL reactor contains approximately 2000 1.8-in. i.d. 40-ft long tubes filled with supported nickel catalyst. As it is released, the heat is absorbed by boiling water in the shell, and the reaction temperature is controlled by controlling the amount of recycle gas blended with the make-up feed. Some additional control is attainable by varying the pressure on the shell side. Scale-up of this type of design is relatively simple since it is necessary to pilot only one of the 2000 tubes and to ensure uniform gas flow through the tubes by proper mechanical design. Thus, one can be reasonably sure of performance on the basis of piloting just one tube.

The main advantage of this design over the adiabatic systems (*e.g.* product gas recycle) is that potentially it can achieve almost complete methanation in one reactor rather than in a series of reactors. There is a greater possibility of excessively high, local, catalyst surface temperatures with this design than with any other. This would lead to more rapid catalyst deterioration and higher catalyst consumption. In this type of reactor system, it is essential to be able to control the high temperature in the catalyst. This is achieved mainly through design of tube dimensions and formulation of catalysts. Methods of predicting the radial and axial temperature profiles for such a reactor are covered amply in the literature (*55*).

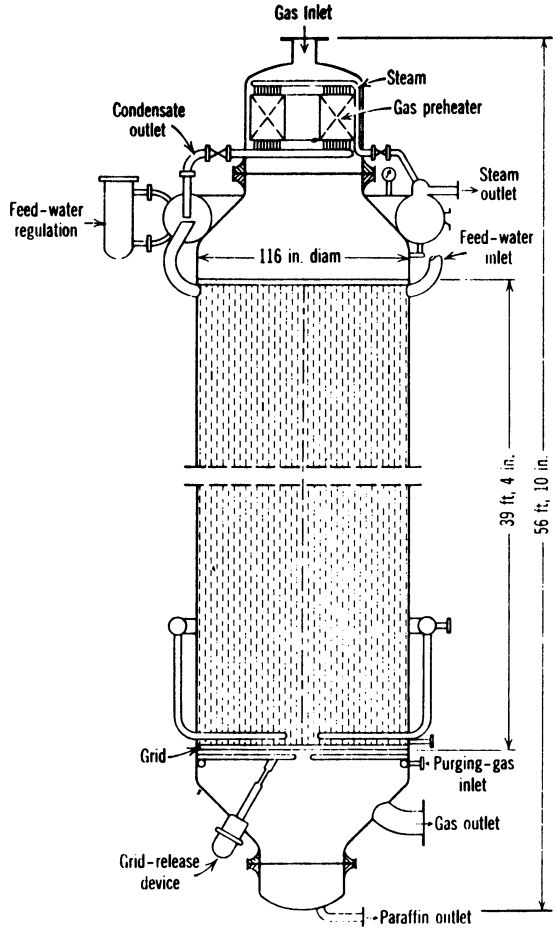

Figure 14. Fixed bed reactor (45)

It is essential to stretch out the reaction zone over as much of the tube length as possible. This will ensure maximum utilization of the tube surface for transfer of heat to the shell side (boiling water). In the extreme, if the reaction were complete in the first couple of inches of the 40-ft tube, very little of the generated heat would be removed, and, in effect, the reactor would operate adiabatically with a disastrous temperature rise. There are also radial temperature gradients with temperatures being maximum along the center line of the tube. The larger the tube diameter, the higher this maximum temperature.

In addition to these bulk temperature effects, which can be readily predicted, local hot spots can develop at the point of reaction. This phenomenon is aggravated in this system because the recycle:make-up

gas ratio may be only 2:1 whereas the ratio required in order to limit the temperature rise to *e.g.* 220°C is estimated at 20:1. Thus, much higher temperatures are potentially possible at the reacting surface with this system than with the product gas recycle system. Prediction of these local hot spots is not easy. It was shown, however, that cooling of the hot spot after completion of the reaction is so hindered that the high temperature lasts sufficiently long for sintering of catalyst crystallites to occur, with resulting decrease in catalyst activity (*56*).

Fluidized Catalyst Reactor. Two systems have been proposed, based on large scale operation of the Fischer–Tropsch process (to produce liquid hydrocarbons) at SASOL and at Carthage Hydrocol. The SASOL system was designed by M. W. Kellogg and has been operating for about 20 years (*57, 58, 59, 60*).

This system (Figure 15) is based on a large catalyst circulation rate to provide the necessary mass to absorb the large heat of reaction. The

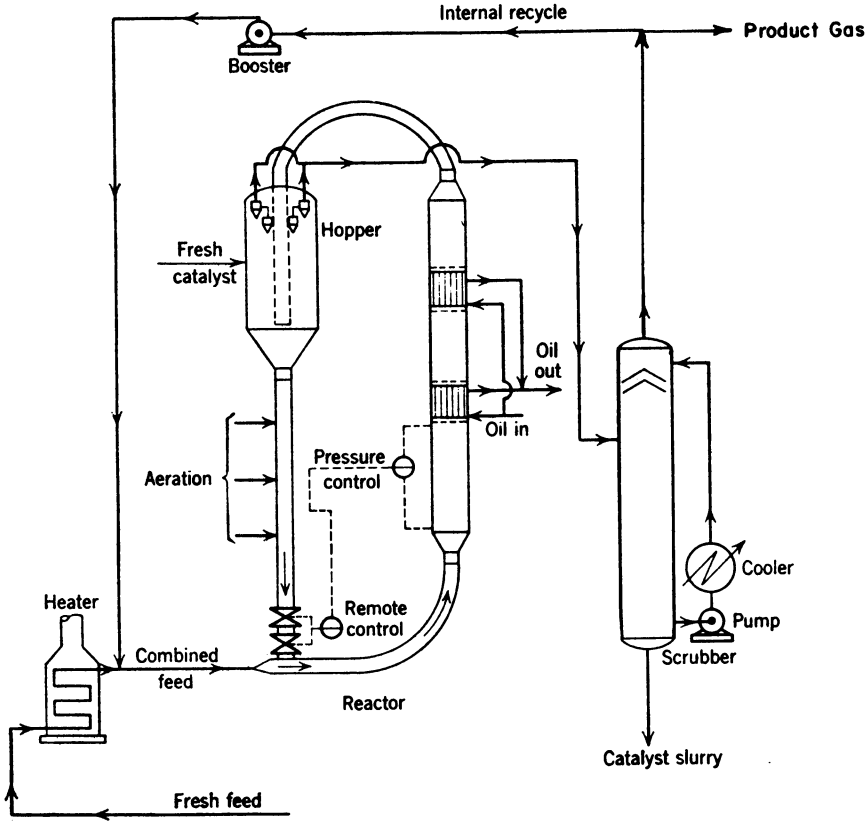

"Encyclopedia of Chemical Technology"

Figure 15. Flow sheet for SASOL fluidized bed system (45)

circulating catalyst is entrained by the fresh gas feed plus recycle gas (1:2) in a transport reactor. Generated heat is removed in appropriately located waste heat boilers. The temperature rise through the reactor is about 10°C. In the SASOL operation, an iron catalyst made from mill scale is used. Entrainment losses are tolerable because the catalyst is cheap, the life of the catalyst is only about six months, and the entrainment losses provide a purge for spent catalyst.

The Carthage Hydrocol system was designed by Hydrocarbon Research; it operated about 10 years before it was shut down in 1957. The

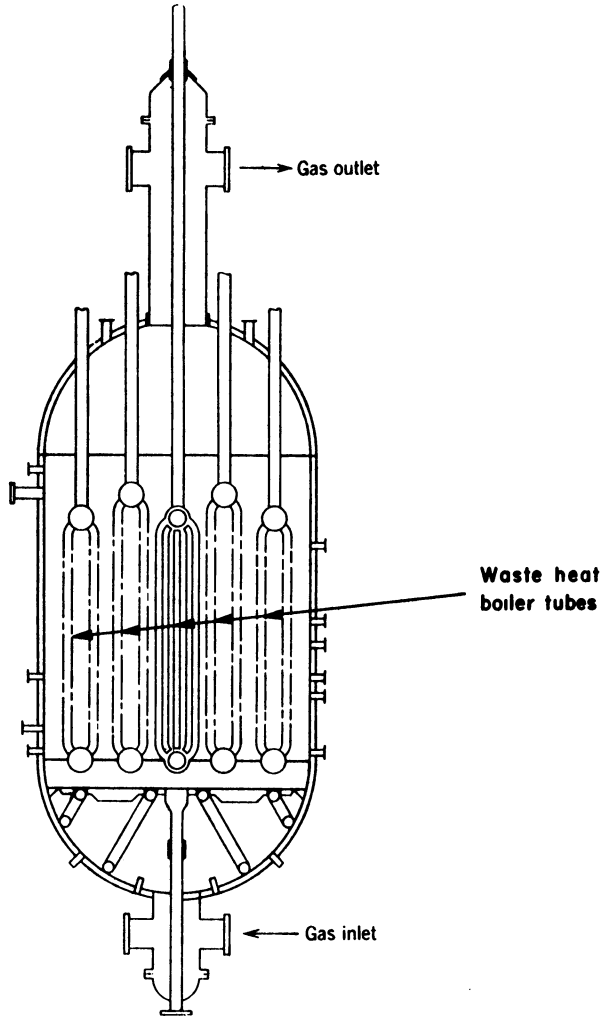

"Encyclopedia of Chemical Technology"

Figure 16. Hydrocol reactor (45)

overall flow sheet is the same as that for the SASOL system except for the design of the reactor. In the Hydrocol reactor (Figure 16) (*45*), the catalyst remains in the reactor rather than being withdrawn, circulated, and entrained as in the SASOL system. Heat is removed by waste-heat boiler tubes submerged in the bed.

The catalyst losses in either system are moderate and not excessively costly when inexpensive iron catalyst is used (as for production of liquid hydrocarbons). It is questionable, however, whether comparable losses of expensive nickel catalysts (for methanation) could be tolerated. For this reason, it is quite likely that the fluidized catalyst system will be used for methanation only after a cheap methanation catalyst is developed.

Steam-Moderated Process. The basic idea behind this approach is to limit the extent of conversion of the methanation reaction, Reaction 1, by adding steam to the feed gases. This process simultaneously provides for (*46*) elimination of the CO shift, Reaction 2, to get a 3:1 H_2:CO ratio from the make-up gas ratio of about 1.5:1; and avoidance of carbon laydown by operation under conditions in which carbon is not a thermodynamically stable phase (*see* Chemistry and Thermodynamics section above).

The basic advantages of this process are: (a) elimination of a mechanical device (recycle gas compressor) for controlling the adiabatic temperature rise, (b) combination of CO shift with methanation, (c) significant increase in byproduct steam recovery, and (d) significant capital advantages.

Kinetically Limited Process. Basically, this system limits the temperature rise of each adiabatically operated reactor to safe levels by using high enough space velocities to ensure only partial approach to equilibrium. The exit gases from each reactor are cooled in external waste heat boilers, then passed forward to the next reactor, and so forth. This resembles the equilibrium-limited reactor system as shown in Figure 8, except, of course, that the catalyst beds are much smaller.

The possible advantages of this system over the equilibrium-limited reactor system are smaller catalyst beds, lower gas recycle requirements, and lower capital requirements. The possible disadvantages of this system are (a) practically no turn-down since any turn-down would be equivalent to decreased space velocities, closer approach to equilibrium, and higher temperature rises; (b) maldistribution of gases across the bed would give rise to excessive temperature rises in zones of low flow; and (c) considerably shortened catalyst life because of possible high local or zonal temperature and, concurrently, greater chances for carbon laydown.

This design is theoretically possible, and it is even intriguing as a way to reduce capital. Practically, there are severe technical risks which

would require extensive piloting to resolve. The justification for such expense is questionable in light of the marginal benefits in capital.

Slurry Methanation. This process is being investigated by Chem Systems under contract with the American Gas Association and the Office of Coal Research (*47*). It is based on passing make-up synthesis gas, with or without gas recycle, up through a slurry of catalyst in oil. The heat of reaction is removed by (a) internal cooling in the reactor, or (b) external cooling to cool a large stream of circulating catalyst–oil slurry, or (c) evaporative cooling by evaporation of a portion of the oil in the reactor, or (d) combinations of the above.

The internal cooling system was applied to the Fischer–Tropsch process by the U. S. Bureau of Mines (*48, 49*), the British Fuels Board (*54*), and Rheinprussen–Koppers (*52, 53*). The external cooling system was applied to the Fischer–Tropsch process by I. G. Farben (*61*).

Interesting features of this process include the potential for one-stage methanation to completion without the need for gas recycle. This feature was cited by Chem Systems, but, according to Rheinpruessen–Koppers' work on the Fischer–Tropsch (*52, 53*), gas recycle was necessary with high H_2:CO ratios. Drawbacks include such factors as catalyst attrition (*48, 50*), and low volume productivities of the methanator (less than one-tenth that reported for fixed bed adiabatic reactors) (*48, 50, 52, 53, 61*).

Literature Cited

1. Sabatier, P., Senderens, J. B., *C.R. Acad. Sci.* (1902) **134**, 514.
2. Joint Army–Navy–Air Force Thermochemical Table, 2nd ed., Nat. Bur. Stand., Nat. Stand. Ref. Data Ser. (1971) **37**.
3. Rossini, F. D., Pitzer, K. S., Taylor, W. J., Ebert, J. P., Kilpatrick, J. E., Beckett, C. W., Williams, M. G., Werner, H. G., "Selected Values of Properties of Hydrocarbons," Nat. Bur. Stand. Circular (1947) **C461**.
4. Vlasenko, V. M., Uzefovich, G. E., *Russ. Chem. Rev.* (1969) **38** (9), 728.
5. Mills, G. A., Steffgen, F. W., "Catalytic Methanation," *Catal. Rev.* (1973) **8** (2), 159.
6. Nicolai, J., d'Hurt, M., Jungers, J. C., *Bull. Soc. Chim. Belg.* (1946) **55**, 160.
7. Fischer, F., Pichler, H., *Brennst. Chem.* (1933) **14**, 306.
8. Schuster, F., Panning, G., Buelow, H., *Brennst. Chem.* (1935) **16**, 368.
9. Yates, J. T., *Chem. Eng. News* (August 26, 1974) 19–29.
10. Akers, W. W., White, R. R., *Chem. Eng. Prog.*, (1948) **44**, 553.
11. Binder, G. G., White, R. R., *Chem. Eng. Prog.* (1950) **46** (11), 563.
12. Gilkeson, M. M., White, R. R., Sliepcevich, C. M., *Ind. Eng. Chem.* (1953) **45** (2), 460.
13. Dew, J. N., White, R. R., Sliepcevich, C. M., *Ind. Eng. Chem.* (1955) **47** (1), 141.
14. Smith, B. D., White, R. R., *Amer. Inst. Chem. Eng. J.* (1956) **2** (1), 46.
15. Lobo, P. A., Sliepcevich, C. M., White, R. R., *Ind. Eng. Chem.* (1956) **48** (5), 906.
16. Hougen, O. A., Watson, K. M., "Chemical Process Principles," Part 3, pp. 943–958, John Wiley & Sons, New York, 1947.

17. Hausberger, A. L., Atwood, K., Knight, C. B., private communication.
18. Fischer, F., Tropsch, H., Dilthey, P., *Brennst. Chem.* (1925) **6**, 265.
19. Gudkov, S. F., Chernyshev, A. B., *Izv. Akad. Nauk SSSR Otd. Tekh. Nauk* (1955) No. 5, 154.
20. Chernyshev, A. B., Gudkov, S. F., *Izbr. Tr.* (1956) 307.
21. Schlesinger, M. D., Demeter, J. J., Greyson, M., *Ind. Eng. Chem.* (1956) **48**, 68.
22. Field, J. H., Demeter, J. J., Forney, A. J., Bienstock, D., *Ind. Eng. Chem. Prod. Res. Develop.* (1964) **3**, 150.
23. Dirksen, H. A., Linden, H. R., *Inst. Gas Technol. Res. Bull.* (1963) **31**.
24. Rehmat, A., Randhava, S. S., *Ind. Eng. Chem. Prod. Res. Develop.* (1969) **8**, 482.
25. Bousquet, J., Teichner, S. J., *Bull. Soc. Chim. Fr.* (1969) **9**, 2963.
26. Vahala, J., *Chem. Prum.* (1971) **21** (6), 270.
27. Catalyst and Chemicals, Inc., German Patent **1,938,079** (1970).
28. Karn, F. S., Shultz, J. F., Anderson, R. B., *Ind. Eng. Chem.* (1965) **4**, 265.
29. Kurita, H., Tsutsumi, Y., *Nippon Kagaku Zasshi* (1961) **82**, 1461.
30. Schultz, J. L., Karn, F. S., Anderson, R. B., Hofer, L. J. E., *Fuel* (1961) **40**, 181.
31. Forney, A. J., Demski, R. J., Bienstock, D., Field, J. H., *U.S. Bur. Mines Rep. Invest.* (1965) **6609**.
32. Friedman, S., Hiteshue, R. W., U.S. Patent **3,429,679** (1969).
33. Hausberger, A. L., Atwood, K., Knight, C. B., ADVAN. CHEM. SER. (1975) **146**, 47.
34. Sacks, M. E., unpublished data.
35. Jellinek, K., Zakowski, J., *Z. Anorg. Chem.* (1925) **142**, 1.
36. Gruber, G., ADVAN. CHEM. SER. (1975) **146**, 31.
37. Eisenlohr, K. H., Moeller, F. W., Dry, M., ADVAN. CHEM. SER. (1975) **146**, 113.
38. Vorum, D. A., Gas Engineering Handbook, p. 3/116, Industrial Press, New York, 1965.
39. Dent, F. J., *et al.*, 49th Report of the Joint Research Committee of the Gas Research Board and the University of Leeds, London, 1945.
40. Continental Oil Co., Methanation Proposal, 1972.
41. Herbert, W., Tramm, H., *Erdoel Kohle* (1956) **9**, 363.
42. Field, J. H., Forney, A. J., Proc. Synthetic Pipeline Gas, New York (1966), p. 83.
43. Haynes, W. P., Elliott, J. J., Youngblood, A. J., Forney, A. J., *Amer. Chem. Soc., Div. Petrol. Chem., Preprint* **A 121** (Chicago, September, 1970).
44. Forney, A. J., Haynes, W. P., *Amer. Chem. Soc., Div. Fuel Chem., Prepr.* (Washington, D.C., September, 1971).
45. Kirk, R. E., Othmer, D. F., "Encyclopedia of Chemical Technology," 2nd ed., vol. 4, pp. 405–482, Interscience, New York, 1963.
46. White, G. A., Roszkowski, T. R., Stanbridge, D. W., ADVAN. CHEM. SER. (1975) **146**, 138.
47. Blum, D. B., Sherwin, M. B., Frank, M. E., ADVAN. CHEM. SER. (1975) **146**, 149.
48. Schlesinger, M. D., Benson, H. E., Murphy, E. M., Storch, H. H., *Ind. Eng. Chem.* (1950) **42**, 1322.
49. FIAT, Final Report **1267**.
50. Crowell, J. H., Benson, H. E., Field, J. H., Storch, H. H., *Ind. Eng. Chem.* (1950) **42**, 2376.
51. Benson, H. E., Field, J. H., Bienstock, D., Nagel, R. R., Brunn, L. W., Hawk, C. O., Crowell, K. H., Storch, H. H., U.S. Bur. Mines Bull. (1957) **568**.

52. Kölbel, H., Ackermann, P., Proc. World Petrol. Congr., 4th, Rome, 1955, sect. 4C, p. 228.
53. Kölbel, H., "Die Fischer–Tropsch Synthese," in "Chemische Technologie," Winnaker, K., Kuchler, L., Eds., vol. 3, pp. 492–497, Carl Hanser, Munchen, 1959.
54. "Fuel Research, 1956," Report of Fuel Research Board, Dept. of Science and Industry Research, London, 1957.
55. Bird, R. B., Stewart, W. E., Lightfoot, E. N., "Transport Phenomena," p. 279, John Wiley, New York, 1960.
56. Ruckenstein, E., Petty, C. A., *Chem. Eng. Sci.* (1972) **27**, 937.
57. Hoogendoorn, J. C., Salomon, J. H., *Brit. Chem. Eng.* (1957) **2**, 238.
58. *Ibid.* (1957) **2**, 308.
59. *Ibid.* (1957) **2**, 368.
60. *Ibid.* (1957) **2**, 418.
61. I.G. Farben., German Patent **762,320**. (1935).

Received October 4, 1974.

Equilibrium Considerations in the Methane Synthesis System

G. GRUBER[1]

Cogas Development Co., Princeton, N. J. 08540

Equilibrium calculations are made for the chemical species involved in methane synthesis: CO, CO_2, H_2O, H_2, and CH_4. Complete curves of carbon deposition are presented for all possible starting compositions over a range of pressures and temperatures. Two thermodynamic forms of carbon are investigated, as are the effects of pressure, temperature, and starting composition on equilibrium gas compositions and product gas heating value. Depending on starting composition and type of carbon deposited, increasing the temperature may, or may not, cause equilibrium carbon deposition. Pressure has little practical effect on carbon deposition. Equilibrium methane composition decreases as the temperature increases and increases as the pressure increases. Equilibrium hydrogen and carbon monoxide concentrations decrease with increasing pressure, and increase with increasing temperature. The effects of these phenomena on methane synthesis are discussed.

In the synthesis of methane from carbon monoxide and hydrogen, it is desired to operate the reactor or reactors in such a way as to avoid carbon deposition on catalyst surfaces and to produce high quality product gas. Since gas compositions entering the reactor may vary considerably because of the use of diluents and recycle gas in a technical operation, it is desirable to estimate the effects of initial gas composition on the subsequent operation. Pressure and temperature are additional variables.

It is simple enough to calculate the equilibrium composition for any given starting composition, pressure, and temperature. It is no more difficult to do this for a range of starting compositions, pressures, and

[1] On assignment from FMC Corp., Princeton, N. J. 08540.

temperatures; it merely takes longer. Since the calculations are done by computer, many variables can be examined closely. However, because of the great volume of calculated results, it is important that they be presented in a concise, informative manner. By using a particular type of triangular diagram, one can represent all possible starting compositions of CO, CO_2, H_2, H_2O, and CH_4 on a single coordinate system which is easy to use.

Chemistry

Consider the following reactions which are sufficient to describe the system:

$$CO + 3H_2 \rightleftharpoons CH_4 + H_2O \quad (1)$$

$$CO + H_2O \rightleftharpoons H_2 + CO_2 \quad (2)$$

$$2CO \rightleftharpoons CO_2 + C \quad (3)$$

In addition, it will be convenient to make reference to another reaction

$$CH_4 \rightleftharpoons C + 2H_2 \quad (4)$$

which is not independent of Reactions 1, 2, and 3.

Reactions 1 and 3 are highly exothermic and therefore have equilibrium constants that decrease rapidly with temperature. Reaction 2 is moderately exothermic, and consequently its equilibrium constant shows a moderate decrease with temperature. Reaction 4 is moderately endothermic, and its equilibrium constant increases with increasing temperature. The relationship between temperature and equilibrium constant for these four reactions is depicted in Figure 1 where carbon is assumed to be graphite. Thermodynamic data were taken from Refs. *1* and *2*.

If we allow for carbon deposition in a form other than graphite, the equilibrium constants of Reactions 3 and 4 must reflect the different state. This behavior was in fact reported by Dent *et al.* (*3*); they found that the observed equilibrium constant for Reaction 3 was less than the theoretical equilibrium constant for deposition of graphite based on measurements made at 600°–1200°K. The departure was greatest at 600°K, and the observed and theoretical equilibrium constants approached each other as the temperature increased, becoming equal at about 1100°–1200°K. The difference in free energy between graphite and the actual form of carbon deposited was also determined by decomposing pure CH_4 and by depositing carbon from a CO and H_2 mixture. The findings confirmed the measurements made by decomposing pure CO.

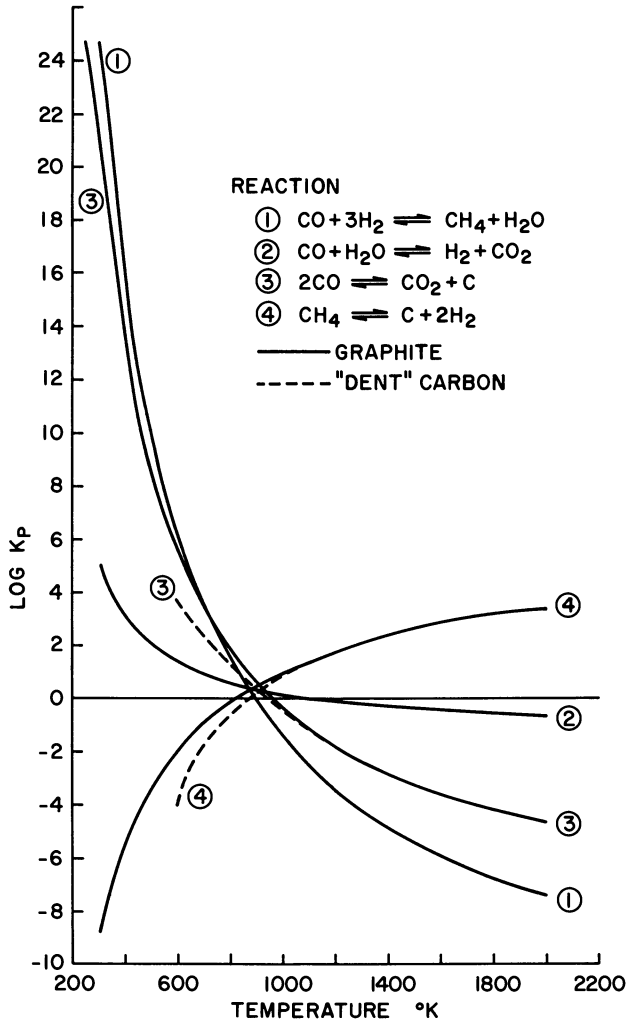

Figure 1. Equilibrium constants as a function of temperature

These experiments were performed over a nickel catalyst, and it is speculated that the anomolous free energy of the deposited carbon may be attributable to the formation of a carbide or a solid solution.

Whatever the exact form of carbon deposition may be, it must be recognized and taken into account in future calculations. The deposited material is called Dent carbon, and equilibrium constants based on its free energy are included in Figure 1. The deposition of carbon as Dent carbon was confirmed qualitatively by Pursley *et al.* (*4*). In other recently reported equilibrium calculations (*5*, *6*, *7*), it was assumed that

carbon deposition was in the form of graphite. In this paper, calculations are based on both graphite and Dent carbon.

Calculation of Carbon Deposition

If we consider the system consisting of the six species—CO, H_2, H_2O, CO_2, CH_4, and C—together with the three independent reactions—1, 2, and 3—the system can be uniquely defined by specifying three species. As a matter of convenience, we select the three species as H_2, CO, and CO_2. Furthermore, by normalizing the composition so that the number of moles of the species sums to unity, we only have to specify two species explicitly. H_2 and CO are chosen, and therefore the composition of CO_2 is implied. In order to calculate carbon deposition for any given starting temperature, the procedure is to solve Equations 1 and 2 for the equilibrium composition, ignoring carbon deposition. After the equilibrium composition is obtained, a check is made to see if the ratio $(CO)^2/CO_2$ according to Equation 3 would lead to carbon deposition. If carbon deposition is indicated, then the entire calculation is repeated using Equations 1, 2, and 3 in order to calculate the amount of carbon deposited. By using the above procedure, a line is defined which divides the coordinate region into two areas: one where graphite may deposit, and one where graphite may not deposit—on the basis of the equilibrium calculations. A typical graph of this type is shown in Figure 2.

Coordinate Systems

As was indicated above, any possible composition of CO, CO_2, H_2, H_2O, and CH_4 (solid carbon also) may be depicted on the coordinate system if the independent species are selected to be H_2, CO, and CO_2. Furthermore, the sum of the species is set to unity and only H_2 (ordinate) and CO (abscissa) are explicitly plotted. Pure H_2 is indicated by the point (0, 1.0), and pure CO by the point (1.0,0). Similarly, pure CO_2 is at the point (0,0), and compositions corresponding to pure H_2O (−1,1) and pure CH_4 (⅔,⅔) are also indicated. Water, for example, in terms of the independent species is expressed as

$$H_2O = H_2 + CO_2 - CO$$

and therefore the point on the graph corresponds to $X = -1$ and $Y = 1$. Similarly, CH_4 may be expressed as

$$CH_4 = 2H_2 + 2CO - CO_2$$

and, since CH_4 is represented by three moles of the independent species, upon normalizing $Y = \frac{2}{3}$ and $X = \frac{2}{3}$. In general, for a mixture of arbitrary composition, the coordinates are given by

$$Y = \frac{H_2O + H_2 + 2CH_4}{H_2O + H_2 + CO_2 + CO + 3CH_4} \quad (5)$$

$$X = \frac{CO - H_2O + 2CH_4}{H_2O + H_2 + CO_2 + CO + 3CH_4} \quad (6)$$

Some important features of the coordinate system are:

(a) A point on the graph does not represent a unique starting composition, but rather an equivalent starting composition expressed in terms of the independent components of the system CO, H_2, and CO_2.

(b) Only a single value of a single property of an equilibrium mixture can be represented by a single curve on the coordinate system.

(c) A family of curves is used to represent the range of a single property.

(d) The single property, or variable, will be temperature, pressure, heating value, or composition of a particular species at equilibrium; thus, the entire range of possible starting compositions is covered.

Furthermore, compositions may be found graphically by a lever rule. All mixtures of pure CO_2 and pure H_2 fall along the ordinate, the distance from pure CO_2 being inversely proportional to the amount of pure CO_2

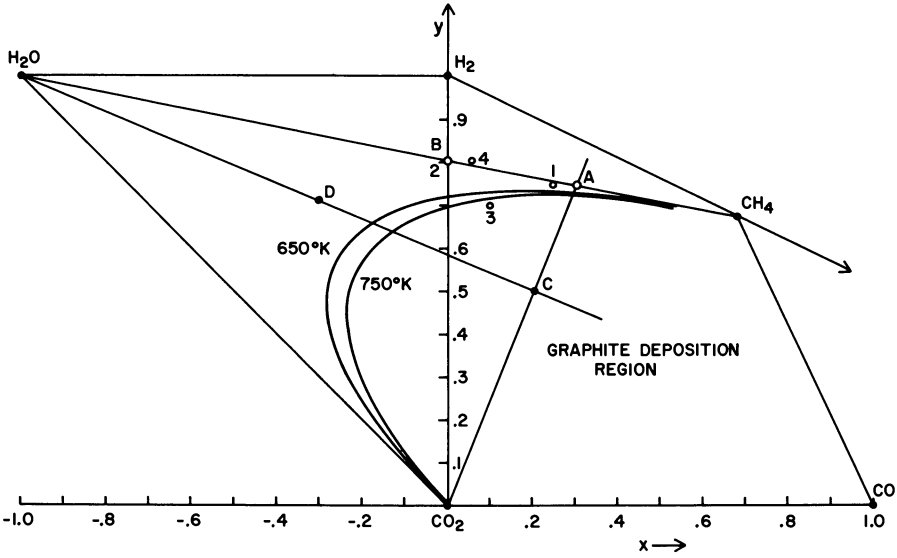

Figure 2. Graphite deposition as a function of composition and temperature at 30 atm

in the mixture. Similar rules hold for any pair of pure components or, in fact, for any pair of mixtures with the exception of methane and mixtures containing methane. Since one mole of methane is equivalent to three moles of independent species, methane concentrations must be weighted by a factor of three.

Generally speaking, the area of physical reality for gaseous mixtures corresponds to the region bounded by the straight lines connecting the pure components in Figure 2. The region formed to the right of the CH_4–CO line and below the extension of the H_2O–CH_4 line corresponds to mixtures of CH_4, CO, and solid C, and, although physically realizable, it is not considered here. The two curves in Figure 2 divide the graph into graphite-forming and non-graphite-forming regions. These curves are for 30 atm pressure at 650° and 750°K, conditions which are typical of many proposed methanation processes (*4, 8, 9, 10*). The region below and to the right of the curve is where graphite might be deposited.

Let us assume that Point A in Figure 2 corresponds to a stoichiometric mixture of H_2 and CO. If pure CO_2 is added to the mixture, Point C may be reached by moving along the line connecting the point and pure CO_2. Similarly, if pure H_2O is added, the composition moves along the line connecting Point C and pure H_2O until Point D is reached. Point B can be reached by adding H_2 and removing H_2O, which point incidentally corresponds to a stoichiometric mixture of H_2 and CO_2, or it may be viewed as a stoichiometric mixture of H_2 and CO with an excess of water.

Suppose that a starting mixture corresponding to Point A is allowed to react according to Equation 1 to produce some CH_4 and H_2O. The composition of this new mixture is still represented by Point A. If water is now removed from the mixture, the composition moves along the line connecting Point A and pure H_2O to a Point E. The extension of this line intersects the point for pure CH_4. If the mixture, whose composition is represented by Point E, is allowed to react further, and if the water produced is subsequently removed, the point representing the composition will move along line A–E toward pure CH_4. One objective is to approach pure methane without causing deposition of carbon or graphite, and these curves provide a rapid picture of how this may be done by operating at different starting compositions and temperatures, even with multiple stages. It is emphasized that we are dealing with equilibrium calculations, and we can make no predictions for non-equilibrium situations.

Carbon and Graphite Deposition

Pressure. The curves for two temperatures (Figure 2) indicate the areas of graphite deposition. Before we consider the effects of higher

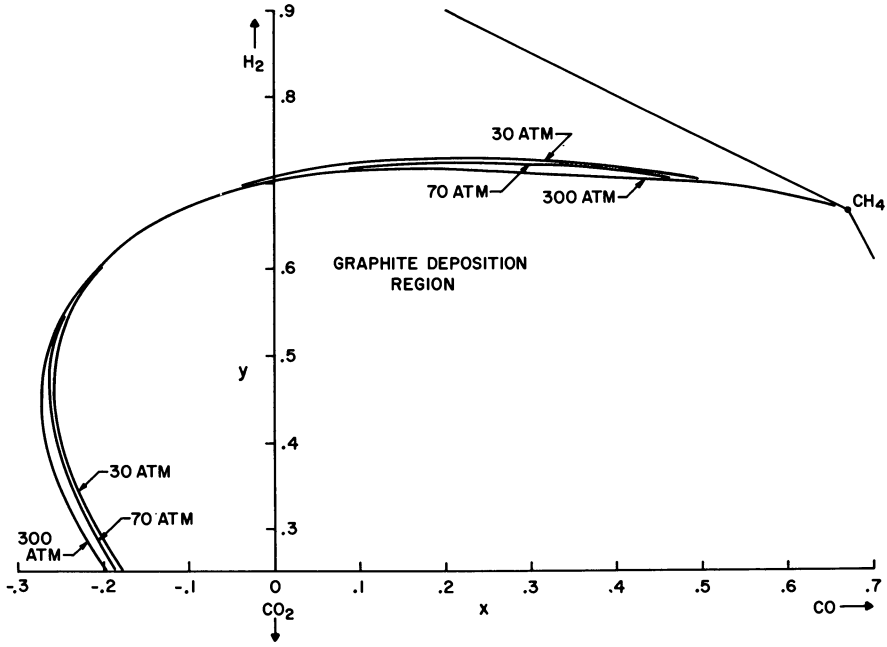

Figure 3. Effect of pressure and composition on graphite deposition at 700°K

temperatures, the effect of pressure will be examined. Figure 3 depicts the graphite deposition curves for three pressures at 700°K. This graph uses the same coordinate system, but it is plotted on a larger scale. We start by considering the effects of pressure on the two two-component systems that are represented by Reactions 3 and 4. An increase in pressure favors the reverse of Reaction 4 which has the effect of decreasing the graphite formation area in the vicinity of pure methane. Thus the intersection of the graphite deposition curve with the pure H_2–CH_4 line moves toward pure CH_4. With Reaction 3, an increase in pressure enhances the deposition of graphite and the intersection of the graphite deposition curve with the X axis will move closer to pure CO_2. This behavior again leads to an intersection of the graphite deposition curve for two different pressures. For the temperature indicated (700°K), the effect of pressure on the location of the graphite deposition curve is not large, although the effect is more pronounced at higher temperatures.

Temperature. We shall now examine the effect of temperature on the graphite deposition curve, considering a larger temperature range and the deposition of Dent carbon. Figure 4 depicts the graphite deposition curves for temperatures of 650°–2000°K. The upper temperature is far above the maximum capability of catalysts which are being proposed to carry out the methanation reaction on a large scale (*6*); however, it is

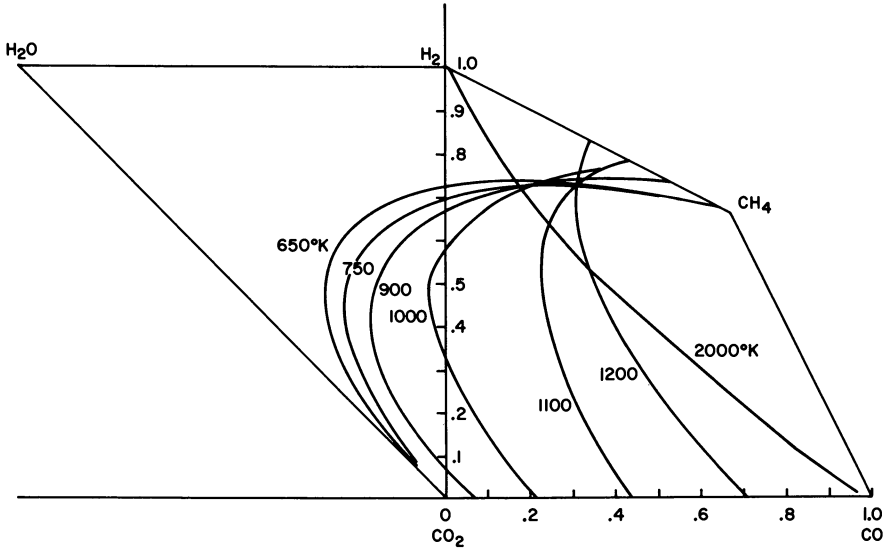

Figure 4. Graphite deposition at 30 atm and 650°–2000°K

interesting to carry out the calculations to these high temperatures with the assumption that no other reactions will occur.

Let us first consider mixtures of pure CO and CO_2, all points of which lie on the *X* axis. The equilibrium in this system is fully described by Equation 3. As the temperature increases, the equilibrium constant decreases, and CO becomes stable. It is apparent (Figure 4) that, as the temperature increases, the intersections of the curves for different temperatures move close to pure CO, thus increasing the region of no graphite deposition.

Pure CO_2 is stable with respect to carbon deposition, as is pure H_2, but there is a large composition range where mixtures of H_2 and CO_2 will deposit graphite. Thus at lower temperatures the deposition curves intersect the ordinate at two points; at higher temperatures, they retain their characteristic shape for some time, changing gradually to the almost straight line of the 2000°K curve.

In the region of pure CH_4, the equilibrium is governed by Equation 4. For this reaction, the equilibrium constant increases with temperature so that at high enough temperatures there will be appreciable dissociation of CH_4 to H_2 and graphite. In the lower temperature range considered here, the thermodynamic equilibrium indicates only a very small amount of dissociation so the intersection of the graphite deposition curve with the H_2–CH_4 line occurs at almost pure CH_4. As the temperature increases, the point of intersection will move toward pure H_2 on the H_2–CH_4 line.

So far, we have discussed graphite deposition only in terms of the two reactions, Reactions 3 and 4. As the temperature increases, graphite deposition by Reaction 4 is favored, and it is retarded by Reaction 3. The net result is that the graphite deposition curves for two temperatures will intersect at some point (*e.g.*, the two curves for 900° and 1000°K). The quantitative description of curves depends on the interactions of all the species.

Because of the opposite effects of temperature on the stability of CO and CH_4, the odd result is that, as the temperature increases, graphite deposition is less likely for starting mixtures which are near stoichiometric, but it is more difficult to produce pure methane by removing water and allowing the mixture to react further. Because of equilibrium considerations, the final approach to pure methane must be done at a relatively low temperature.

If it is assumed that the solid deposit is not graphite but rather that it has the thermodynamic properties of Dent carbon, the situation is quite different. At the lower temperatures considered, Dent carbon is much less likely to be deposited than graphite as indicated by the curve for 600°K in Figure 5. As the temperature increases, the behavior of Dent carbon approaches that of graphite, and the carbon deposition region becomes greater. At approximately 1100°K, the curves for Dent carbon and graphite are the same. At higher temperatures, it is assumed that Dent carbon and graphite also behave identically regarding deposition.

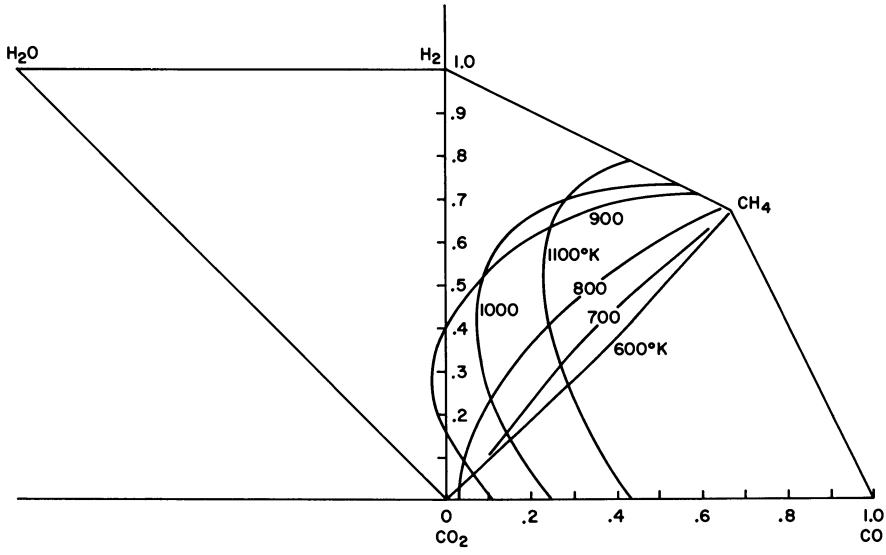

Figure 5. Deposition of DENT carbon at 30 atm

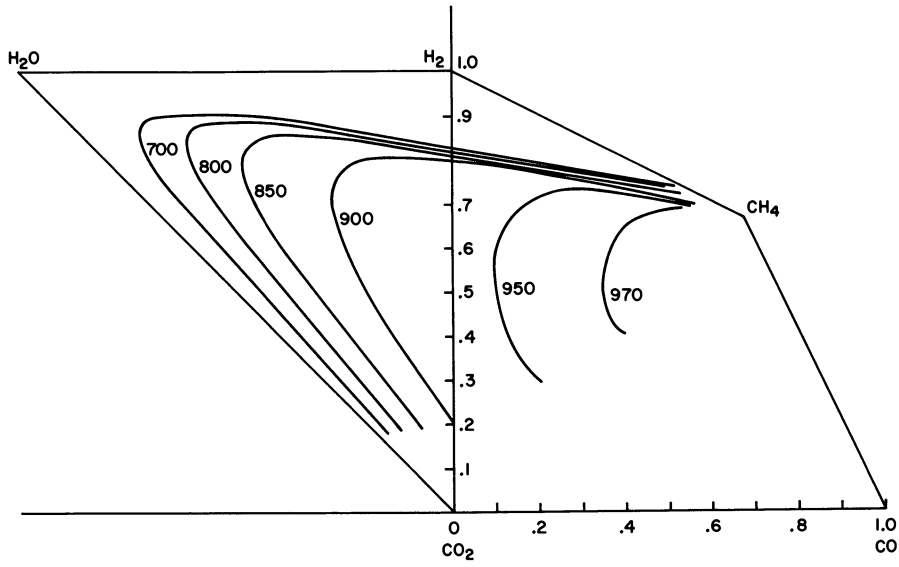

Figure 6. Higher heating value of CO_2- and H_2O-free equilibrium mixtures as a function of starting composition at 50 atm and 700°K

Since the effects of temperature on Reactions 3 and 4 are in opposite directions, the different temperature curves also intersect as with graphite. If it is assumed that carbon deposition is governed by the thermochemistry of Dent carbon rather than that of graphite, it is obvious that there is a much greater region where deposition will not take place.

Equilibrium Compositions and Heating Value

The preceeding discussion was confined mostly to the carbon deposition curves as a function of temperature, pressure, and initial composition. Also of interest, especially for methane synthesis, is the composition and heating value of the equilibrium gas mixture. It is desirable to produce a gas with a high heating value which implies a high concentration of CH_4 and low concentrations of the other species. Of particular interest are the concentrations of H_2 and CO since these are generally the valuable raw materials. Also, by custom it is desirable to maintain a CO concentration of less than 0.1%. The calculated heating values are reported as is customary in the gas industry: on the basis of one cubic foot at 30 in. Hg and 15.6°C (60°F) when saturated with water vapor (*11*). Furthermore, calculations are made and reported for a CO_2- and H_2O-free gas since these components may be removed from the mixture after the final chemical reaction. Concentrations of CH_4, CO, and H_2 are also reported on a CO_2 and H_2O-free basis.

The higher heating value is plotted on the composition coordinate in Figure 6. These curves are for 50 atm and 700°K. The contours of constant heating value increase uniformly in the direction of pure methane. These contours, of course, are very similar to the contours of CH_4 concentration which are plotted in Figure 7 for the same conditions, 50 atm and 700°K.

The hydrogen concentration contours for 50 atm and 700°K (Figure 8) indicate that there is appreciable unreacted hydrogen after equilibrium is reached. It is clear that multiple reaction stages are required to approach pure methane.

The carbon monoxide concentration contours for 50 atm and 700°K (Figure 9) indicate that the equilibrium CO leakage will not be high if equilibrium is reached when the initial composition is near the stoichiometric line.

Figure 10 depicts the effect of temperature on higher heating value and on CH_4, H_2, and CO concentrations for four different starting compositions. The four starting compositions are:

Y	*X*	
.75	.25	stoichiometric
.8	0	stoichiometric
.7	.1	hydrogen deficient
.8	.05	hydrogen rich

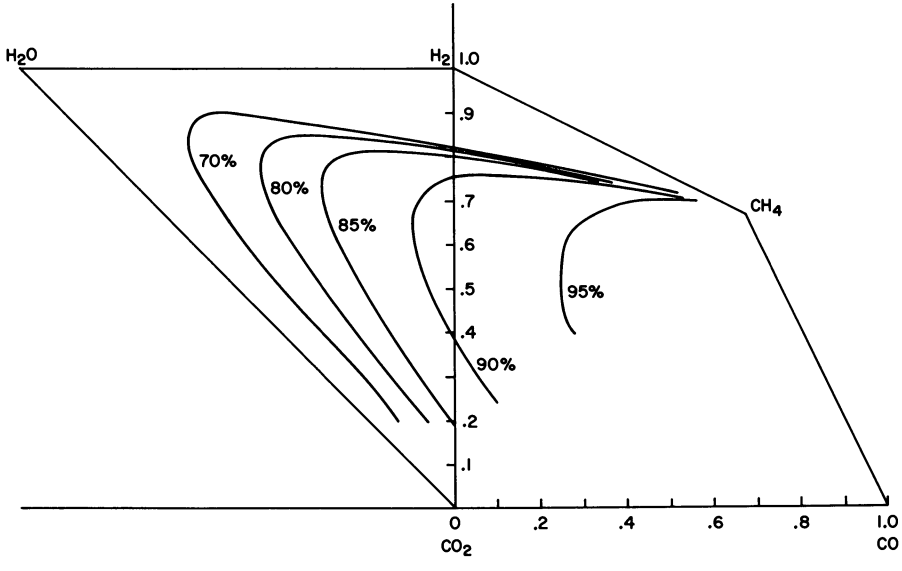

Figure 7. CH_4 concentration of equilibrium mixtures at 50 atm and 700°K

In this context, stoichiometric implies any composition point on the line connecting pure water and pure methane. These mixtures have an H_2/CO ratio of 3.0 and contain either excess water or methane. Thus, they are stoichiometric with respect to hydrogen and carbon monoxide according to Reaction 1. Points falling below the line are deficient in hydrogen, and points above the line are hydrogen rich. In Figures 10A and 10B the heating value and methane concentration decrease as a function of temperature for all four starting compositions. Conversely, the hydrogen and carbon monoxide concentrations increase (*see* Figures 10C and 10D). The equilibrium CO leakage is about the same for the two stoichiometric points, but it is considerably larger for the hydrogen-deficient starting composition.

Figure 11 depicts the effect of pressure on higher heating value and equilibrium composition for these same four starting compositions, all at 700°K. Generally, the effect of pressure decreases as the pressure increases, with most of the change occurring in the region up to 200 atm. For all of the compositions, as well as the higher heating values, the curves for the two stoichiometric and for the hydrogen-deficient starting points are similar. The hydrogen-rich starting composition is different; this is more apparent on Figure 11 because it is plotted on a larger scale than Figure 10.

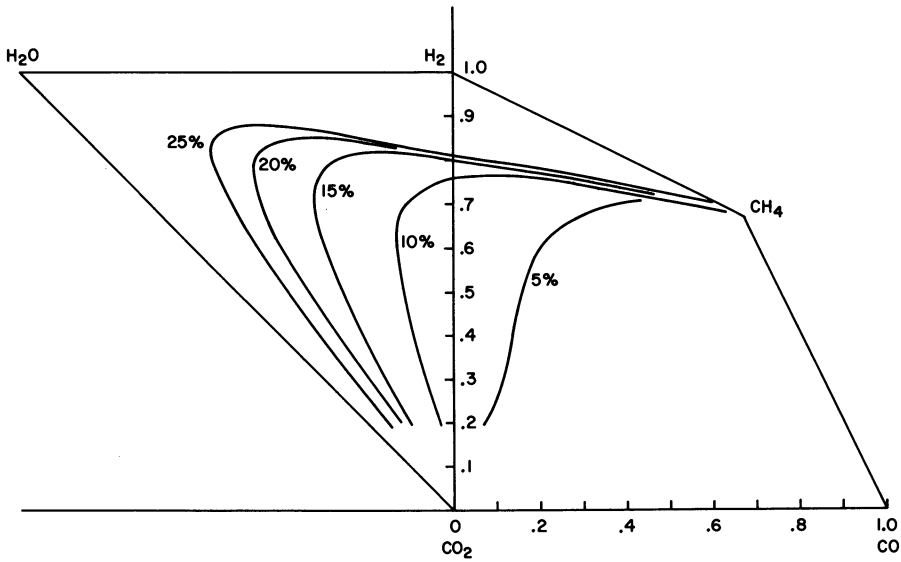

Figure 8. H_2 concentration of equilibrium mixtures, H_2O- and CO_2-free, at 50 atm and 700°K

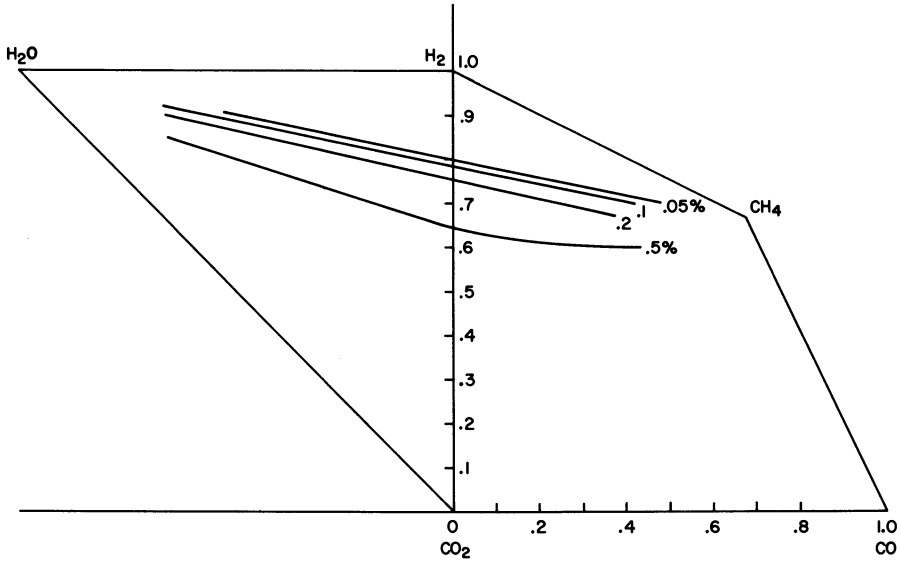

Figure 9. Equilibrium CO concentration, H_2O- and CO_2-free, at 50 atm and 700°K

General Discussion

Various schemes have been proposed for carrying out the methane synthesis reaction; some of these are now in use (*6, 12, 13, 14*).

A major engineering problem is removal of the large amount of heat generated during the synthesis, and numerous way of accomplishing this have been considered. The reactor temperature may be controlled by recycling product gas, with or without the water being condensed, or by otherwise diluting the reacting mixture with an excess of any of the products or reactants. This effectively changes the overall mixture composition. In addition, the fresh feed composition is widely variable depending on the source of the feed gas. Nevertheless, the charts presented here are applicable to a gas of any composition, and they allow one to determine immediately if there is a possibility of carbon deposition at any given temperature. Figure 5, for example, indicates that it is not possible to approach pure CH_4 at a high temperature without carbon deposition, and that a catalyst with a high temperature capability is not universally useful but is dependent on the starting composition of the mixture. In any event, the final stage of the reaction to approach pure CH_4 must be carried out at a low temperature.

Summary

An investigation was made into the equilibria of the methanation reaction, coupled with the shift reaction and the carbon deposition reaction. Of particular interest is the exploration of regions where carbon deposition is possible according to thermodynamic criteria assuming that carbon is deposited as graphite or as Dent carbon. The carbon-laydown curves are plotted on a unique coordinate system which corresponds to the starting composition variables that are commonly used. The effects of pressure, temperature, and starting composition on carbon laydown are investigated over a range of practical interest as well as beyond. All possible starting compositions are considered at temperatures of 600°–

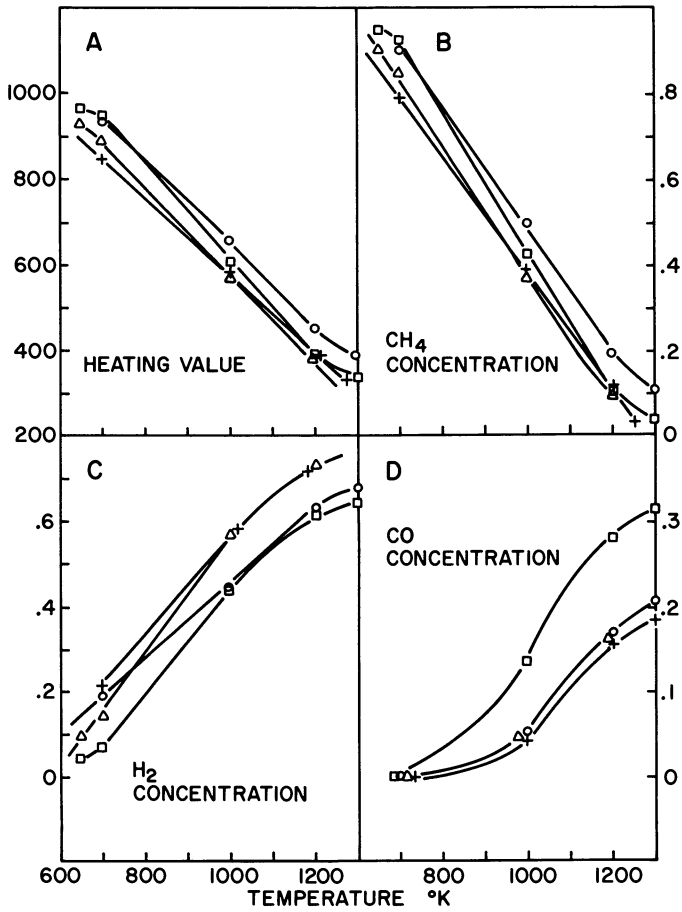

Figure 10. Effect of temperature on concentration at 50 atm
Starting compositions (values of Y, X): ○: 0.75, 0.25; △: 0.8, 0; □: 0.7, 0.1; and +: 0.8, 0.05

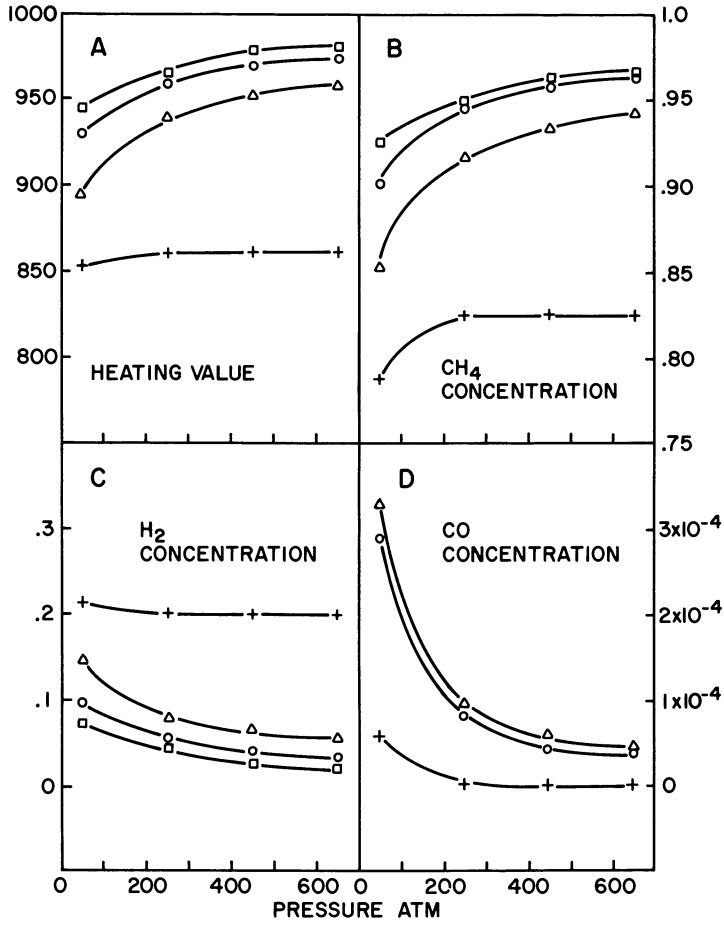

Figure 11. Effect of pressure on concentration at 700°K
Starting compositions as in Figure 10

2000°K (329°–1727°C) and at pressures of 30–300 atm (426–4395 psig). In addition, the effects of pressure, temperature, and starting composition on equilibrium composition and product gas heating value are examined. The figures presented provide a useful tool for rapid scanning of the effects of starting gas composition, pressure, and temperature on product gas quality and useful operating regions. The utility of the graphs is not limited to a single-stage reaction, but it can also be used for multiple-stage reactors with arbitrary amounts of diluents (H_2O, CO_2, CH_4) and recycle gas, which may change from stage to stage. Additionally, the pressure and temperature of each stage may be examined independently.

Literature Cited

1. Joint Army–Navy–Air Force Thermochemical Table, 2nd ed., Nat. Bur. Stand., Nat. Stand. Ref. Data Ser. (1971) **37.**
2. Rossini, F. D., Pitzer, K. S., Taylor, W. J., Ebert, J. P., Kilpatrick, J. E., Beckett, C. W., Williams, M. G., Werner, H. G., "Selected Values of Properties of Hydrocarbons," Nat. Bur. Stand. Circular (1947) **C461.**
3. Dent, J. F., Moignard, L. A., Blackbraun, W. H., Herbden, D., "An Investigation into the Catalytic Synthesis of Methane by Town Gas Manufacture," 49th Report of the Joint Research Committee of the Gas Research Board and the University of Leeds (1945) **GRB20.**
4. Pursley, J. A., White, R. R., Sliepcevich, C., "Reaction Kinetics," *Chem. Eng. Prog. Symp. Ser.* (1958) **48** (4), 51–58.
5. Lunde, P. J., Kester, F. L., *Ind. Eng. Chem. Proc. Res. Develop.* (1974) **13** (1).
6. Mills, G. A., Steffgen, F. W., *Catal. Rev.* (1973) **8** (2), 159–210.
7. Greyson, M., in "Catalysis," P. H. Emmet, Ed., vol. 4, chap. 6, Reinhold, New York, 1956.
8. Lee, A. L., Feldkirchner, H. L., Tajbl, D. G., "Methanation of Coal Hydrogasification," *Amer. Chem. Soc., Div. Fuel Chem., Prepr.* **14** (4), Part I, 126–142 (September, 1970).
9. Wen, C. Y., Chen, P. W., Kato, K., Galli, A. F., "Optimization of Fixed Bed Methanation Processes," *Amer. Chem. Soc., Div. Fuel Chem., Prepr.* **14** (3), 104–163 (September, 1970).
10. Forney, A. J., McGee, J. P., "The Synthane Process," Amer. Gas Ass. Pipeline Gas Symp., 4th, Chicago, 1972.
11. McClahahan, D. N., *Oil Gas J.* (Feb. 20, 1967) 84–90.
12. Greyson, M., *et al., U.S. Bur. Mines Rep. Invest.* (1965) **6609.**
13. Forney, A. J., Haynes, W. P., "The Synthane Coal to Gas Process: A Progress Report," *Amer. Chem Soc., Div. Fuel Chem., Prepr.* (September, 1971).
14. Schoubye, P. J., *Catalysis* (1970) **18** (1), 118.

RECEIVED October 4, 1974.

Development of Methanation Catalysts for the Synthetic Natural Gas Processes

A. L. HAUSBERGER, C. BERT KNIGHT, and KENTON ATWOOD

Catalysts and Chemicals, Inc., Louisville, Ky. 40210

It was shown in laboratory studies that methanation activity increases with increasing nickel content of the catalyst but decreases with increasing catalyst particle size. Increasing the steam-to-gas ratio of the feed gas results in increased carbon monoxide shift conversion but does not affect the rate of methanation. Trace impurities in the process gas such as H_2S and HCl poison the catalyst. The poisoning mechanism differs because the sulfur remains on the catalyst while the chloride does not. Hydrocarbons at low concentrations do not affect methanation activity significantly, and they reform into methane; at higher levels, hydrocarbons inhibit methanation and can result in carbon deposition. A pore diffusion kinetic system was adopted which correlates the laboratory data and defines the rate of reaction.

In September 1970, Catalysts and Chemicals, Inc. (CCI) began a research and development program on methanation catalysts for the production of a high Btu, synthetic natural gas (SNG) by either coal or naphtha gasification. In 1971, CCI entered into an agreement with El Paso Natural Gas Co. to demonstrate the commercial feasibility of the methanation step in the production of SNG from coal. The pilot plant was designed in late 1971 and started up in early 1972. Because of the widespread interest and concern about the methanation step in the overall production of SNG from coal, this project was opened to other participants in 1972. Western Gasification Co. and COGAS Development Co. decided to participate in the pilot plant program.

This is a report on the basic work done in the laboratory to develop the catalysts for the methanation of synthetic gas from coal, and it also reports on the development of an applicable kinetic system. This report does not include any of the subsequent pilot plant test work.

In the laboratory, more than 160 bench-scale tests involving more than 40 catalysts were made in order to determine the optimum catalysts and process conditions for this application. Initial tests used commercially available catalysts, but early findings indicated that a whole new series of catalysts was required.

The comprehensive research program included all facets necessary for the development of these catalysts. Laboratory tests were conducted to determine the necessary catalyst loading, the design operating conditions, the effect of particle size, the effect of various trace constituents on catalyst performance, and finally, resistance of the catalyst to thermal upsets. This paper presents only those findings which have direct significance for the kinetic model which was selected. Of particular importance to the development of the most active catalyst and the kinetic model for this new methanation application were laboratory studies of the effects on catalyst activity of (a) the nickel content of the catalyst, (b) the particle size of the catalyst, (c) the steam/gas ratio (S/G) in the process gas, and (d) trace impurities in the process gas.

Table I. Designations for Nickel-Containing Catalysts

	Support	
Nickel Content, %	*Silica*	*Alumina*
50	C150-1-02	C150-1-03
40	C150-2-02	C150-2-03
30	C150-3-02	C150-3-03

We discuss extensively the kinetic system we used and the basis for selecting this system. During our development work, we referred frequently to the literature and to the kinetics reported by previous investigators. An extensive literature search was made, and a comprehensive bibliography is presented.

Effect of Nickel Content on Catalyst Activity

For the methanation reaction in the process of converting coal to a high Btu gas, various catalyst compositions were evaluated in order to determine the optimum type catalyst. From this study, a series of catalysts were developed for studying the effect of nickel content on catalyst activity. This series included both silica- and alumina-based catalysts, and the nickel content was varied (Table I).

This study was run in a laboratory bench-scale unit with 0.75-in. reactor tubes. The catalysts were sized to 10×12 mesh and diluted nine-to-one with SiO_2 in order to spread the reaction out through the bed and to permit measurement of temperature profiles, the profile being an

Table II. Test Conditions for Study of Effect of Nickel Content

Catalyst Loading		*Gas Composition*		*Test Conditions*	
Volume, cm^3	5.0	CO, %	3	inlet T, °C	260
Size, mesh	10 × 12	CO_2, %	4	pressure, psig	370
Bed, L/D	7.31	H_2 %	12	space velocity,[a] vol/vol hr	25,000–95,000
Bed dilution	9/1	CH_4, %	81	superficial linear velocity,[a] ft/sec	0.343–1.302
		S/G	0.35		

[a] Space velocity: the volume of outlet dry gas per hour at standard conditions of 15.6°C and 1 atm, given per volume of catalyst.
[b] Linear space velocity: based on 371°C and outlet flow rate.

excellent indicator of catalyst activity. Space velocities were also varied in an attempt to move away from equilibrium CO leakages in order to assess the relative activity of the different catalysts.

The catalysts were reduced with 100% H_2 at 371°C and an inlet space velocity of 1000/hr. Because of the carbon-forming potential of a dry gas recycle composition and the cost of reheating the recycle if the water produced by the methanation reaction is removed, a wet gas recycle composition was used. The catalyst loading, gas composition, and test conditions for these tests are listed in Table II, and the effects of nickel content are compared in Table III.

The temperature profiles for each catalyst at two different space velocities are plotted in Figure 1. The catalysts with lower nickel content had reasonable activity, but the activity obviously decreased with nickel content. At 25,000/hr space velocity, the 30% nickel-on-alumina catalyst used 50% of the bed to obtain the maximum temperature whereas with 50% nickel the reaction used only 30% or the bed. The method used to prepare the C150-3-02 catalyst resulted in a non-reduceable nickel silicate

Table III. Nickel Content of Catalyst *vs.* H_2 and CO Leakage

Catalyst	*Nickel Content, %*	*Outlet Dry Gas Space Velocity, vol/vol hr*	*CO Leakage, %*	*H_2 Leakage, %*
C150-1-02	50	93,000	0.18	6.93
C150-2-02	40	96,000	0.80	13.10
C150-3-02	30	96,000	3.35	22.30
C150-1-03	50	88,600	0.66	10.70
C150-2-03	40	96,000	0.27	16.88
C150-3-03	30	96,000	1.24	16.40

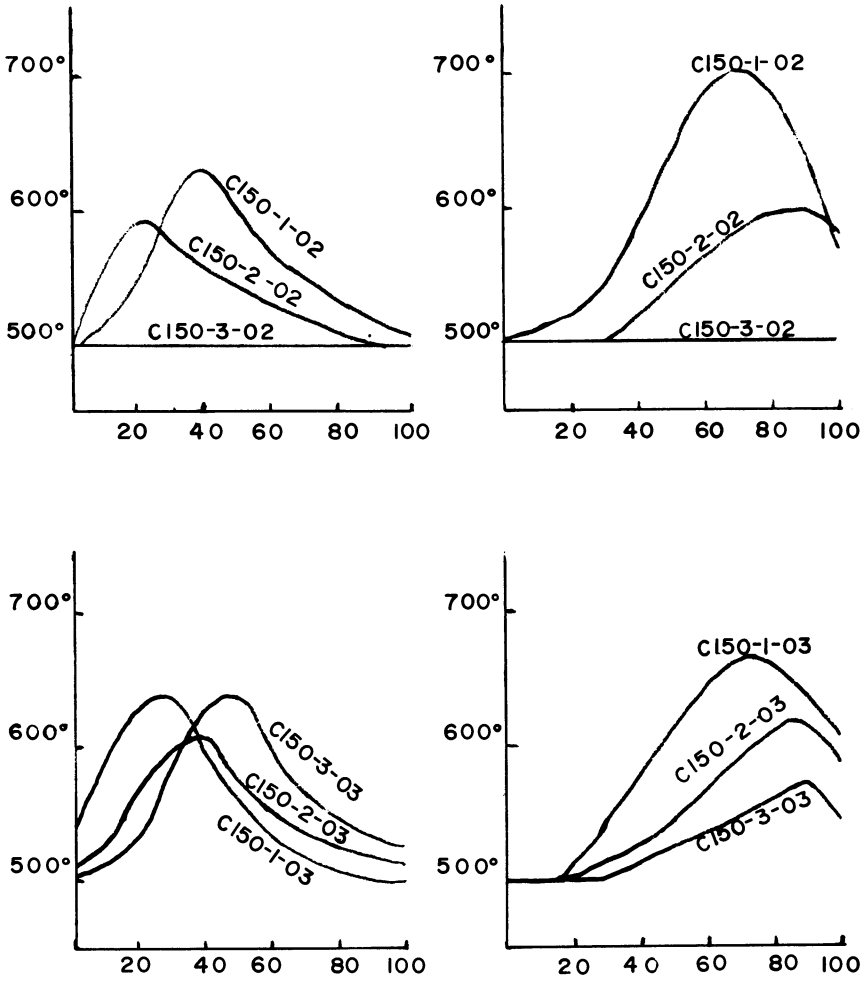

Figure 1. Temperature (in °F) vs. bed depth (in %)
Top: silica-supported catalysts; bottom: alumina-supported catalysts; left: 25,000 space velocity; and right: 95,000 space velocity

which had no activity. Each test was continued for at least 300 hrs. At various times a test condition would be repeated, and the percentage of the bed used for the reaction revealed that the catalyst had not aged. Carbon analysis indicated that no carbon deposition occurred under the conditions of these tests.

Effect of Particle Size on Catalyst

Particle size was studied with the C150-1-02 catalyst. The C150-1-02 mixture was tabletted in three different sizes: 1/8 × 1/16, 3/16 × 3/32, and 3/16 × 3/16 in. The catalyst was reduced by the procedure described

Table IV. Test Conditions for Particle Size Study

Catalyst Loading		*Gas Composition*		*Test Conditions*	
Type	C150-1-02	CO, %	5.0	inlet T, °C	260–288
Volume, cm^3	10.0	CO_2, %	4.0	pressure, psig	350
Form	tablets	H_2, %	23.0	space velocity, vol/vol hr	20,000 40,000 60,000
Size, in.	3/16 × 3/16 3/16 × 3/32 1/8 × 3/32	CH_4, %	68.0	superficial linear velocity, ft/sec	0.075–0.250
Bed, L/D	1.46	S/G	0.35–0.40		

above, and it was then tested under the conditions of primary wet gas recycle methanation. Catalyst loading, gas composition, and test conditions are outlined in Table IV. The findings from these experiments are summarized in Table V.

As particle size decreases, hydrogen leakage decreases and hot spot temperature in the bed is higher. Thus the smaller particle size has greater activity (*see* Table VI). A kinetic system which defines the reaction in terms of CO and CO_2 methanation and CO shift conversion was used to determine the activity (*see* last column of Table VI).

Table V. Study of Catalyst Particle Size

Temperature, °C			*Space Velocity,*	*Outlet Analyses*		*Activity Constant*
Inlet	*Hot Spot*	*Outlet*	*vol/vol hr*	*CO, %*	*H_2, %*	Kw *CO*[a]
C150-1-02, 3/16 × 3/16 in.						
292	428	394	20,000	<.03	7.3	40,674
291	393	382	40,000	<.03	10.4	36,659
290	387	360	60,000	<.03	14.8	39,407
						Avg. 38,713
C150-1-02, 3/16 × 3/32 in.						
294	414	391	20,000	<.03	7.3	59,788
295	425	388	40,000	<.03	9.9	51,052
						Avg. 55,420
C150-1-02, 1/8 × 1/16 in.						
296	434	388	20,000	<.03	6.8	78,902
296	418	398	40,000	<.03	8.7	66,045
294	431	402	60,000	<.03	12.2	73,464
						Avg. 72,804

[a] $-\frac{dCO}{dV} = KwCO\left[\frac{\text{moles CO}}{\text{moles flow}} - \frac{\text{moles CO}_{eq.}}{\text{moles flow eq.}}\right]$

Table VI. Effect of Particle Size on Relative Activity

Particle Size, in.	*CO Methanation* Kw	Kw_x/Kw_o[a]
3/16 × 3/16	38,713	1.00
3/16 × 3/32	55,420	1.43
1/8 × 1/16	72,804	1.88

[a] Kw_o is taken as the base case Kw. $Kw\sigma$ is the observed Kw_x for each size.

If we assume that the activity is universely proportional to particle size:

$$\frac{Kw_o}{Kw_x} = \left(\frac{Dx}{Do}\right)^n$$

then n approximately equals 0.9 or Kw is proportional to $(1/D)^{0.9}$ where D is the equivalent sphere diameter. Since the kinetics are based on diffusion control, it was assumed that Kw was proportional to $1/D$. These data give fairly good agreement since the packing and flow in the small diameter laboratory tubes would also cause some error.

Effect of Steam-to-Gas Ratio on Catalyst Activity

In the various laboratory studies when the outlet gas composition was not at equilibrium, it was observed that the steam-to-gas ratio (S/G) significantly affected the hydrogen leakage while the carbon monoxide still remained low. On the assumption that various reactions will proceed at different rates, a study was made to determine the effect of S/G on the reaction rate. The conditions for this test are presented in Table VII; the findings are tabulated in Table VIII.

Significant differences were observed when S/G was varied from 0.15 to 0.40. At the lower S/G ratios there is no CO shift conversion whereas there is CO shift conversion at the higher S/G ratios. When the data are evaluated and activity constants for CO and CO_2 methanation and CO shift conversion are determined, the activity for methanation remains the same regardless of the S/G. However, with high S/G, shift conversion occurs at about 25% of the rate of CO methanation. At low S/G, no shift conversion is observed.

Effect of Trace Constituents in the Process Gas on Catalyst Activity

When SNG is made from coal, the methanation feed gas can contain various trace constituents which could affect performance. The coal can contain various amounts of sulfur, chloride, and nitrogen. These components will mostly be converted to H_2S, HCl, NO_x, and NH_3 (the NH_3

can be scrubbed or condensesd out of the gas), and they are therefore potential catalyst poisons. In addition to these inorganic compounds, various hydrocarbon compounds are formed in the gasifier. Most of the heavier substances can be separated; however, the C_2 and C_3 hydrocarbons are expected in the methanator feed gas.

Two other components, methanol and benzene, were included in this study. Methanol is important in processes using Rectisol systems for CO_2 removal prior to methanation. Benzene was considered in order to determine the effect of aromatics on catalyst activity and potential carbon formation.

Table IX lists the substances included in this study. The general conditions are given in Table X. Each impurity was added separately to the gas mixture and passed over C150-1-03 in order to determine its effect on catalyst activity. These tests were run under the primary methanation conditions, but in a small 3/8-in. tube reactor on sized, 10 × 12 mesh, catalyst.

Sulfur. In Test 1, H_2S was added at 2–3 ppm to the dry feed gas. The effect of H_2S on catalyst activity is summarized in Table XI.

Tests 2 and 3 were run in the same reactor as Test 1. In order to confirm the initial activity, the catalyst was started up without added sulfur. The catalyst picked up sulfur in both these tests and was deactivated even though no sulfur was added to the feed; this indicates that sulfur remained in the reactor after Test 1. This is a common problem encountered when working with sulfur in laboratory test reactors. The sulfur reacts with the steel walls of the reactor. Then, even though sulfur is removed from the feed, sulfur evolves from the walls of the reactor and it is either picked up by the catalyst or it appears in the effluent from the reactor. With continuous addition of sulfur, the CO leakage continues to increase.

In Test 1 (3 ppm sulfur in the feed gas), the catalyst showed continuous deactivation; it did not maintain some intermediate level of

Table VII. Conditions for Study of Steam-to-Gas Ratio

Catalyst Loading		*Gas Composition*		*Test Conditions*	
Type	C150-1-03 C150-4-03	CO, %	5.0	temperature, °C	260–454
Volume, cm^3	10.0	CO_2, %	4.0	pressure, psig	20,000
Size, in.	3/16 × 3/32	H_2, %	23.0	space velocity, vol/vol hr	20,000
Bed, L/D	1.46	CH_4, %	68.0	superficial linear velocity, ft/sec	0.078
S/G	0.15–0.40				

Table VIII. Effect of

Catalyst[a]	Time on Stream, hrs	Inlet S/G	Temperature, °C Inlet	Hot Spot	Outlet
C150-1-03	33	.365	259	364	270
	79	.368	259	360	270
	93	.308	260	336	268
	35	.15	261	407	267
	40	.15	261	412	267
	51	.182	261	373	267
	58	.02	260	440	270
	61	.02	260	429	269
	65	.02	260	431	268
C150-4-03	33	.365	259	356	268
	79	.368	259	352	270
	93	.308	259	336	267
	35	.15	260	388	266
	40	.15	259	398	268
	51	.182	260	360	267

Catalyst	Time on Stream, hrs	Inlet S/G	Kw *CO*	Kw CO_2
C150-1-03	40	.15	37,173	29,734
	51	.18	49,564	39,645
	65	.02	45,434	36,342
	79	.37	37,173	29,734
C150-4-03	40	.15	49,564	39,645
	51	.18	—	—
	65	.02	49,564	39,645
	79	.37	54,520	43,610

[a] C150-1-03: 50% nickel on alumina; and C150-4-03: 60% nickel on alumina.

Table IX. Trace Impurities Studied

Substance	Comment
H_2S	RSH and COS were not included since they are expected to hydrogenate to H_2S over the nickel catalyst.
HCl	
NO*x*	NH_3 was not included since it can be separated by condensation or scrubbing.
CH_3OH	MeOH is included because of use of the Rectisol system is expected.
C_2, C_3	Ethane, ethylene, propane, and propylene are the light hydrocarbons expected in the process gas.
Benzene	Benzene was included in order to study the effect of aromatics on the catalyst in the event of catalytic sulfur removal rather than use of the Rectisol system.

Steam-to-Gas Ratio

Inlet Gas, %			*Outlet Gas, %*			*Equilibrium Gas, %*		
CO	CO_2	H_2	*CO*	CO_2	H_2	*CO*	CO_2	H_2
4.34	4.13	20.14	.247	5.26	6.45	.007	3.54	2.73
3.42	6.25	14.60	.183	6.34	4.81	.016	6.50	2.46
3.12	1.54	14.30	.165	3.01	4.97	.001	.933	2.35
7.31	4.52	16.90	.459	8.75	2.80	.022	7.21	1.52
7.31	4.52	16.90	.503	8.50	2.24	.022	7.21	1.52
4.28	4.26	14.70	.255	6.10	2.34	.020	4.86	2.10
4.18	5.52	17.70	.167	4.31	1.69	.080	5.44	1.83
4.18	5.52	17.70	.159	4.43	1.69	.037	5.36	1.25
4.18	5.52	17.70	.170	4.51	1.82	.061	5.41	1.60
4.34	4.13	20.14	.223	4.53	4.68	.007	3.54	2.73
3.42	6.25	14.60	.114	6.10	3.64	.016	6.50	2.46
3.12	1.54	14.30	.124	2.70	3.36	.001	.933	2.35
7.31	4.52	16.90	.138	8.77	2.69	.022	7.21	1.52
7.31	4.52	16.90	.228	8.50	2.27	.022	7.21	1.52
4.28	4.26	14.70	.139	6.00	1.65	.020	4.86	2.10

Kw *Shift*	Kw *CO*	
	Average	*Corrected to 1/4 × 1/4 in. Tablets*
0		
0		
0	42,336	23,814
13,011		
0		
—	51,216	28,809
—		
13,630		

Table X. General Conditions for Study of Trace Impurities

Catalyst Loading		*Gas Composition*		*Test Conditions*	
Type	C150-1-03	CO, %	5–7	temperature, °C	315
Volume, cm^3	10.0	CO_2, %	4–6	pressure, psig	350
Size, mesh	10 × 12	H_2, %	20–25	space velocity, vol/vol hr	10,000
		CH_4, %	62–71	S/G	.35

Table XI. Effect of Sulfur Poisoning

Test	Initial CO Conv., %	Initial Kw CO Meth.	Final CO Conv., %	Final Kw CO Meth.	S Added to Catalyst, %	S in Feed, ppm	Calcd. Inlet Sulfur, ppm	Time on Stream, hrs
1	99.8	81,500	6.4	1000	0.295	2–3	3.1	54
2	98.6	65,500	85.5	25,500	0.274	0	0.93	139
3	98.2	65,000	84.3	25,000	0.125	0	0.26	240

activity. For Tests 2 and 3, inlet sulfur concentration was calculated on the basis of the amount of sulfur found on the catalyst and the time on stream. With 0.13–0.30% sulfur on the catalyst, 60–90% of the activity was lost. Although Tests 2 and 3 were never conducted as originally planned (*i.e.* feeding 1 ppm sulfur in the feed gas), it was felt that the results of Tests 2 and 3 prove satisfactorily the severe poisoning effect of sulfur on C150-1-03. RSH and COS were not studied as sources of sulfur because, under the conditions of the test, they are expected to hydrolyze or hydrogenate to H_2S and poison the catalyst the same as H_2S.

Chloride. C150-1-03 was tested under primary wet gas conditions to determine the effect of chloride on catalyst performance. Chloride

Table XII. Chloride Poisoning Test

Days	Conditions	Findings
1–5	no chloride added	conversion of CO was steady 99.1% with constant hot spot locations 31% into the bed.
6–21	0.52 ppm Cl added on dry gas basis	apparent slight decrease in conversion (avg. = 98.7%); hot spot moved down into bed to 69% level.
22–29	2–4 ppm Cl added on dry gas basis.	overall average conversion was 98.5% during this period; hot spot remained at the 69% level.
30–33	all chlorides removed from feed	conversion did not change when chlorides were removed (98.6%); hot spot also remained unchanged.
34–47	11–14 ppm Cl added on dry gas basis	conversion decreased steadily during this period of high chloride levels to only 84.0% on the 47th day; hot spot moved down into the bed to the 94% level. on the 37th day, the unit had to be shut down to repair a leak on the inlet to the reactor; the catalyst was kept under CO_2 during this period.
48–51	all chlorides removed from feed again	conversion continued to decrease and was 75.8% on the 51st day when the test was stopped. The hot spot remained at the 94% level, nearly the very bottom of the bed.

was expected to be very detrimental to catalyst activity, but the manner of deactivation was uncertain. The chloride was added to the system as hydrogen chloride in the feed water, up to 14 ppm on a dry gas basis. The test was conducted in a single reactor unit with an electric furnace heater. The feed water served as the source of steam and chloride.

Table XII provides a synopsis of the findings. Figure 2 depicts the change in hot spot location caused by increased chloride levels. Analysis

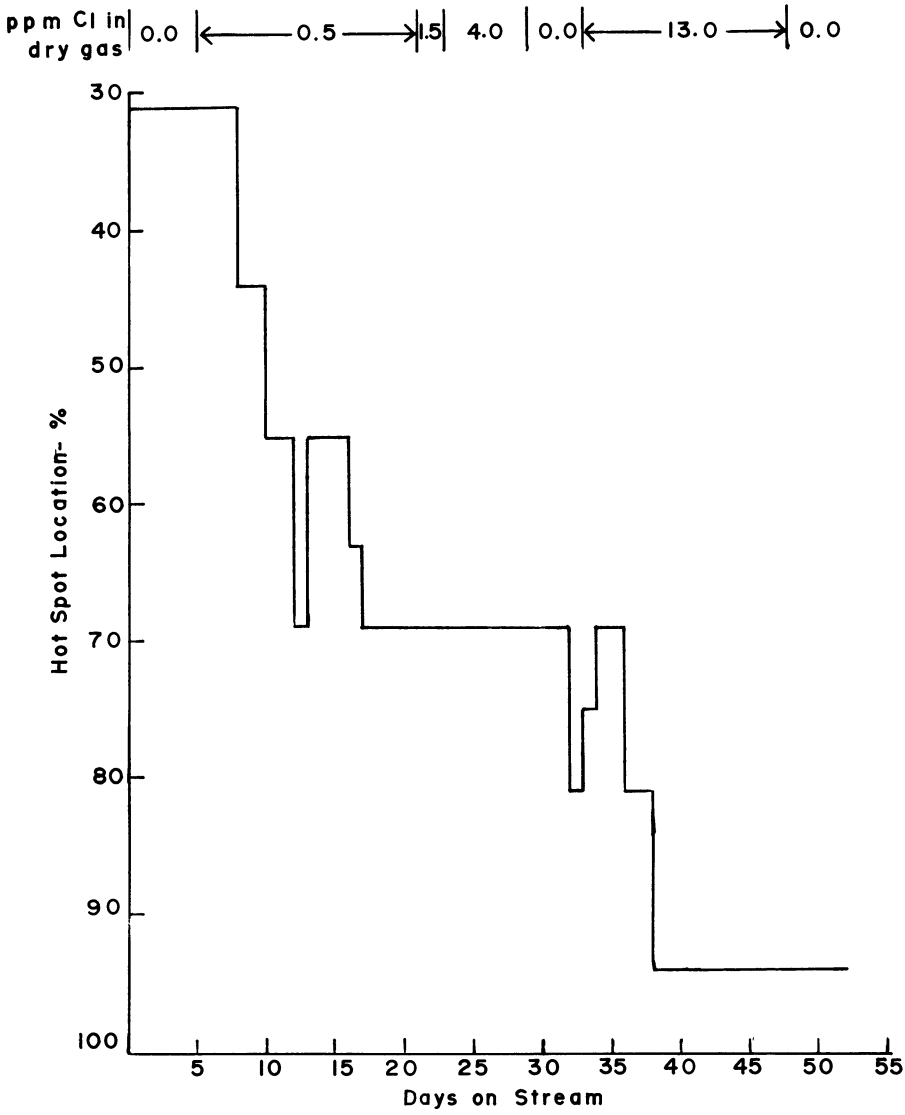

Figure 2. Study of chloride poisoning: hot spot location vs. *time on stream*

of the discharged catalyst is presented in Table XIII. New catalyst analyzed at less than 0.01% chloride.

The chloride level was raised to above 5 ppm in the feed gas because the hot spot had moved down to the 69% level and remained there. Note that percent conversion changed significantly only when the hot spot reached the bottom of the bed. When the chloride was removed, neither hot spot location nor percent conversion improved.

Hydrogen chloride is a permanent irreversible poison to the methanation activity of C150-1-03 even though most of it is not picked up by the catalyst but is observed in the effluent gas. Only 0.02–0.04% was found on the discharged catalyst, but any amount of chloride in the feed gas is detrimental to catalyst activity.

Table XIII. Analysis of Discharged Catalyst

	Chloride, wt %	
Catalyst	*Wet Method*	*XRF Method*[a]
Top one-third	0.051	0.04
Middle one-third	0.039	0.02
Bottom one-third	0.039	<0.01
Average	0.043	0.023

[a] XRF: x-ray fluorescence.

Nitrogen Dioxide. Nitrogen dioxide can be formed in the gasifier from the nitrogen present in the coal. Since NO_2 is an acid gas, it was included in the study as a potential poison. This study was conducted with C150-1-03 in the electric furnace reactor unit. The catalyst was tested under primary wet gas conditions with up to 8 ppm NO_2 in the dry feed gas. Table XIV provides a synopsis of the test results.

NO_2 at concentrations up to 8 ppm(v) in the inlet gas did not poison the C150-1-03 catalyst. The location of the hot spot fluctuated between the 31 and 44% levels. The hot spot did not drop sharply down into the catalyst bed as it had during the poisoning studies with H_2S and HCl.

Alkanes and Alkenes. For this study, C150-1-01 and C150-1-03 were tested under primary wet gas conditions with ethylene, ethane, propylene, and propane being added to the feed gas. This study was made in order to determine whether these hydrocarbons would deposit carbon on the catalyst, would reform, or would pass through without reaction. The test was conducted using the dual-reactor heat sink unit with a water pump and vaporizer as the source of steam. All gas analyses were performed by gas chromatography. The test was stopped with the poisons still in the feed gas in order to preserve any carbon buildup which may have occurred on the catalysts.

Table XIV. Effect of NO_2 on Catalyst Activity

Days	*Conditions*[a]	*Findings*
1–8	no NO_2 added	average 99.1% conversion of CO with hot spot located 31–44% into bed
9–13	1–2 ppm(v) NO_2 added	average 99.1% conversion with hot spot located at steady 31%; no change
14–28	2–7 ppm(v) NO_2 added	average 99.2% conversion with hot spot located 31–44% into bed

[a] ppm (v): parts per million by volume.

The gas analyses (Table XV) demonstrated that the catalysts were not visibly affected by these alkanes or alkenes. The CO and H_2 leakages remained low throughout the test, rising slightly after hour 181 when the jacket temperature was raised. The disappearance of the ethane, ethylene, propane, and propylene is attributed to reforming reactions even though a continuous trace ethane leakage was observed. Reforming of such small amounts of hydrocarbons would not cause a discernible difference in the gas analyses. There was no downward movement of the hot spot during the test, and carbon deposition did not occur. These observations support our conclusion that ethylene, ethane, propylene, and propane undergo reaction over the catalyst but do not poison it.

Methanol. In another series of tests, the effect of methanol—which can be carried over from the Rectisol scrubber system—on catalyst activity was determined by adding methanol to the water before vaporizing into the unit. The methanol was added to give 0.01–1.0% on a dry gas basis. Up to 1000 ppm, methanol had no effect on activity as evidenced by no change in the H_2 and CO leakages. When methanol was increased to 1%, the temperature profile moved down through the bed but with no noticeable effect on H_2 and CO leakage. When methanol was removed, the hot spot returned to its original location in the catalyst bed. The effluent H_2O contained no methanol during the test; therefore the methanol reformed to methane.

Benzene. Benzene is ordinarily scrubbed out by a Rectisol system before the methanators. However, if a different H_2S removal system were used, benzene could pass through the system and then hydrogenate, plug up the catalyst pores, or reform. Benzene was therefore included in this poison study.

C150-1-03 and C150-4-03 catalysts were loaded into the small dual-tube reactor. The unit was equipped with inlet saturators which served as the source of benzene. Poison levels of 0–5% were tested. The findings

Table XV. Effect of Light

Time on Stream, hrs	Outlet S/G	Temperature, °C Top	Hot Spot	Bottom	Catalyst Bed above Hot Spot, %	Inlet Gas Composition, % CO	CO_2	H_2	CH_4
C150-1-01 Catalyst[a]									
15	.531	369	369	308	11.5	5.07	5.13	26.73	63.07
23	.538	399	399	309	11.5	5.17	5.43	28.71	60.69
73	.536	372	372	311	11.5	4.27	4.77	24.38	67.37
95	.538	388	388	311	11.5	4.92	4.23	24.57	69.67
111	.537	446	446	326	11.5	4.73	6.68	24.90	64.17
161	.530	441	441	357	11.5	4.05	6.77	24.55	69.75
C150-1-03 Catalyst[a]									
6	.507	387	401	312	0.0	5.07	5.13	26.73	63.07
23	.484	404	404	316	6.9	5.17	5.43	28.71	60.69
41	.505	406	406	316	6.9	5.06	5.19	25.28	69.01
66	.485	368	383	318	20.7	4.91	4.16	21.95	71.80
95	.483	362	383	320	20.7	4.92	4.23	24.57	69.67
111	.505	419	434	340	20.7	4.73	6.68	24.90	64.17
131	.500	426	426	360	6.9	4.91	10.99	26.31	64.35
161	.497	421	430	364	20.7	4.05	6.77	24.55	69.75

Catalyst	C, % Discharged	C, % New	S, % Discharged	S, % New	Reduction, %
C150-1-01	3.08	2.58	.048	.06	62.0
C150-1-03	6.14	5.84	.066	.09	76.3

(Table XVI) demonstrate that at low levels benzene had no noticeable effect on activity; the benzene was reforming to methane, carbon oxides, and hydrogen. At higher levels, $> 5\%$, catalyst activity declined which was demonstrated by the hot spot's moving down the catalyst bed and by the increase in CO and H_2 leakage. In addition, benzene and cyclohexane were observed in the effluent. At very high benzene levels, carbon formation was observed over the C150-1-03 catalyst.

Although benzene is not a poison such as H_2S and HCl, it does depress activity by reforming and adsorption onto the catalyst. At high levels it can produce carbon.

Discussion of Kinetic System

In various fields of commercial catalyst practice, it has been customary for more than 30 years (*1*) to use a very simple first order, or psuedo first order, equation in preliminary converter design where very great changes in conditions are not made. This equation, for constituent X, may be written as

$$Kw = SVW \log_{10} \left(\frac{X_{in} - X_{eq}}{X_{out} - X_{eq}} \right)$$

$$= SVW \log_{10} A \qquad (1)$$

Hydrocarbons on Catalyst Activity

Inlet Gas Composition, %				*Outlet Gas Composition, %*							
C_2H_4	C_2H_6	C_3H_6	C_3H_8	CO	CO_2	H_2	CH_4	C_2H_4	C_2H_6	C_3H_6	C_3H_8
—	—	—	—	<.01	4.70	3.46	91.84	—	—	—	—
—	—	—	—	.0125	4.76	3.15	92.09	—	—	—	—
.154	.060	.186	.473	<.01	4.31	2.99	88.06	<.01	.066	<.01	.0081
.235	.061	.276	.548	<.01	4.04	2.81	94.86	<.01	.072	<.01	.0041
.326	.051	.338	.475	.005	7.21	2.81	90.62	<.01	<.01	<.01	<.01
.333	.059	.481	.556	<.01	6.32	3.66	85.49	<.01	.0101	<.01	<.01
—	—	—	—	.0025	4.50	2.45	93.05	—	—	—	—
—	—	—	—	.008	4.56	2.67	92.77	—	—	—	—
.447	.088	.491	.162	<.01	5.17	2.21	104.6	<.01	.0095	<.01	<.01
.443	.093	.608	.669	<.01	5.01	2.36	88.35	<.01	.014	<.01	.0019
.235	.061	.276	.548	<.01	4.20	2.79	95.48	<.01	.021	<.01	.0007
.326	.051	.338	.475	.005	7.24	2.05	91.03	<.01	<.01	<.01	<.01
.353	.045	.321	.547	.0373	11.7	2.71	86.32	<.01	.0018	<.01	<.01
.333	.059	.481	.556	<.01	6.29	3.20	99.42	<.01	.0039	<.01	<.01

[a] Discharged catalyst properties.

where Kw is a rate constant at a specific pressure and temperature, and SVW is total wet gas space velocity expressed as standard cubic feet of total gas per hour and cubic foot of bulk catalyst. X is given in pound moles per hour, and X_{in} refers to the amount of constituent entering the section of catalyst for which the space velocity is measured, X_{out} is the amount leaving the section, and X_{eq} is the amount which would pass through the section under equilibrium conditions. For reactions with large heats, it is necessary to divide the catalyst bed into a number of sections so that each section is essentially isothermal.

Equation 1 has as its basis the concept that diffusion, either through pores or to the gross surface of the catalyst particle, controls the reaction rate. When the control is strictly by the gas film surrounding the catalyst, one would have to convert Equation 1 to

$$Kw^* \sqrt{L} = SVW \log_{10}A \quad (2)$$

where L is the catalyst bed depth in feet. This is necessary because the controlling film thickness is reduced as gas velocities are increased. In general, Equation 1 is satisfactory for commercial reactors. Equation 1 is the specific solution of

Table XVI. Effect of Benzene

Catalyst	Time on Stream, hrs	Catalyst Bed above Hot Spot, %	Inlet Gas Composition, % CO	CO_2	H_2	C_6H_6
C150-1-03	32	0.0	5.91	5.90	23.11	—
	58	16.7	5.57	5.76	23.36	0.161
	123	33.3	3.81	6.34	23.73	0.410
	251	33.3	4.31	4.63	26.24	1.86
	304	100.0	4.47	7.26	25.79	3.64
	335	50.0	3.55	4.98	21.75	—
C150-4-03	32	0.0	5.91	5.90	23.11	—
	51	16.7	5.98	5.59	24.53	0.102
	84	33.3	3.81	5.65	23.02	1.09
	89	41.7	3.81	5.65	23.02	0.361
	145	50.0	3.44	5.06	24.5	0.404
	251	66.7	4.31	4.63	26.24	1.19
	304	83.3	4.47	7.26	25.79	5.53
	335	66.7	3.55	4.98	21.75	—

$$-\frac{dX}{dV} = 6.07 \times 10^{-3}\, Kw \left(\frac{\mathrm{X}}{\text{gas flow}} - \frac{\mathrm{X}_{eq}}{\text{gas flow}_{eq}}\right) \tag{3}$$

This may also be written as:

$$-\frac{dX}{dv} = 6.07 \times 10^{-3}\, Kw\, (N_{\mathrm{X}} - N_{\mathrm{X}_{eq}}) \tag{4}$$

This refers to the total gas flow through a plane of catalyst where N_x is the mole fraction of X in the gas passing through the plane, $N_{x_{eq}}$ is the mole fraction of X at equilibrium under conditions at this point in the catalyst bed, and dv is the incremental catalyst volume.

Another equation which is helpful for computer use is:

$$\mathrm{X}_{in} - \mathrm{X}_{out} = \left(1 - 10^{\frac{-Kw}{SVW}}\right)(\mathrm{X}_{in} - \mathrm{X}_{eq}) \tag{5}$$

When there is no volume change in the reaction, Equations 1 and 5 may be readily derived from Equation 3 or Equation 4.

The solution of Equation 3 is complicated when there is a volume change in the reaction which removes constituent X. For these reactions, Equation 3 may be used with dX replaced by ΔX and dV by ΔV. The solution can be made as accurate as desired if the increments are sufficiently small.

on Catalyst Activity

Outlet Gas Composition, %				
CO	CO_2	H_2	C_6H_6	C_6H_{12}
.0025	5.45	2.13	—	—
.0025	6.99	2.61	—	—
.0025	6.32	3.58	0.053	—
.01	5.31	7.38	1.281	.04589
.01	6.83	18.93	5.74	.29693
.01	5.69	12.50	—	—
.0025	5.49	1.96	—	—
.0025	5.82	2.71	0.095	.00037
.0025	5.82	3.05	0.297	—
.005	6.56	3.22	0.720	.00015
.005	5.77	4.57	0.139	—
.01	5.18	9.06	1.018	.00279
.02	6.02	11.13	7.211	.1443
.01	5.18	9.35	—	—

Equation 5 can be used as is, but a more accurate solution is given by:

$$X_{in} - X_{out} = \left(1 - 10^{\frac{-Kw}{SVW}}\right)\left(X_{in} - X_{eq} \times \frac{\text{flow}}{\text{flow}_{eq}}\right) \quad (6)$$

Equation 6 was used to correlate the data of this paper; however, a more accurate approximation solution of Equation 3 is given by:

$$X_{in} - X_{out} = \left(1 - 10^{\frac{-Kw\ \text{flow}^*}{SVW\ \text{flow}_{eq}}}\right)(X_{in} - X_{eq}) \quad (7)$$

where flow* is the volume of gas which would pass if 100% of constituent X were reacted.

Finally, a fairly complicated exact solution of Equation 3 may be derived. It must be noted, however, that Equation 3 itself cannot be strictly accurate since the diffusion of only a single constituent has been considered.

In the application of Equation 3 to the methanation of CO by the reaction $CO + 3H_2 \rightleftharpoons CH_4 + H_2O$, starting with a mixture of *e.g.* 90% CO and 10% H_2 and using CO as X would lead to the erroneous conclusion that methanation is impossible under these conditions. The requirement is that Equation 3, operating on one constituent, can only be accurate (even when diffusion is strictly controlling) if X is present at a low concentration. To solve the 90% CO–10% H_2 case previously men-

tioned, it would be necessary to consider the diffusion of constituents other than CO.

In view of the above as well as the fact that all the various approximate solutions of Equation 3 give about the same answer when the reactant concentration is low, it did not seem worthwhile to seek better accuracy in the solution of Equation 3.

Equation 7, however, is of interest when one compares various kinetic equations. It may be rewritten as:

$$X_{in} - X_{out} = \left(1 - 10^{\frac{-Kw \times Q}{SVW}}\right)(X_{in} - X_{eq}) \tag{8}$$

Thus, Equation 7 is a special case of Equation 8 where

$$Q = \text{flow}^*/\text{flow}_{eq} \tag{9}$$

In computer operations with other kinetic systems, Equation 8 may be used, and all the unique features of the kinetic system may be incorporated into the value of Q which may of course be a very complex expression. This technique is of interest only in that it simplifies the work necessary to analyze data using any specific kinetics for a chemical reaction. The technique requires sectioning the catalyst bed; in most cases with normal space velocities, 50–100 sections which require 2–3 min of time on a small computer, appear to be sufficient even when very complex equations are used.

Kw in the foregoing equations is a function of pressure and temperature. Although the effect of pressure and temperature on strictly diffusion-controlled processes is small, the effect of these variables on surface reactions is generally quite large. Thus, although diffusion may be the major contributor to the mathematical form of the kinetic equations, a residuum of influence from the basic process taking place at the end of the catalyst pores will also affect the rate constant. The usual balance achieved with respect to pressure is a rate that increases with the square root of the total pressure. Since essentially all of the experimental work in this project was at essentially the same pressure, this study gives no information on the pressure dependence of rate. It should be noted, however, that the form of several proposed kinetic equations (*2*, *3*) would give this type of pressure–rate relationship. Data are available from commercial ammonia plant methanators and from laboratory studies relative to them which demonstrate this type of pressure dependence.

For this reason, a square root of pressure term was introduced into the equation for *Kw*. Further experimental work would be desirable if pressures greatly different from 25 atm were to be used.

The effect of temperature on *Kw* was introduced through an activation energy term. This follows the normal form for this type of reaction, with a very high activation energy below the threshold temperature and a lower value at higher temperatures that tends to diminish with increasing dependence of reaction rate on diffusion as the temperature is raised. Activation energies for rate data derived from experiments (*4–10*) on the hydrogenation of CO and CO_2 at low pressures and low temperatures using small catalyst particles 0.01–0.03 in. in diameter are generally 15,000–30,000 cal/g mole. On the other hand, for work at higher pressures and temperatures with commercial size catalyst (1/8–1/4 in. in diameter), values of 0–10,000 cal/g mole are obtained (*2, 3, 7, 8, 10, 11*).

In the early phases of this study, temperature surveys were run on various catalysts in order to determine the threshold temperature for CO methanation. The data in Table XVII, calculated for 0.25-in. C150-1-02 catalyst, are rather typical.

Table XVII. Threshold Temperature for CO Methanation

Average Temperature, °C	Kw	*Activation Energy, cal/g mole*[a]
160	170	—
183	710	24,000
198	6020	61,000
213	11850	21,000
276	24300	6,100

[a] Calculated from previous temperature value.

In general, since these tests were made on unaged catalyst, a *Kw* value below several thousand indicates that the catalyst is not practical for commercial use. Therefore, from a utilitarian standpoint, these data indicate a threshold temperature slightly below 200°C. Because of the small amount of reaction at the lower temperatures as well as the effect of small temperature errors on the calculation of the activation energy, the values at the three lowest temperatures are not very consistent; however, the average value of 35,000 cal/g mole is not in bad agreement with the findings of other investigators. The value of 6100 cal/g mole is typical for the diffusion control region.

The laboratory data on C150-1-01 and C150-1-02 catalysts for CO hydrogenation reveal that there is essentially no change in the *Kw* value between 260°, 315°, and 371°C. This would suggest an activation energy of zero. Although these data show a small, essentially zero, temperature dependence from 260°–370°C (*11*), the difficulties in unraveling the relationship between the rates of CO and CO_2 methanation, and the water–gas shift reaction ($CO + H_2O \rightleftharpoons CO_2 + H_2$) prevent one from

Table XVIII. Ratio of Activities of C150-1-01 and Other Commercial Catalyst

Ref.	Reactant	Literature Equation	Activity Ratio of C150-1-01/Other Catalyst: Literature Equation[a]	Activity Ratio of C150-1-01/Other Catalyst: Equation 5[a]
13	CO	$r = \frac{p_{CO}p_{H_2}^3}{(A+Bp_{CO}+Dp_{CO_2}^4+Ep_{CH_4})}$	9000	5.8
11	CO	$r = \frac{1.1p_{CO}p_{H_2}^{1/2}}{1+1.5H_2}$	1.2	2.3
14	CO	$r = \frac{Kp_{CO}p_{H_2}^{1/2}}{1+K_2p_{H_2}+K_3p_{CH_4}}$	2.3	2.6
15,16	CO_2	$r = \frac{C_1p_{CO_2}pH_2^4}{(p_{H_2}^{1/2}+Cp_{CO_2}+C_3)}$	2.2	3.9
17,18	CO_2	$r = \frac{Kp_{CO_2H_2}^4}{(1+K_1p_{H_2}+K_2p_{CO_2})^5}$	6.2	13.1

[a] Equation used to derive activities.

deriving a good value for the activation energy for any one reaction. Because of these tests as well as various reported studies (*2, 3, 7, 8, 10, 11*), an activation energy value of 5000 cal/g mole was used below 371°C whereas 2000 cal/g mole was used above 371°C. One must bear in mind that below the threshold temperature any predicted performance would be virtually meaningless. It may be noted that a kinetic equation which in practice is very close to the simple *Kw* expression (*2, 3*) uses 6900 cal/g mole for the activation energy over the entire temperature range (274°–482°C).

Finally, one must know the effect of catalyst particle size on *Kw*. For a pore diffusion-controlled reaction, activity should be inversely proportional to catalyst particle diameter, that is directly proportional to external catalyst surface area.

Several studies (*9, 10, 12*) show that above 204°C pore diffusion will control catalyst activity if the particle diameter is > 0.02–0.03 in. This is far smaller than the particle diameter of any practical commercial catalyst.

In this investigation (Table VIII), it was found that *Kw* values for CO hydrogenation depend on the 0.9 power of the reciprocal of particle diameter. In view of this and the literature, a linear (first power) dependence on the reciprocal of particle diameter was used in the *Kw* expression. Accuracy of measurement is certainly insufficient to distinguish between a 0.9 and a 1.0 power dependence.

The use of Equation 3 was applicable at 274°–482°C at pressures of 20–40 atm, and it is assumed it would be applicable over the range of 1 to 70 or 80 atm. The equation is not valid if the feed contains H_2S or HCl since these are permanent irreversible poisons.

Characteristic of most equations for surface-controlled kinetics, as opposed to diffusion-controlled kinetics, are a number of partial pressure terms, often to high powers. When large changes in partial pressures are made, differences between the observed and the calculated reaction can easily equal a factor of 1000 or more. When diffusion-type kinetics are used, one seldom finds differences exceeding a factor of two or three. While this may not seem very accurate, comparison of the two methods is rather startling.

The activities of two catalysts, C150-1-01 and another commercial catalyst, were compared (Table XVIII). Catalyst activity was determined (a) from the literature data using their kinetics, and (b) by Equation 5. Then the same procedure was followed for the C150-1-01 catalyst using typical data. The activity ratios are presented in Table XVIII.

It is evident that the equation for Ref. *13* has broken down completely for CO hydrogenation. The other equations (*11*, *14*) for CO hydrogenation gave correlations similar to those obtained by the simple kinetics. These equations are all, however, of relatively simple form. They use low activation energies and in general show an activity dependence on the square root of the pressure, similar to that of the simple kinetics.

For the CO_2, the literature kinetics gave more reasonable correlation than the simple kinetics though the difference is not great. However, Ref. *15* (*16*) involves methanation of $> 50\%$ CO_2 in H_2 under conditions where Equation 3 would break down, and Ref. *17* (*18*) involves only the initial hydrogenation (less than the first 1 or 2%) of the CO_2 present. Furthermore, there is a possibility that the reverse shift would produce enough CO to poison the CO_2 methanation in these experiments which would make it difficult to obtain agreement between various runs.

A number of measurements made on the methanation of CO_2 may be correlated by using Equation 5 with the same values of ΔH as for the CO hydrogenation. On the basis of diffusion considerations, the value of KwS for CO_2 hydrogenation was taken as 80% of that for CO hydrogenation. Attempts were made to correlate data when both CO and CO_2 were methanated by using simple diffusion for both with the CO_2 rate set at 80% of the CO rate. In order to get good agreement with experimental data, it is necessary to introduce a variable water–gas shift reaction activity.

An examination of some laboratory runs with diluted C150-1-02 catalyst can illustrate this problem. In one run with 304°C at inlet, 314°C at exit, and 97,297 outlet dry gas space velocity, the following results were obtained after minor corrections for analytical errors. Of the CO present (out of an inlet 2.04 mole %), 99.9885% disappeared in reaction while the CO_2 present (from an initial 1.96%) increased by over 30%. Equilibrium carbon oxides for both methanation reactions were essentially zero whereas the equilibrium CO based on the water–gas shift reaction at the exit composition was about one-third the actual CO exit of 0.03 mole %. From these data, activities for the various reactions may be estimated on the basis of various assumptions (*see* Table XIX for the effect of two different assumptions).

Table XIX. Effect of Different Assumptions on *Kw* Values

	Kw	
Reaction	*Assumption 1*	*Assumption 2*
Water–gas shift	350,000	50,000
CO_2 methanation	56,000	0
CO methanation	70,000	150,000

For the first assumption, the value of *Kw* for the shift appears to be too high. It must be this high because it is necessary to make CO_2 appear while both CO_2 and CO are being consumed rapidly by methanation. The data may be tested to see if the indicated rate appears unreasonable from the standpoint of mass transfer to the gross catalyst surface. Regardless of the rate of diffusion in catalyst pores or the surface reaction rate, it is unlikely that the reaction can proceed more rapidly than material can reach the gross pill surface unless the reaction is a homogeneous one that is catalyzed by free radicals strewn from the catalyst into the gas stream.

The following equation has been derived for testing mass transfer limitation to the gross catalyst particle (*19*).

$$Kw = \frac{8100}{D}\sqrt{\frac{L \times SVW}{M \times D \times T}} \tag{10}$$

where $\overline{M}$ is average molecular weight of the gas, T is temperature in °Rankine, D is catalyst particle diameter in inches, and L is bed depth in feet. For this calculation for a diluted bed, SVW and L must be computed as if all the active catalyst were gathered in one place. In this experiment then L is 0.02 feet, SVW is 130,000 (counting the steam present), D is 0.078 in., $\overline{M}$ is about 16, and T is 1048. This leads to a limiting Kw of about 150,000.

Although 150,000 is somewhat of an average value for expected maximum *Kw* and uncertainties in the computations make the minimum *Kw* about 15,000 (below 15,000 no mass transfer to gross surface could be expected to be limiting whereas the maximum possible *Kw* might be over 1,000,000), assumption 2 certainly gives the more reasonable explanation of the data.

Many reports discussed the inhibition of CO_2 methanation by CO (*6, 9, 12, 20, 21, 22, 23*). At 160°C and 300 psig, there is indication that as little as 65 ppm CO would stop CO_2 methanation (*12*). Under atmospheric pressure with 0.015-in. catalyst (*9*), CO poisoning of CO_2 methanation was demonstrated with 200 ppm CO at temperatures as high as 230°C. It is expected that poisoning of CO_2 methanation by CO will be observed at lower CO concentrations when catalyst particle diameters are smaller. This is because the smaller particle will be poisoned throughout whereas the poisoning effect will decrease at some depth in the pores of a larger sized catalyst and some significant methanation of CO_2 will be able to take place. It is noteworthy that the only data obtained in this investigation where poisoning was likely at very low CO concentrations (*e.g.*, Table I) were obtained with very small catalyst particles.

It is concluded that a fully satisfactory system for calculating simultaneous reactions of CO and CO_2 with H_2 and H_2O will require a schedule of the effect of CO on CO_2 methanation as a function of temperature. This effect will probably be different with different particle sizes. From a commercial standpoint, the particle size range may be too small to require much difference in the treatment of the data, but in the laboratory very small particle size may lower the CO methanation rate. A simple kinetics system such as that derived from Equation 3 may be satisfactory for all the reactions. It is unlikely that reliable data will be collected soon for the shift reaction (since it is of a somewhat secondary nature and difficult to study by itself), and therefore a more complicated treatment is not justified.

For CO methanation, one of the simple literature kinetic systems (*2, 3*) should be as reliable or better than the one used in this study. With CO_2 methanation, it is less certain that a simple system is indicated. It is probably of more urgency to elucidate the quantiative effect of CO on CO_2 methanation than to find a complex kinetic expression for the CO_2–H_2 reaction itself.

It is expected that the actual rate of CO methanation will always be high, at least under industrial conditions, whereas the CO_2 methanation rate will vary from about the same as that for CO down to zero, depending on operating pressure, temperature, CO content of the gas, and catalyst particle size. Meanwhile a water–gas shift (or reverse shift) reaction will be occurring at all times at a fairly high rate.

Literature Cited

1. Loupichler, F. G., *Ind. Eng. Chem.* (1938) **30,** 578–586.
2. Lee, A. L., Feldkirchner, X. X., Tajbl, D. G., "Methanation for Coal Hydrogasification," *Amer. Chem. Soc., Div. Fuel Chem., Prepr.* **14** (4) Part 1, 126–142 (City, September, 1970).
3. Lee, A. L., "Methanation for Coal Gasification," Clean Fuel for Coal Symp. (Chicago, September, 1973).
4. Bousquet, J. L., Teichner, S. J., "Methanation of CO by H_2 in Contact with Catalysts Prepared from Ni Hydroaluminate," *Bull. Soc. Chim. Fr.* (1969) 2963–2971; CONOCO Library Transl. **TR 71-15.**
5. Luyten, L., Jungers, J. C., "The Kinetics of the Catalytic Synthesis of CH_4 in Nickel," *Bull. Soc. Chim. Belg.* (1945) **54,** 303–318.
6. Nicoli, J., d'Hont, U., Jungers, J. C., "Methanation of CO_2," *Bull. Soc. Chim. Belg.* (1946 **55,** 160–176.
7. Pour, V., "Hydrogenation of CO_2 on Nickel Catalysts, I. Kinetics," *Coll. Csech. Commun.* (1969) **34,** 45–56.
8. Pour, V., "Hydrogenation of CO_2 on Nickel Catalysts, II. Effectiveness Factor," *Coll. Csech. Commun.* (1969) **34,** 1217–1228.
9. Van Herwijnen, T., Van Doesburg, H., DeJong, W. A., "Kinetics of the Methanation of CO and CO_2 on a Nickel Catalyst," *J. Catalysis* (1973) **28,** 391–402.
10. Vlasenko, V. M., Runson, M. T., Yuzefovich, "Kinetics of CO_2 Hydrogenation on Nickel Catalyst," *Kinet. Katal.* (1961) **2,** 525–528.
11. Pursley, J. A., White, R. R., Sliepcovich, C., "The Rate of Formation of CH_4 from CO and H_2 with a Nickel Catalyst at Elevated Pressures," *Chem. Eng. Prog. Symp. Ser.* (1952) **48** (4), 51–58.
12. Vlasenko, V. M., Yuzefovich, "Hydrogenation of CO and CO_2 over Nickel Catalysts," *Kinet. Katal.* (1965) **6,** 938–941.
13. Akers, W. W., White, R. R., "Kinetics of CH_4 Synthesis," *Chem. Eng. Progr.* (1948) **44** (7), 553–556.
14. Bienstock, D., *et al.*, "Pilot Plant Development of the Hot Gas Recycle Process for the Synthesis of High Btu Gas," U.S. Bur. Mines Rep. Invest. (1961) **5841.**
15. Binder, G. C., White, R. R., "Synthesis of CH_4 from CO_2 and H_2," *Chem. Eng. Progr.* (1950) **46,** 563–574.
16. Binder, G. C., White, R. R., Amer. Documentation Inst., Washington, document **2834.**
17. Dew, J. N., White, R. R., Sliepcevich, C. M., "Hydrogenation of CO_2 on Nickel–Kieselguhr Catalyst," *Ind. Eng. Chem.* (1955) **47,** 140–146.
18. Dew, J. N., Ph.D. Dissertation, University of Michigan, 1953.
19. Wheeler, A. Emmett, "Catalysis," vol. 12, pp. 140–150, Reinhart, New York, 1955.
20. Fisher, F., Pichler, H., *Brennst. Chem.* (1933) **14,** 306–310.
21. Rehmat, A., Randhava, S. S., "Selective Methanation of CO," *Ind. Eng. Chem. Prod. Res. Develop.* (1970) **9** (4).
22. Schuster, F., Panning, G., Buelow, H., *Brennst. Chem.* (1935) **16,** 368.
23. Vlasenko, V. M., Yuzefovich, "Methanation of the Catalytic Hydrogenation of Oxides of Carbon to CH_4," *Usp. Khim.* (1969) **38,** 1622–1647; transl.: *Russ. Chem. Rev.* (1969) **38,** 728–739.

RECEIVED October 4, 1974.

4

Formulation and Operation of Methanation Catalysts

GEORGE W. BRIDGER and COLIN WOODWARD

Research Department, Imperial Chemical Industries Ltd., Agricultural Division, P.O. Box 6, Billingham, Cleveland, TS23 1LE, England

The basic requirements for a satisfactory nickel methanation catalyst are ease of reducibility, activity, and stability. Plant designs usually require that the catalyst be reduced at a temperature no higher than reactor operating temperature. High activity is associated with high nickel surface area, and stability is obtained by maximizing strength and resistance to sintering. During plant operation, it is advantageous in planning shutdowns and catalyst replacements to be able to predict the future useful life of a catalyst charge. By monitoring the temperature profile in the catalyst bed, the depth of unused catalyst remaining after attainment of design exit conditions can be determined graphically. From a study of the history of the catalyst charge, its probable future useful life can then be predicted.

Methanation is the final stage in the purification of synthesis gas in which small concentrations of CO and CO_2 (0.1–0.5%) are removed catalytically by reaction wtih hydrogen:

$$CO + 3H_2 \rightarrow CH_4 + H_2O \quad \Delta H_{573^\circ K} = -51.8 \text{ kcal/mole}$$

$$CO_2 + 4H_2 \rightarrow CH_4 + 2H_2O \quad \Delta H_{573^\circ K} = -41.9 \text{ kcal/mole}$$

The methanation process commonly operates at pressures up to 30 atm, and, with the nickel catalyst which is almost universally used for the process, the inlet temperature is about 300°C (~570°F). Almost complete conversion of the oxides of carbon occurs giving a product synthesis gas containing less than 5 ppm $CO + CO_2$. The temperature rise for the exothermic methanation reactions is typically 35°C (63°F).

Catalyst Formulation

The catalysts used in the process are essentially nickel metal dispersed on a support material consisting of various oxide mixtures such as alumina, silica, lime, magnesia, and compounds such as calcium aluminate cements. When the catalyst is made, the nickel is present as nickel oxide which is reduced in the plant converter with hydrogen, usually the 3:1 H_2:N_2 synthesis gas:

$$NiO + H_2 \rightarrow Ni + H_2O \quad \Delta H_{573°K} = -0.8 \text{ kcal/mole}$$

The heat of reaction is negligible and there is no significant change in temperature in the catalyst bed during reduction. Design limitations in most modern plants require that the catalyst should preferably be reduced at its normal operating temperature, around 300°C (570°F). Once some metallic nickel has been formed, however, methanation begins with the corresponding temperature rise which accelerates reduction of the catalyst further down the reactor. Clearly, the reduction process will continue after the reactor is on-line so that it is common for the activity of the catalyst to continue to increase for some time until an equilibrium state, corresponding to a particular degree of reduction of the nickel, is reached. If engineering considerations permit, the reduction process can be accelerated without detrimental effect upon the catalyst by increasing the temperature to ~350°C (~660°F).

A good methanation catalyst is one which is physically strong, is reducible at 300°C (570°F) and has high activity. In order to provide a long life, it must retain these properties in use. Lives of 3–5 years are commonly obtained from charges of Imperial Chemical Industries, Ltd. (ICI) catalyst 11-3, depending on the temperature of operation and the presence of poisons in the synthesis gas, factors which are discussed below. These properties can be obtained by careful attention to the formulation and manufacture of the catalyst.

Methanation activity is related to the surface area of the nickel metal obtained when the catalyst is reduced. The highest surface area of metal and the highest activity are obtained when the nickel is produced as very small crystallites, usually < 100 A in diameter. One of the functions of the other oxides in the catalyst is to support this fine dispersion of nickel crystallites so that they are available for reaction. The oxides mixed with nickel also retard growth or sintering of the metal to form large crystallites with a lower surface area and lower activity. The nickel can be dispersed among the other oxides in various ways with resultant different degrees of mixing (*e.g.*, by impregnation of a preformed oxide support with a soluble nickel compound or by coprecipitating a nickel compound

together with the other materials such as aluminum or magnesium as hydroxides or carbonates). These materials are worked up by drying, decomposing, etc., and pelleting or extruding precipitated materials to produce the final catalyst.

Intimate mixing of the components can lead to the formation of compounds or of solid solutions of the components which are difficult to reduce at 300°C but which, when reduced, contain well dispersed and well stabilized nickel. Methanation catalysts in practice therefore are compromises which combine optimum reducibility with activity and stability. As an example of compound formation, alumina readily forms with nickel

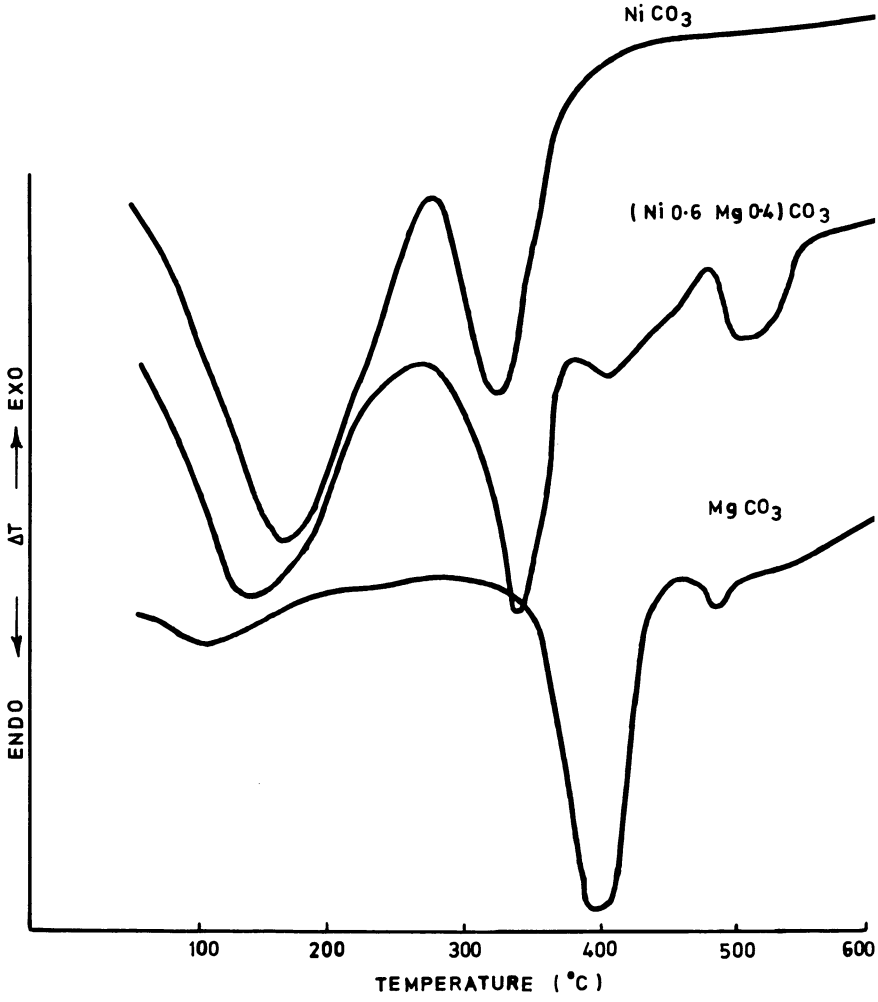

Figure 1. DTA curves of basic carbonates

oxide spinel compounds of the type $NiO \cdot Al_2O_3$. A temperature around 1000°C (1832°F) is necessary for combination when NiO is mixed with α-Al_2O_3, but with finely divided NiO and γ-Al_2O_3 temperatures around 500°C (~930°F) are sufficient. When the oxides are coprecipitated, "spinel precursors" can be detected in the dried precipitate, and such catalysts have to be reduced at temperatures as high as 500°C (~930°F). They are, therefore, unsuitable for use in conventional ammonia synthesis methanation units.

Magnesia forms solid solutions with NiO. Both MgO and NiO have face-centered cubic lattices with NaCl-type structures. The similarity between the ionic radii of the metals (Ni^{2+} = 0.69 A, Mg^{2+} = 0.65 A) allows interchangeability in a crystal lattice, and thus the formation of solid solutions with any proportion of the two oxides is possible. Such solid solutions are more difficult to reduce than NiO alone. Thus Takemura *et al.* (*1*) demonstrated that NiO reduced completely at 230°–400°C (446°–752°F) whereas a 10% NiO–90% MgO solid solu-

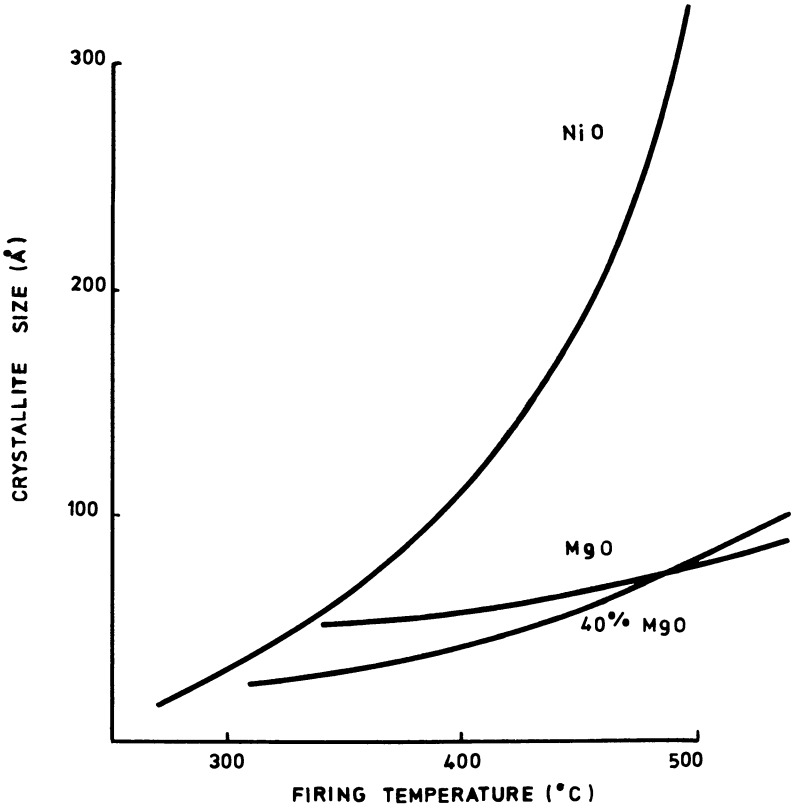

Figure 2. Variation of crystallite size with calcination temperature

tion reduced in two stages, one at 230°–400°C and the other at 500°–600°C (930°–1112°F). For ease and completeness of reduction in a methanation catalyst, therefore, excessive solid solution formation should be avoided. As indicated above, however, solid solution formation is beneficial in retarding crystal growth of NiO during manufacture and of reduced Ni during operation. During manufacture, a precipitated nickel compound such as the carbonate has to be converted into nickel oxide, and, in order to obtain small NiO crystallites, it is desirable that the calcination temperature be the minimum compatible with efficient conversion of $NiCO_3$ to NiO. Differential thermal analysis (DTA) (Figure 1) reveals that this endothermic process occurs in two main stages with maxima around 150°C (302°F) and 340°C (644°F) and that the presence of some magnesia in a solid solution raises the required temperature by only about 15°C (27°F). The presence of MgO, however, does retard the growth of NiO during calcination (*see* Figures 2, 3, and 4). For example, Figure 2 shows that calcination at 500°C (932°F) for 4 hrs increases NiO crystallite size to 300–400 A whereas the crystallite size of an NiO–MgO solid solution (60:40 w:w) would be only about 80 A after the same treatment. Figures 3 and 4 depict the effect of calcination duration on crystal growth at different temperatures. Crystallite size is proportional to $T^{0.25}$ for NiO alone and to $T^{0.12}$ for NiO–MgO and for MgO alone.

Figure 5 depicts the effect of calcination temperature on subsequent catalyst activity after reduction at 300°C (572°F). Activity was measured in laboratory tubular reactors operating at 1 atm with an inlet gas composition of 0.40% CO, 25% N_2, and 74.6% H_2, and an inlet temperature of 300°C. Conversion of CO is measured and catalyst activity is expressed as the activity coefficient k in the first order equation:

$$\text{rate} = k\, p_{CO}\, P^{0.3} \left(1 - \frac{K}{K_p}\right) e - \frac{E}{RT}$$

The reducibility of the catalyst is demonstrated in Figure 6 which shows the activity of catalysts, measured as described above, after reduction to constant activity at temperatures of 280°–350°C (536°–662°F). It will be seen that ICI catalyst 11-3 compares favorably with other catalysts which contain larger amounts of alumina and consequently are more difficult to reduce at acceptable temperatures.

In summary, therefore, we have found it beneficial to include a small amount of MgO (2–3%) in ICI methanation catalyst 11-3. This provides the ideal compromise between ease of reducibility and sintering resistance. By this means, a catalyst is produced which is readily reduced at 300°–350°C (572°–662°F); loss of activity caused by sintering is not a problem

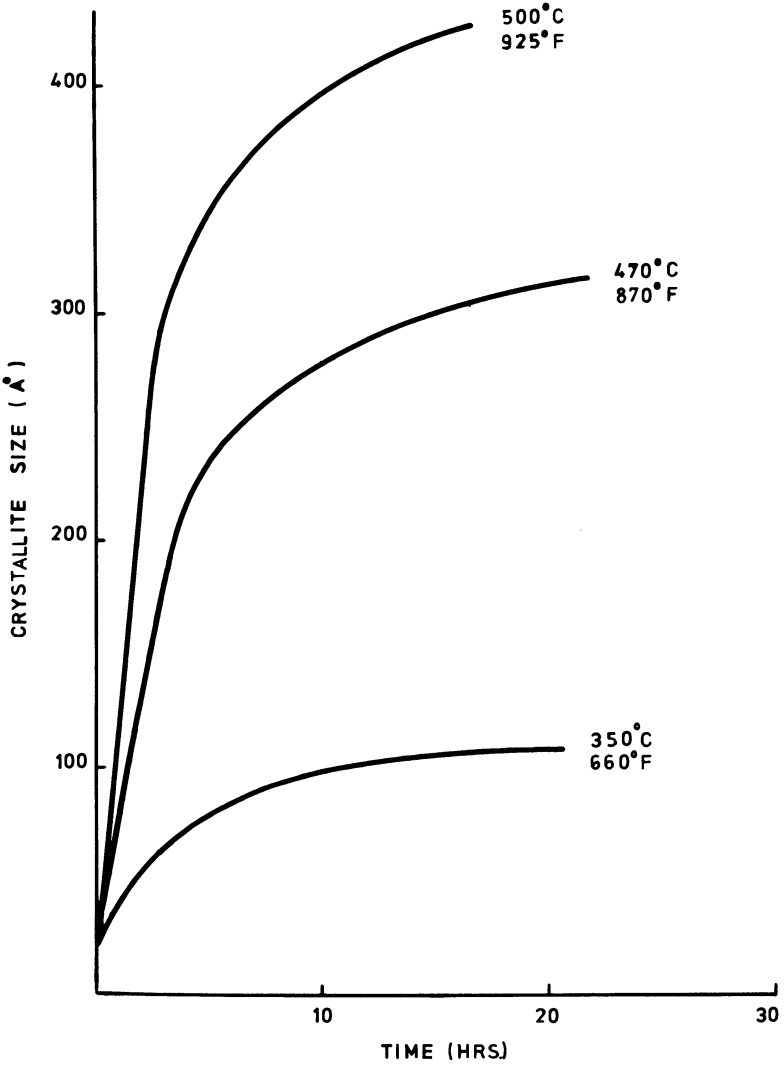

Figure 3. Variation of NiO crystallite size with time

during several years' normal operation at temperatures up to 350°C (660°F). This good performance has been confirmed by experience in many plants including ICI's three 1000 tons/day ammonia plants at Billingham, England.

Poisons

With a well constituted catalyst of this type, sintering is not an important cause of activity loss at normal operating temperatures even if the

catalyst is occasionally overheated. The principal cause of loss of activity is poisoning. Sulfur compounds are virulent poisons for nickel catalysts, but, in the synthesis gas purification stream, the methanation catalyst is protected by the LT (low temperature) shift catalyst in the preceding stage which is an efficient sulfur guard. Therefore in normal operation,

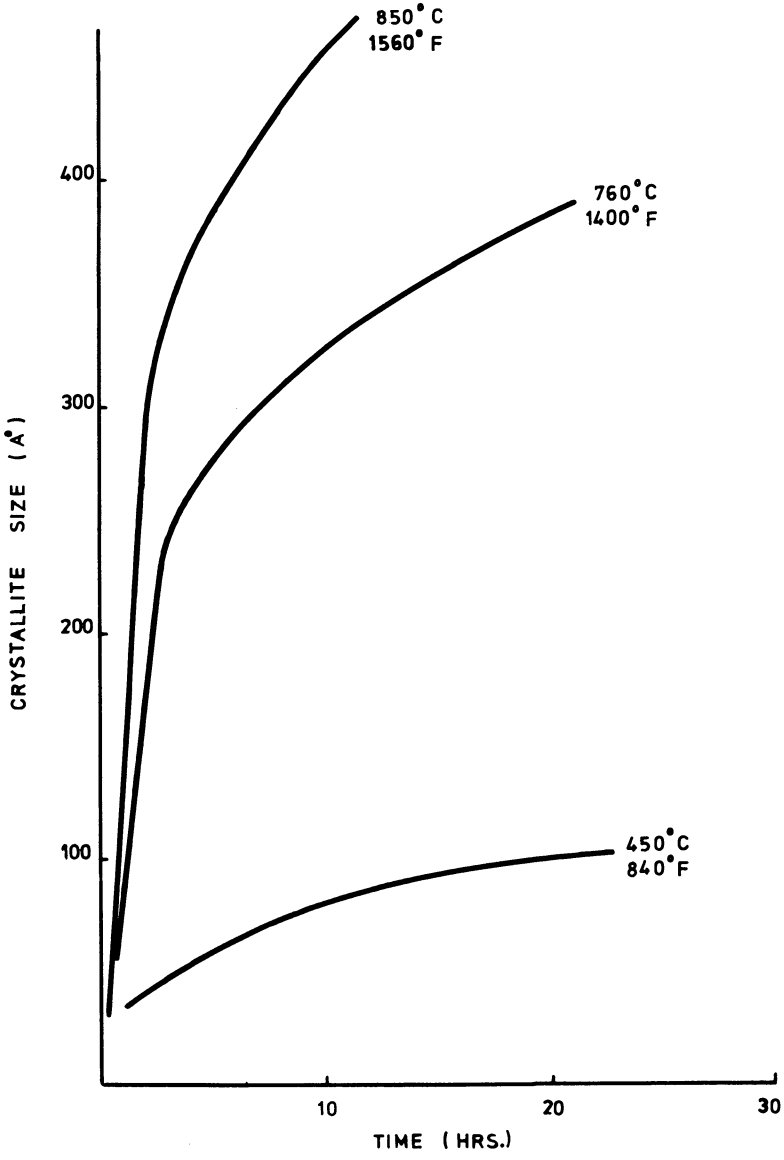

Figure 4. Variation of NiO–40% MgO crystallite size with time

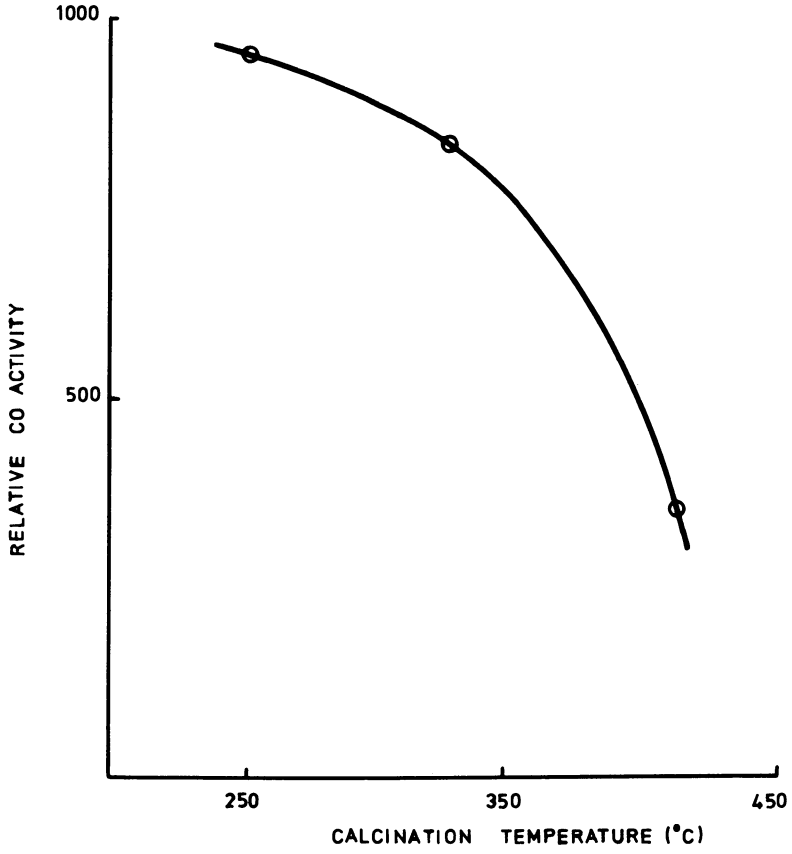

Figure 5. Activity vs. calcination temperature

the methanation catalyst is unlikely to be exposed to sulfur. The exception to this would be if the LT shift converter were partially by-passed, in which instance sulfur could reach the methanation catalyst. Serious deactivation of the catalyst can occur; for example, one catalyst that contained about 30% NiO (before reduction) had significant loss of activity when the sulfur content exceeded ~0.1%.

The poisons most likely to be encountered in an ammonia plant are those originating in the CO_2-removal system which precedes the methanator. Carry-over of a small amount of liquid into the methanator, which is almost inevitable, is not normally serious. Plant malfunction, however, can sometimes result in large quantities of CO_2-removal liquor being pumped over the catalyst, and this can be very deleterious. Table I lists the effects of common CO_2-removal liquors on methanation catalyst activity.

Prediction of Catalyst Life

In the operation of a methanator, it is important to be able to estimate the remaining future useful life of a catalyst charge at any moment. The question to be answered is: Should this catalyst charge be changed during the shutdown planned for x weeks time, or is it good enough to last until the next shutdown planned for a year hence? Strictly, therefore, the requirement is for a yes/no answer rather than a precise prediction, the assumption being that changing a catalyst will never be the sole reason for a shutdown. This is reasonable because, if the cost of plant downtime is compared with the cost of a catalyst charge, it is clearly economical to change catalyst rather than to run the risk of a catalyst failure causing an additional shutdown.

Methanation converters on most ammonia plants are overdesigned, both for safety reasons and as a result of increases in catalyst activity since

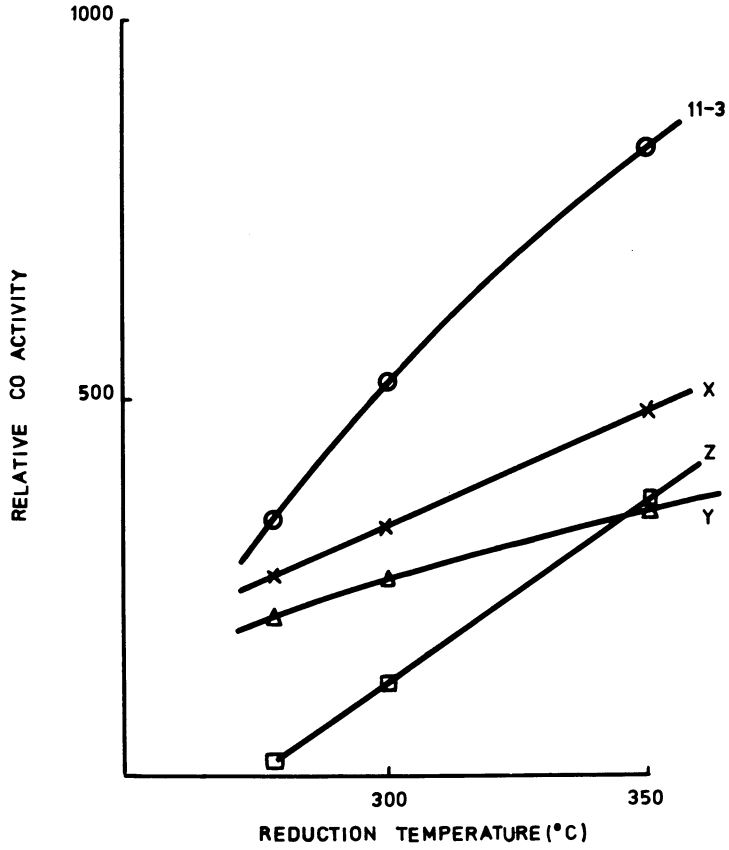

Figure 6. Activity vs. *reduction temperature*

Table I. Poisoning Effects of CO_2-Removal Systems

Process	*Chemicals*	*Effect*
Benfield process	aqueous potassium carbonate	blocking of pores of methanation catalyst by evaporation of potassium carbonate solution
Vetrocoke process	aqueous potassium carbonate–arsenious oxide	as Benfield, also As_2O_3 is poison—about 50% of activity is lost when As = 0.5%
Benfield DEA	aqueous potassium carbonate + 3% diethanolamine	as Benfield, DEA is harmless
Sulphinol	sulpholane, water, di-2-propanolamine	sulpholane will decompose and give sulfur poisoning
MEA, DEA	mono- or di-ethanolamine in aqueous solution	no poisoning effect
Cold Rectisol	methanol	no poisoning effect

plants were built. Consequently, at the beginning of the catalyst's life, most of the methanation is virtually completed in the first 25% of the bed, and monitoring of exit gas composition gives no information about die-off of the catalyst. Catalyst deactivation occurs normally by a poisoning mechanism, and, as poisoning continues, the volume of active catalyst remaining will eventually be insufficient to meet the required duty. Although the thermodynamic exit levels of CO and CO_2 are about 10^{-4} ppm, in practice these are not attained because of kinetic and other limitations and the actual exit concentrations during normal operation are of the order of 1–2 ppm.

A technique has been devised for calculating when exit carbon oxides will exceed any given design level and hence predicting the future useful life of the catalyst charge. The method is based on accurate measurement of the temperature profile in the bed by a movable thermocouple or a series of fixed thermocouples. A point on the profile is selected at which conversion is nearly complete. This point can, for example, be taken as the point at which 5°F (2.8°C) temperature rise remains. The total temperature rise across a methanator is typically 60°F (33°C). The 5°F point provides a good compromise between selecting a point near the top of the temperature rise so that pressures and temperatures can be regarded as nearly constant for the remainder of the bed and minimizing

inaccuracies in temperature measurement. Obviously, if the method is valid, any selected point will give the same result. The method also assumes that CO methanates before CO_2, which is commonly accepted (*2*), so that over the last part of the catalyst bed only the completeness of CO_2 methanation need be considered.

The temperature profile obtained by a movable thermocouple has the form in Figure 7. For highest accuracy, the maximum possible number of readings should be made in the region of the 5°F point. This profile is interpreted graphically to obtain a catalyst life prediction (the mathematical derivation of the technique appears in the Appendix). The method assumes first order reaction kinetics with respect to CO_2 (*2*). If the gradient of the temperature profile at the 5°F point is drawn, *i.e.* the tangent to the curve at this point, this is a measure of the rate of reaction at this point in the bed. If catalyst activity is assumed to be constant in the remainder of the bed, this can be used to estimate the further depth of bed required for reaction to reach any selected carbon oxides level. Design limits may be imposed by the requirement that total $CO + CO_2$ be low enough so as to avoid poisoning ammonia synthesis catalyst (*e.g.*, $CO + CO_2 > 10$ ppm). More commonly, however, the main objective is to minimize ammonium carbamate, NH_4COONH_2, in the synthesis gas loop for which a limit of $CO_2 > 2$ ppm appears desirable.

The last 5°F temperature rise at the end of the bed corresponds to methanation of about 465 ppm CO_2; typically methanation of 1% CO_2 produces a temperature rise of 108°F (60°C), that of 1% CO a rise of

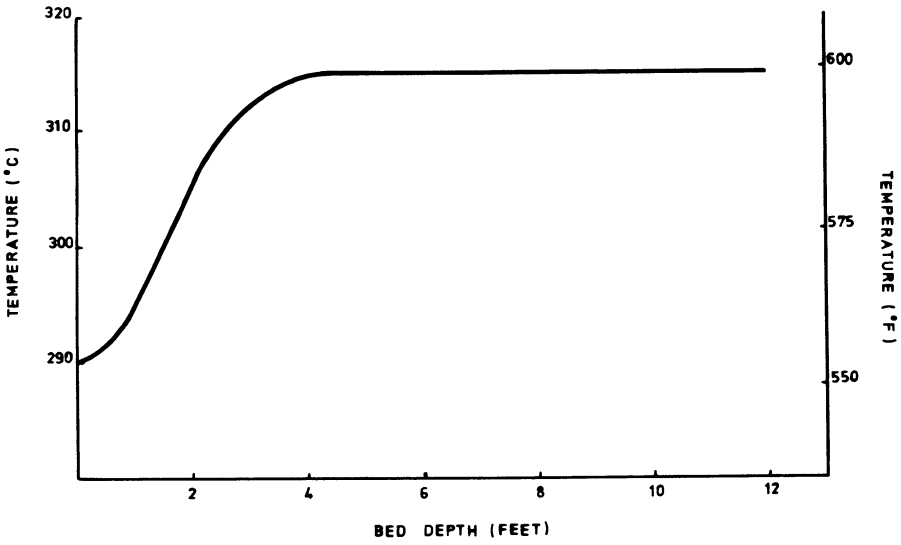

Figure 7. Typical methanator temperature profile

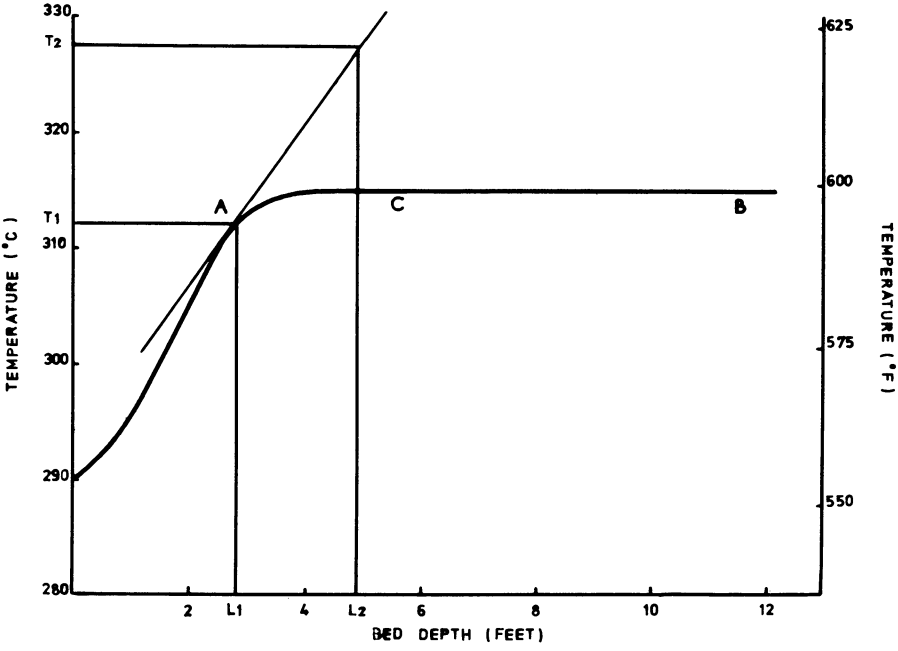

Figure 8. Location of effective end of bed

133°F (74°C). It can be shown (*see* Appendix) that an exit level of 2 ppm CO_2 corresponds to the point at which the tangent intersects a horizontal line drawn 28°F (16°C) above the 5°F point. The graphical constructions are therefore as presented in Figure 8. This permits identification of the present position of the effective end of the bed and hence of the amount of reserve catalyst remaining. In our experience, the effective end of the bed is usually located by this method as 1–1.5 ft below the point at which maximum temperature is measured. This figure obviously depends on the shape of the profile, *i.e.* on the activity of the catalyst, and should be regarded as not more than an indication. It is then necessary to study the previous history of the charge in order to estimate the rate of profile movement and likely future useful life of the charge.

The main disadvantage of this technique is that it relies on very accurate temperature measurement, particularly near the top of the temperature profile, so that the position of the 5°F point can be established and the tangent accurately constructed. Also, the end of the bed is predicted only from kinetic considerations when, in fact, other factors may be more important. In practice, however, although this introduces some scatter into successive measurements—as does variation in the duty required of the methanator—the technique has proved very satisfactory.

Typical findings are represented in Figure 9 where, if the present rate of catalyst die-off continues, the end of useful catalyst life will be reached when the current end of the bed reaches the actual end of the bed which in this instance will be after about six years on line.

Conclusion

In summary, therefore, we can say that methanation catalysts for these applications are very satisfactory in terms of activity, strength, and stability. In the absence of detrimental malfunctions, one can expect favorable operating experience, and we have demonstrated a simple and convenient method by which the future useful life of an on-line catalyst can be estimated.

Acknowledgments

We are pleased to acknowledge our indebtedness to colleagues P. J. Baldock and A. Parker for the x-ray crystallographic studies, to P. Snowden who devised the life prediction technique, and to Imperial Chemical Industries Ltd. for permission to publish this paper.

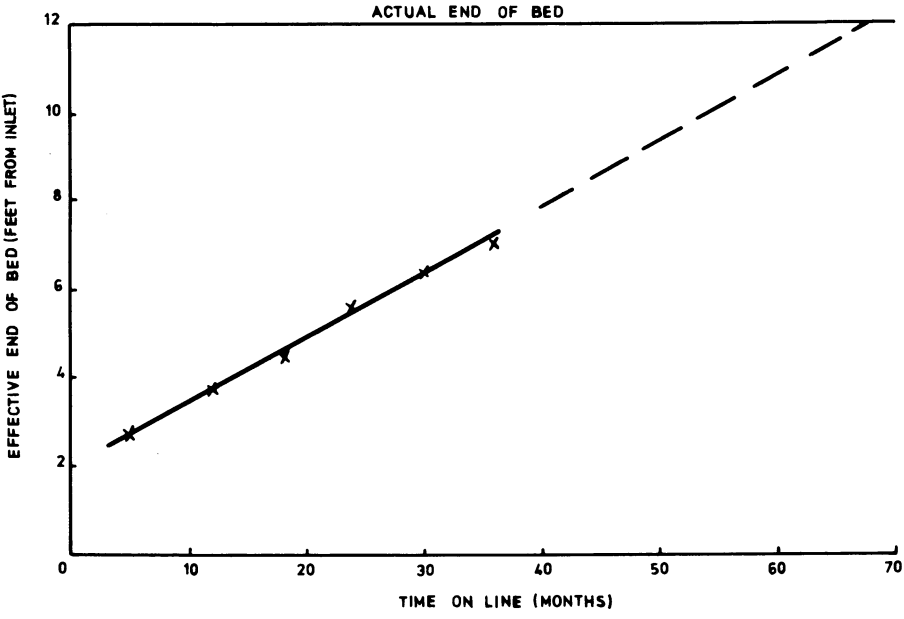

Figure 9. Future useful life prediction

Appendix: Derivation of Graphical Method

The CO_2 methanation reaction is

$$CO_2 + 4H_2 \rightarrow CH_4 + 2H_2O + H$$

where H is the heat of reaction. The rate of conversion of CO_2 in a short section of catalyst bed with length dl can be calculated from the first order rate equation

$$dX = k_o p\ P^a \left[1 - f\left(\frac{K}{K_p}\right)\right] e^{-\frac{E}{R}\left(\frac{1}{T} - \frac{1}{T_o}\right)} \quad (1)$$

where dX is the moles CO_2 converted per second and unit volume of bed, k_o is the rate constant at T_o, p is the partial pressure of CO_2, P is the total pressure, T is the temperature of bed section in °K, a is the total pressure coefficient, and K_p is the equilibrium constant for the reaction

$$K = \frac{(p_{CH_4})\ (p_{H_2O})^2}{p(P_{H_2})^4}$$

Since the system is far from equilibrium (the actual CO_2 concentration even at the exit of the bed is about 2 ppm whereas the equilibrium concentration is 10^{-4} ppm), K is small compared with K_p and the term $[1 - f(K/K_p)]$ becomes unity, *i.e.* the effect of the reverse reaction can be ignored. Equation 1 then becomes

$$dX = k_o\ p\ P^a\ e^{-\frac{E}{R}\left(\frac{1}{T} - \frac{1}{T_o}\right)} \quad (2)$$

Considering the small section of bed of length dl and cross-sectional area A, heat from reaction $= dX \cdot HA \cdot dl$ cals/sec. Therefore the temperature rise dT across the section of bed is given by

$$dT = \frac{dX \cdot HA \cdot dl}{GC} \quad (3)$$

where G is the gas flow rate in moles/sec, and C is the specific heat of gas per mole at T and P. Rearranging Equation 3 and combining with Equation 2, we obtain

$$dX = \frac{C}{H} \cdot \frac{G}{A} \cdot \frac{dT}{dl} = k_o\ p\ P^a\ e^{-\frac{E}{R}\left(\frac{1}{T} - \frac{1}{T_o}\right)}$$

The temperature gradient at a point in the bed where the temperature is T is therefore

$$\frac{dT}{dl} = \frac{HA}{CG} \cdot k_o\ P^a\ p\ e^{-\frac{E}{R}\left(\frac{1}{T} - \frac{1}{T_o}\right)}$$

Now, for a point A near the top of the profile (*see* Figure 8) at temperature T_1, the temperature gradient $(dT/dl)_1$ is given by

$$\left(\frac{dT}{dl}\right)_1 = \left(\frac{HA}{CG}\right)_1 k_o \, P_1{}^a p_1 e^{-\frac{E}{R}\left(\frac{1}{T_1} - \frac{1}{T_o}\right)}$$

Substituting for k_o in Equation 2, we obtain

$$dX = \left(\frac{dT}{dl}\right)_1 \left(\frac{CG}{HA}\right)_1 \frac{P^a \, p \, e^{-\frac{E}{R}\left(\frac{1}{T} - \frac{1}{T_o}\right)}}{P_1{}^a p_1 e^{-\frac{E}{R}\left(\frac{1}{T_1} - \frac{1}{T_o}\right)}}$$

By considering only the last section of the bed where little conversion occurs, we can make several simplifications. The total pressure is virtually constant and $P_1 = P$. Hence,

$$dX = \left(\frac{dT}{dl}\right)_1 \left(\frac{CG}{HA}\right)_1 \frac{p}{p_1} \, e^{-\frac{E}{R}\left(\frac{1}{T} - \frac{1}{T_1}\right)} \tag{4}$$

The temperature change is also small so that the exponential term can be taken as unity. The molar flow G can be assumed to be constant between A and B and the CO_2 conversion is proportional to the change in CO_2 partial pressure, dp. The volume of the section of bed is Adl so that the rate of CO_2 conversion, dX, is therefore:

$$dX = \frac{G}{Adl} \cdot \frac{dp}{P}$$

When this is combined with Equation 4, after simplification we get

$$\frac{dp}{P} = \left(\frac{dT}{dl}\right)_1 \cdot \frac{C}{H} \cdot \frac{P}{p_1} \cdot dl$$

Integrating between A and C, we obtain

$$ln \, \frac{p_2}{p_1} = \left(\frac{dT}{dl}\right)_1 \cdot \frac{C}{H} \cdot \frac{P}{p_1} \cdot (L_2 - L_1) \tag{5}$$

where p_2 is the partial pressure of CO_2 at bed depth L_2. For a typical methanation system, $C = 4 \times 10^{-3}$ kcal/mole °F, $H = -41.9$ kcal/mole, and $P = 30$ atm.

Taking A as the point 5°F below maximum temperature, 465 ppm CO_2 remain to be methanated at this point. Take design exit CO_2 concentration as 2 ppm. Equation 5 then reduces to

$$2.303 \log_{10}\left(\frac{2}{465}\right) = -\left(\frac{dT}{dl}\right)_1 \cdot \frac{4 \times 10^{-3}}{41.9} \cdot \frac{1}{465 \times 10^{-6}} \cdot (L_2 - L_1)$$

$$(L_2 - L_1) = \frac{28.0}{\left(\frac{dT}{dl}\right)_1}$$

Since

$$\left(\frac{dT}{dl}\right)_1 = \frac{T_2 - T_1}{L_2 - L_1}$$

$$T_2 - T_1 = 28.0\ ^\circ\text{F}$$

Hence a line drawn 28°F above the 5°F point will intersect the tangent to the profile at the 5°F point at the position corresponding to the present end of the catalyst bed.

Literature Cited

1. Takemura, Y., Morita, Y., Yamamoto, K., *Bull. Jap. Petrol. Inst.* (1967) **9**, 13.
2. Van Herwijnen, T., Van Doesburg, H., De Jong, W. A., *J. Catal.* (1973) **28**, 391.

RECEIVED October 4, 1974.

Synthesis of Methane in Hot Gas Recycle Reactor Pilot Plant Tests

W. P. HAYNES, A. J. FORNEY, J. J. ELLIOTT, and H. W. PENNLINE

United States Energy Research and Development Administration, Pittsburgh Energy Research Center, 4800 Forbes Ave., Pittsburgh, Pa. 15213

Four pilot plant experiments were conducted at 300 psig and up to 475°C maximum temperature in a 3.07-in. i.d. adiabatic hot gas recycle methanation reactor. Two catalysts were used: parallel plates coated with Raney nickel and precipitated nickel pellets. Pressure drop across the parallel plates was about 1/15 that across the bed of pellets. Fresh feed gas containing 75% H_2 and 24% CO was fed at up to 3000/hr space velocity. CO concentrations in the product gas ranged from less than 0.1% to 4%. Best performance was achieved with the Raney-nickel-coated plates which yielded 32 mscf CH_4/lb Raney nickel during 2307 hrs of operation. Carbon and iron deposition and nickel carbide formation were suspected causes of catalyst deactivation.

Development of large scale, catalytic methanation reactors is necessary to complete the commercialization of plants for converting coal to substitute natural gas. Major objectives in developing a catalytic methanation system are to achieve efficient removal of the heat of reaction so as to minimize thermal deactivation of catalyst as well as catalyst deactivation by other causes such as chemical poisoning and structural changes. The hot gas recycle (HGR) reactor, in which large quantities of partially cooled product gas are circulated through the catalyst bed, provides one satisfactory method of removing large amounts of heat from the catalyst surface. In early United States Bureau of Mines experiments with the HGR reactor, however, catalysts had short lives on the order of 200 hrs (*1*). Our work attempted to extend the life of the catalyst in the HGR reactor system, to determine the effects of some of the process variables, and to compare the performances of a bed of pelleted nickel catalyst and a bed of parallel plates coated with Raney nickel.

Pilot Plant Description

The reactor in the HGR pilot plant was constructed of type 304 stainless steel, 3-in., schedule 40 pipe that was 10 ft long and flanged at each end. In three experiments (HGR-10, HGR-12, and HGR-14), the catalyst bed consisted of grid assemblies of parallel, type 304 stainless steel plates that had been flame spray coated with Raney nickel. The 6-in. long grid assemblies were stacked to the desired bed height and conformed to the inside diameter of the reactor. Grid plates were aligned perpendicular to the plate alignment of adjacent grids. Prior to assembly, each plate was sand blasted on both sides, flame sprayed with a bond coat, and finally flame sprayed with the Raney nickel catalyst to form a Raney nickel coating ~0.02-in. thick. In experiment HGR-13, the reactor was charged with 0.25-in. pellets of a commercial grade, precipitated nickel catalyst. *See* Table I for physical properties of the catalyst beds.

Table I. Catalyst Bed Data from

Parameter	*HGR-10, Flame-Sprayed Raney Nickel*	*HGR-12, Flame-Sprayed Raney Nickel*
Nickel, wt %	42[a]	42[a]
Activated, %	70[b]	70[b]
Plate thickness, in.	0.25	0.25
Space between bare plates, in.	0.224	0.224
Avg. bond coat thickness, in.	0.006	0.006
Avg. catalyst thickness, in.	0.026	0.022
Bed diameter × length, in.	3.07 × 60	3.07 × 60
Bed volume, ft^3	0.257	0.257
Unactivated catalyst, lb	3.72	2.86
Superficial area of catalyst, ft^2	12.7	12.7
Void fraction	0.421	0.436

[a] Before leaching.

The basic HGR reactor scheme is presented as a simplified flow-sheet (Figure 1). The main reactor containing the parallel plate grid assemblies is the subject of this report. The second stage reactor, an adiabatic reactor charged with a precipitated nickel catalyst, was operated intermittently; it will be discussed in a later report. Additional heat exchangers (not shown in the flowsheet) were used in the pilot plant to compensate for system heat losses, to achieve a measure of heat recuperation, and to control the gas temperature into the hot gas compressor and into the main reactor. The main catalyst bed is cooled by direct transfer of the reaction heat to the slightly cooler gas stream flowing through the bed. The recycle stream is appropriately cooled before being returned to the reactor. The hot recycle stream may be cooled (a) directly without con-

densation, or (b) by cooling a portion of the recycled product gas sufficiently to condense out the water vapor and then returning the resultant cold recycle gas along with the hot recycle gas. After a final heat exchange, the mixture of cooled recycle gas and fresh feed gas comprise a feed to the HGR reactor at a controlled temperature that may be 50°–150°C lower than the reactor outlet temperature, depending on the total amount of gas recycled and the amount of heat exchange.

Charcoal absorption towers (not included in the flowsheet) were used to keep the sulfur content in the fresh feed gas less than 0.1 ppm in equivalent volume of H_2S.

Catalyst Preparation

The metal plates to be coated with Raney nickel were type 304 stainless steel. Plate surfaces were prepared by sand blasting with an iron-free

Hot Gas Recycle Reactor Tests

HGR-13, *Supported Nickel*	*HGR-14,* *Flame-Sprayed Raney Nickel*
25	42[a]
100% reduced	70[b]
—	0.046
—	0.135
(1/4 × 1/4 in. cylindrical	0.006
pellets)	0.022
3.07 × 24	3.07 × 24
0.103	0.103
6.80	3.84
18.6	11.4
0.370	0.515

[b] Leaching of aluminum stopped when 70% of the theoretical amount of hydrogen had evolved.

grit and then flame spraying on a light coat of bonding material about 0.006 in. thick. After the surface was bond coated, the Raney nickel alloy powder (80–200 mesh) was flame sprayed on to the desired thickness. The plates were assembled in parallel and inserted in the reactor. The Raney nickel was then activated by passing a 2-wt % NaOH solution through the catalyst bed to dissolve the aluminum phase and leave a spongy surface of highly active free nickel. Activation was stopped after 70% of the aluminum in the Raney alloy had reacted. It is believed that the remaining unreacted alloy provides a base on which the activated nickel remains anchored. The extent of reaction was determined by measuring the hydrogen evolved by these three reactions, in each of which three moles of H_2 are evolved for every two moles of Al that reacted (top of next page):

$$2Al + 2NaOH + 2H_2O \rightarrow 2NaAlO_2 + 3H_2$$
$$2Al + NaOH + 4H_2O \rightarrow NaAlO_2 + Al(OH)_3 + 3H_2$$
$$2Al + 3H_2O \rightarrow Al_2O_3 + 3H_2$$

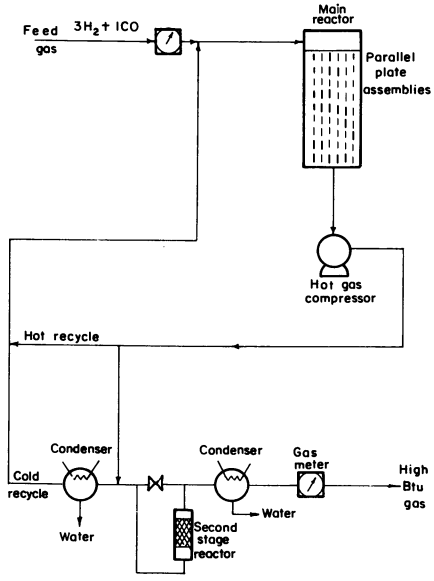

Figure 1. Flowsheet of hot gas recycle process

After the aluminum had reacted, the catalyst was washed with water of pH *ca.* 6.8 until the pH of the effluent water reached ~7.2.

Once the catalyst was activated and washed, it was always kept under hydrogen until it was put into methanation service at the desired operating pressure and temperature. Before the catalyst was cooled to take it out of service, the reactor was purged with hydrogen. It was kept in a hydrogen atmosphere during cooling, depressurizing, and while in a standby condition.

In experiment HGR-13, the commercial grade precipitated nickel catalyst was in a reduced and stabilized condition when it was charged into the reactor. No special activation treatment was needed. It was, however, kept under hydrogen at all times until the temperature and pressure of the system were brought to synthesis conditions, at which time the synthesis feed gas was gradually fed into the system to start the run.

Procedures and Results

General. The flame-sprayed Raney nickel catalyst was used in ex-experiments HGR-10, HGR-12, and HGR-14, the pelleted precipitated catalyst in experiment HGR-13. Reactor conditions as a function of

stream time for experiments HGR-10, HGR-12, HGR-13, and HGR-14 are presented graphically by computer printout in Figures 2, 4, 6, and 8, respectively. Carbon monoxide concentrations and heating values of the product gases and methane yields are depicted graphically as a function of stream time in Figures 3, 5, 7, and 9. The total recycle ratio was calculated on the basis of stream analyses; it fluctuated widely because of the high sensitivity of the calculated values to small changes in stream analyses. All runs were made at 300 psig.

The major process parameters at selected periods in the four experiments are listed in Tables II, IV, VII, and VIII. Carbon recoveries ranged from 63 to 91%. Most of the losses occurred in connection with the recycle compressor system, and they decreased correspondingly the volume of product gas metered. Such losses, however, did not affect significantly the incoming gas to the main reactor or reactor performance.

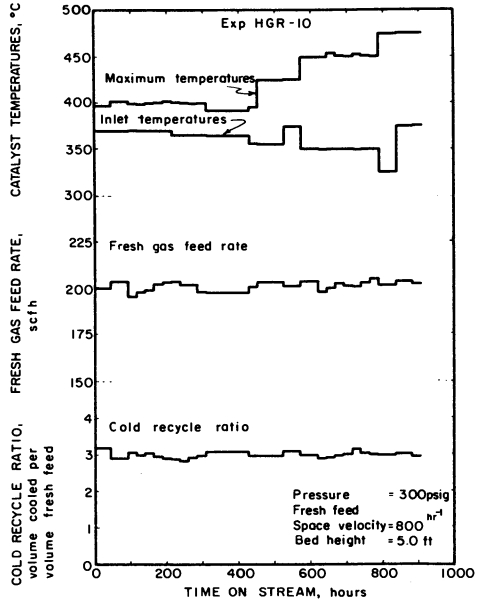

Figure 2. Reactor conditions for experiment HGR-10

Experiment HGR-10. Experiment HGR-10 operated at 300 psig with recycle ratios being varied to give temperature rises across the catalyst bed of 50°–150°C (Figure 2). Temperature control was excellent. Total operating time was relatively short, 910 hrs. The initial CO concentration in the product gas at 0.3% was higher than the desired value of $< 0.1\%$ (Figure 3). Over the entire experiment, the average rate of catalyst deactivation, expressed as increase in the percent carbon monoxide in the

Table II. Operating Data from Selected Periods in Experiment HGR-10

Parameter	*Period 5*	*Period 15*	*Period 26*
Time on stream, hrs	168	527	887
Fresh gas			
rate, scfh	200	204	204
H_2, vol %	75.3	75.3	75.6
CO, vol %	24.3	24.6	24.2
CO_2, vol %	0.2	0.1	0.1
N_2, vol %	0.0	0.0	0.0
CH_4, vol %	0.2	0.1	0.2
H_2O, vol %	0.0	0.0	0.0
H_2/CO	3.10	3.06	3.09
exposure velocity, scfh/ft^2	15.7	16.0	16.1
space velocity, hr^{-1}	779	795	796
Mixed feed gas (wet)			
rate, scfh	9138	3744	2401
H_2, vol %	6.0	13.2	17.7
CO, vol %	1.2	2.9	4.3
CO_2, vol %	1.3	0.7	0.8
N_2, vol %	0.6	1.4	1.7
CH_4, vol %	83.1	76.7	71.4
H_2O, vol %	7.8	5.0	4.1
H_2/CO	5.06	4.61	4.08
inlet superficial velocity, ft/sec	5.44	2.18	1.44
inlet Reynolds number	5000	1960	1180
exposure velocity, scfh/ft^2	51.9	47.5	41.6
space velocity, hr^{-1}	35,600	14,600	9360
Total recycle/fresh gas, v/v	44.7	17.4	10.8
Cold recycle/fresh gas, v/v	3.1	2.99	3.05
Temperature			
gas inlet, °C	370	355	375
maximum catalyst, °C	400	425	475
Pressure, psig	300	300	300
Product gas (wet)			
rate, scfh	48.8	55.5	58.3
H_2, vol %	4.4	9.6	12.1
CO, vol %	0.7	1.6	2.4
CO_2, vol %	1.3	0.8	0.2
N_2, vol %	0.7	1.5	1.8
CH_4, vol %	84.3	80.0	76.6
H_2O, vol %	8.6	6.4	6.3
H_2/CO	6.2	6.0	5.05
Conversion			
H_2, % fresh feed	98.6	96.5	95.4
CO, % fresh feed	99.3	98.2	97.2
(H_2 + CO), % fresh feed	98.7	96.9	95.9
H_2, % mixed feed	27.0	29.9	34.6
CO, % mixed feed	44.4	45.8	46.5
(H_2 + CO), % mixed feed	29.8	32.7	37.0
Usage ratio	3.07	3.01	3.07
Heating value, Btu/scf	952	908	878
Carbon recovery, %	87	91	90

dry product gas per thousand standard cubic feet (mscf) of methane produced per pound of catalyst charged, was 0.23%/mscf/lb (Table II). This is a high rate of deactivation compared with the value of about 0.009%/mscf/lb obtained with Raney nickel catalyst in a tube-wall methanator test (TWR-6) (*2*). Because the experiment was of short duration, methane production per pound of catalyst in experiment HGR-10 was only about 11.8 mscf/lb as compared with 177 mscf/lb in tube-wall reactor test TWR-6.

One probable reason for the relatively poor catalyst performance in experiment HGR-10 was the excessively large deposits of iron and carbon on the catalyst surface. Iron and carbon concentrations (Table III) were

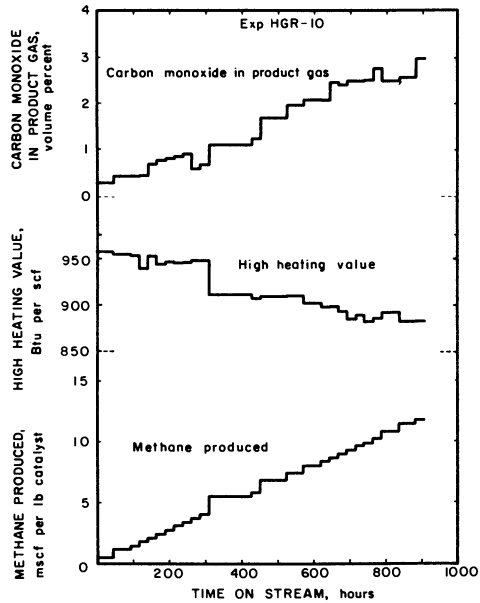

Figure 3. Product gas characteristics in experiment HGR-10

22.0 and 13.4 wt %, respectively, on the catalyst near the gas inlet and 0.8 and 1.9 wt %, respectively, on the catalyst near the gas outlet. It is suspected that the large deposit of iron resulted from decomposition of iron carbonyl carried in from other parts of the reactor system, and that the deposited iron in turn favored formation of free carbon from the incoming carbon monoxide.

Experiment HGR-12. The catalyst bed for experiment HGR-12 was the same as that used in experiment HGR-10 except that the coat of Raney nickel in HGR-12 was slightly thinner (Figure 4). The objective in ex-

Table III. Iron and Carbon Content of Raney Nickel Catalyst Grids after Experiment HGR-10

Grid	*Fe, wt %*	*C, wt %*
A[a]	22.0	13.4
B	17.2	9.1
C	3.5	3.9
D	2.7	3.3
E	2.0	2.5
F	2.1	2.0
G	0.9	1.5
H	0.8	1.6
I	0.8	1.6
Top[b]	0.8	1.9

[a] Gas inlet.
[b] Gas outlet.

periment HGR-12 was to increase catalyst life. The methane produced per pound of catalyst was 39.5 mscf after a total operating time of about 1400 hrs (Figure 5). The overall average rate of catalyst deactivation, 0.091% mscf/lb, was about 40% of that in experiment HGR-10, but it was still 10 times greater than that in experiment TWR-6. The CO concentration increased from 0.1% at the start of the experiment to 3.7% at the end (Table IV).

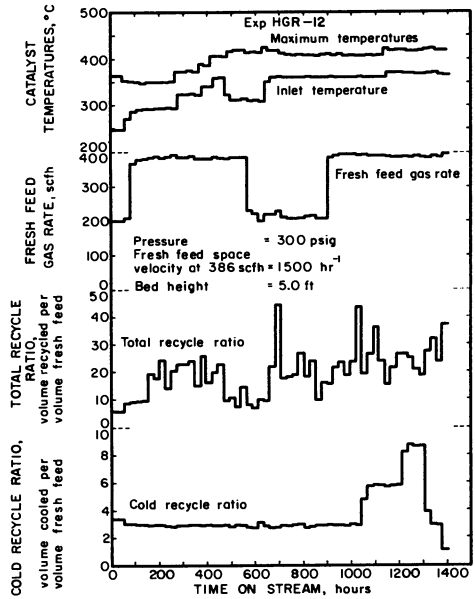

Figure 4. Reactor conditions for experiment HGR-12

In general, the rate of deactivation was much lower at the lower fresh gas feed rate than at the higher feed rates. For example, the rate of deactivation was 0.022%/mscf/lb during the period between 600 and 800 hrs stream time at the lower feed rate of ~206 standard cubic feet per hour (scfh) whereas it was 0.143%/mscf/lb for the period between 100 and 400 hrs when the fresh feed rate was about 386 scfh.

The cold gas recycle (CGR) ratio values (Figure 4) are metered values and are more consistent than the HGR and total gas recycle ratio values which were calculated from gas analyses. Although the calculated total recycle gas flow rate was erratic, catalyst bed temperatures were uniform and easily controlled by varying recycle rate and bed inlet tem-

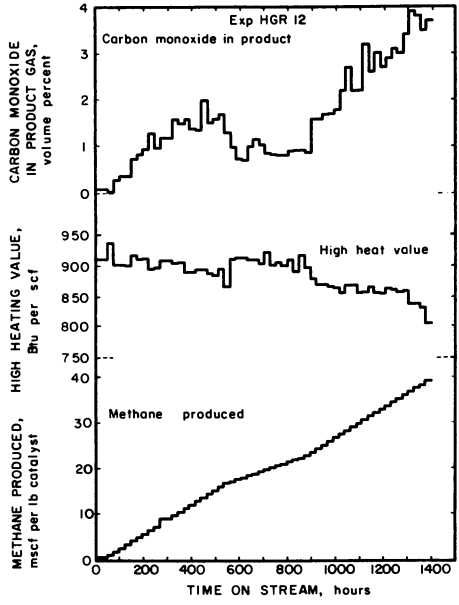

Figure 5. Product gas characteristics in experiment HGR-12

perature. The uniformity of catalyst bed temperature (Figure 4) indicates that the actual recycle rate was much more uniform than the calculated values would indicate. The data plotted in Figures 4 and 5 indicate that raising the maximum temperature of the catalyst bed from 350° to 410°C during stream time of 260–460 hrs did not significantly change the trend of increasing CO concentration in product gas. However, this trend was reversed during the subsequent period of 467–539 hrs when the CO concentration in the product gas decreased from 2.0 to 1.7% (dry). This decrease in CO concentration is attributed mainly to the decrease in the ratio of total recycle gas to fresh gas from ~20:1 to ~8:1 with an attendant increase in residence time. The decrease in total

Table IV. Operating Data from Selected Periods in Experiment HGR-12

Parameter	*Period* 7	20	31	52	55	56
Time on stream, hrs	200	539	803	1307	1379	1403
Fresh gas						
rate, scfh	388	383	206	386	386	393
H_2, vol %	75.5	75.1	75.1	75.6	75.2	75.3
CO, vol %	24.4	24.7	24.7	24.4	24.7	24.6
CO_2, vol %	0.1	0.1	0.1	0	0.1	0
N_2, vol %	0	0	0	0	0	0
CH_4, vol %	0	0.1	0.1	0	0	0.1
H_2O, vol %	0	0	0	0	0	0
H_2/CO	3.09	3.04	3.04	3.10	3.04	3.06
exposure velocity, scfh/ft^2	30.6	30.1	16.2	30.4	30.4	30.9
space velocity, hr^{-1}	1510	1490	804	1500	1500	1530
Mixed feed gas (wet)						
rate, scfh	7380	3450	5820	7760	9670	15,100
H_2, vol %	14.4	20.2	14.9	20.7	22.3	21.9
CO, vol %	2.0	4.2	1.6	4.4	4.2	3.8
CO_2, vol %	0.5	0.4	0.3	0.6	0.8	1.5
N_2, vol %	1.3	0.8	1.2	0.3	0.6	0.8
CH_4, vol %	76.4	70.7	76.6	72.6	66.8	60.8
H_2O, vol %	5.4	3.7	5.4	1.4	5.3	11.2
H_2/CO	7.04	4.82	9.20	4.71	5.34	5.70
inlet superficial velocity, ft/sec	3.88	1.86	3.41	4.61	5.73	8.93
inlet Reynolds number	4270	1870	3060	3910	4810	7510
exposure velocity, scfh/ft^2	95.6	66.3	75.8	153.0	201.0	306.0
space velocity, hr^{-1}	28,800	13,400	22,700	30,200	37,700	58,900
Total recycle/fresh gas, v/v	18.0	7.99	27.2	19.1	24.1	37.4
Cold recycle/fresh gas, v/v	3.01	2.99	3.04	8.71	3.01	1.20
Temperature						
gas inlet, °C	294	310	360	368	366	365
maximum catalyst, °C	353	422	412	420	422	420
Pressure, psig	300	300	300	300	300	300
Product gas (wet)						
rate, scfh	94.6	97.6	45.9	98.8	105.5	127.7
H_2, vol %	10.9	13.0	12.6	17.6	19.9	20.3
CO, vol %	0.8	1.6	0.8	3.3	3.3	3.3
CO_2, vol %	0.5	0.5	0.3	0.6	0.9	1.5
N_2, vol %	1.3	0.8	1.2	0.3	0.6	0.8
CH_4, vol %	79.7	77.5	78.8	75.6	69.0	62.2
H_2O, vol %	6.8	6.6	6.3	2.6	6.3	11.9
H_2/CO	13.6	8.13	15.8	5.33	6.03	6.15
Conversion						
H_2, % fresh feed	96.5	95.6	96.3	94.0	92.8	91.2
CO, % fresh feed	99.2	98.4	99.3	96.5	96.3	95.6

Table IV. Continued

Parameter	*Period* 7	20	31	52	55	56
(H_2 + CO), % fresh feed	97.1	96.3	97.0	94.6	93.6	92.3
H_2, % mixed feed	26.6	39.5	17.2	17.1	12.5	8.18
CO, % mixed feed	62.3	64.4	53.6	26.6	22.8	16.0
(H_2 + CO), % mixed feed	31.1	43.8	20.7	18.7	14.1	9.34
Usage ratio	3.01	2.95	2.95	3.02	2.93	2.92
Heating value, Btu/scf	908	892	899	857	828	802
Carbon recovery, %	80	81	72	83	81	87

recycle ratio was achieved by reducing the HGR ratio to ~5:1 while leaving the CGR ratio constant at 3:1. Correspondingly, the water vapor concentration in the mixed feed to the reactor was decreased slightly from 5.5 to 3.7%, and the resulting temperature spread across the catalyst bed increased from ~51° to 112°C. Total recycle was lowest, 8:1, at 539 hrs stream time.

After experiment HGR-12 was ended, samples of the spent catalyst were taken from various locations in the bed, and Brunauer–Emmett–Teller (BET) pore volumes, and distribution of pore radii were determined for each sample. The findings are presented in Table V as a function of distance from the gas inlet end of the catalyst bed. Additional information on the spent catalyst (for the gas inlet and outlet ends) was obtained by x-ray and chemical analyses. The metal surface area was determined by chemisorbed hydrogen (Table VI). BET surface areas were about one-half that of freshly activated Raney nickel which has a surface area as high as 64 m^2/g. Special catalyst activities as determined by thermogravimetric analysis (TGA) for samples of spent catalyst taken at 0, 6, and 60 in. from the gas inlet were, respectively, 0.0, 0.9, and 18% CO converted to CH_4. Thus, the part of the catalyst nearest the gas outlet was the most active with the lowest carbon content, the largest pore radii (96% of its pore volume had radii > 60 A), the lowest BET surface area (19.5 m^2/g), and the largest free metal surface (4.9 m^2/g). These observations are all consistent if one assumes that the combination of finer pore structure and higher BET surface area at the gas inlet end of the bed indicates a higher carbon concentration and that the nickel pore radii are larger than that of the amorphous carbon deposit.

Experiment HGR-13. A 2-ft bed of commercial catalyst was tested as a packed bed of 0.25-in. pellets (*see* Table I for bed properties). This test was similar to experiment HGR-14 in which the catalyst bed consisted of parallel plates sprayed with Raney nickel. The experiment was

Table V. Characteristics of Spent Raney Nickel Catalyst in Experiment HGR-12

Distance from Gas Inlet, in.	*BET Surface Area, m^2/g*	*Av. Pore Radius, A*	*Pore Vol., cm^3*	*Pore Volume (in %) with Radii of:*				
				<30A	*30–40A*	*40–50A*	*50–60A*	*>60A*
0	34.7	47.1	.083	19.7	11.9	10.8	10.0	47.6
18	31.7	90.6	.146	8.8	6.2	4.9	6.4	73.6
30	34.4	58.6	.101	15.7	9.2	11.6	9.5	54.0
36	32.9	82.0	.135	10.4	7.4	8.0	6.0	68.2
48	24.2	139.0	.168	0.5	3.7	7.5	4.7	83.6
60	19.5	109.5	.107	0	0	0	4	96.0

also designed to determine the effect of varying the fresh feed rate from 2000 to 3000/hr space velocity (with space velocity based on scfh of gas at 1 atm and 32°F/ft^3 of catalyst bed).

Major process conditions for experiment HGR-13 are plotted *vs.* stream time in Figure 6. The total recycle ratio was held relatively constant at ~10:1 which resulted in a constant temperature rise of about 100°C across the catalyst bed (300°C at the inlet, 400°C maximum). Near the end of the experiment, the cold recycle ratio was varied from 8:1 to 1:1. The experiment was ended at 1368 hrs.

The CO concentration in the dry product gas ranged from ~0.02% at the start to 1.2% at 840 hrs, then decreased to 0.88% at 1368 hrs at

Table VI. Properties of Spent Methanation Catalysts

	HGR-12 Catalyst		*HGR-13 Catalyst*		*HGR-14 Catalyst*	
	Inlet	*Outlet*	*Inlet*	*Outlet*	*Inlet*	*Outlet*
X-ray analysis	—	—	Ni	Ni	Ni, Ni_3C	Ni
Chemical analysis						
Ni, %	67.6	80.4	24.0	25.3	83.4	81.9
Al, %	13.1	9.6	—	—	6.23	7.90
C, %	1.74	0.8	5.1	5.2	3.53	0.81
Fe, %	0.35	0.45	0.12	0.20	1.18	1.21
Na, %	0.08	0.06	0.23	0.20	—	—
S, %	0.24	0.13	0.10	0.10	0.19	0.07
BET surface area, m^2/g	34.67	19.50	—	—	30.95	29.7
Metal surface area (chemisorbed hydrogen), m^2/g	1.3	4.9	—	—	—	—
Average pore radius, A	47.07	109.53	—	—	48.01	56.69
Percent pore volume >60A	47.56	95.97	—	—	42.3	64.2

the end of the run (Figure 7). Total methane produced was about 11.5 mscf/lb of catalyst. The heating value of the product was 885–~960 Btu/scf.

The overall deactivation rate was about 0.076%/mscf/lb. During the experiment, the fresh gas rate was varied from ~210 to 320 scfh and finally back to 210 scfh; the corresponding deactivation rates were 0.014, 0.222, and 0.079%/mscf/lb. Thus, the deactivation rate was increased irreversibly by increasing the fresh gas rate.

Typical operating data from selected periods in experiment HGR-13 are presented in Table VII. Period 6, 168 hrs stream time, is typical of conditions at the beginning of the experiment whereas period 54 is repre-

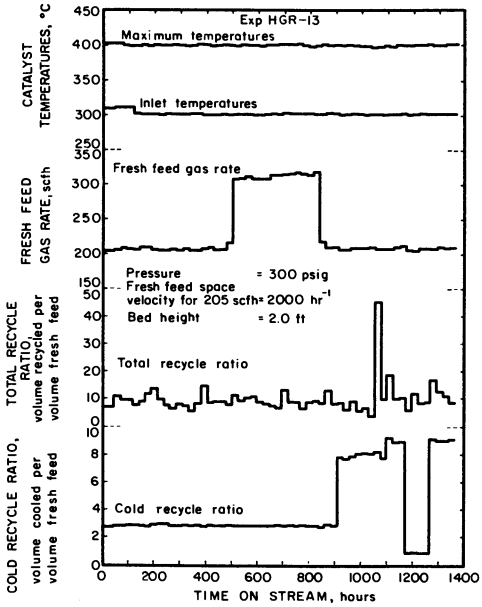

Figure 6. Reactor conditions for experiment HGR-13

sentative of conditions at the end of the experiment. There was very little change in performance during the 336-hr span between periods 6 and 20; for example, the decrease in conversion of $(CO + H_2)$ in the fresh feed gas was very slight, 98.0 to 97.9%. When the fresh feed rate was increased from 2110 to 3020/hr space velocity (*cf.* periods 20 and 22), conversion of $H_2 + CO$ in the fresh feed decreased from 97.9 to 97.1%. A further drop in performance (period 34) may be attributed to continued operation at the higher fresh feed rate of 320 scfh or 3120/hr space velocity.

Although the fresh feed rate was returned to the lower rate of 211 scfh in period 37, the catalyst had definitely lost activity with time (*cf.*

Table VII. Operating Data from

Parameter	*Period* 6	*20*	*22*
Time on stream, hrs	168	504	552
Fresh gas			
rate, scfh	211	216	310
H_2, vol %	75.3	76.4	75.5
CO, vol %	24.6	23.6	24.5
CO_2, vol %	0	0	0
N_2, vol %	0	0	0
CH_4, vol %	0.1	0	0
H_2O, vol %	0	0	0
H_2/CO	3.06	3.24	3.08
exposure velocity, scfh/ft^2	11.3	11.6	16.7
space velocity, hr^{-1}	2050	2110	3020
Mixed feed gas (wet)			
rate, scfh	2260	2090	3400
H_2, vol %	15.2	16.1	16.9
CO, vol %	2.3	2.5	2.6
CO_2, vol %	0.2	0.3	0.6
N_2, vol %	0.9	1.4	1.0
CH_4, vol %	76.9	75.6	74.5
H_2O, vol %	4.5	4.1	4.4
H_2/CO	6.54	6.43	6.41
inlet superficial velocity, ft/sec	1.20	1.11	1.81
inlet Reynolds number	835	772	1240
exposure velocity, scfh/ft^2	21.3	21.0	35.8
space velocity, hr^{-1}	22,000	20,400	33,100
Total recycle/fresh gas, v/v	9.73	8.68	9.98
Cold recycle/fresh gas, v/v	2.98	2.99	3.00
Temperature			
gas inlet, °C	301	300	301
maximum catalyst, °C	401	400	401
Pressure, psig	300	300	300
Product gas (wet)			
rate, scfh	48.1	50.9	79.3
H_2, vol %	8.8	9.0	10.8
CO, vol %	0	0.1	0.4
CO_2, vol %	0.3	0.3	0.7
N_2, vol %	0.9	1.5	1.0
CH_4, vol %	83.0	82.2	80.3
H_2O, vol %	7.0	6.9	6.8
H_2/CO	—	90	27
Conversion			
H_2, % fresh feed	97.3	97.2	96.3
CO, % fresh feed	100	99.9	99.6
(H_2 + CO), % fresh feed	98.0	97.9	97.1
H_2, % mixed feed	45.0	47.2	39.1
CO, % mixed feed	100	96.2	85.3
(H_2 + CO), % mixed feed	52.3	53.8	45.3

Selected Periods in Experiment HGR-13

Period			
34	*37*	*50*	*54*
840	912	1224	1320
320	211	205	210
74.9	74.9	76.1	75.8
24.9	24.9	23.7	24.1
0.1	0.1	0.1	0.1
0	0	0	0
0.1	0.1	0.1	0
0	0	0	0
3.01	3.01	3.21	3.15
17.2	11.3	11.0	11.3
3120	2060	2000	2050
3430	2040	2800	3010
19.1	15.2	17.9	14.0
3.4	2.9	2.3	2.5
0.7	0.6	0.7	0.4
0.9	0.9	0.5	1.2
71.9	76.7	66.8	81.0
4.0	3.7	11.8	0.9
5.69	5.21	7.72	5.69
1.82	1.09	1.49	1.60
1220	753	1010	1120
41.5	19.9	30.5	26.6
33,400	19,900	27,300	29,400
9.73	8.68	12.7	13.3
2.96	2.98	1.01	9.05
301	302	301	301
400	401	401	400
300	300	300	300
81.1	49.0	47.4	38.4
13.1	8.2	13.1	9.2
1.1	0.4	0.6	0.8
0.8	0.6	0.8	0.4
0.9	1.0	0.5	1.3
77.8	83.6	71.0	85.7
6.3	6.2	14.0	2.6
11.9	20.5	21.8	11.5
95.6	97.5	96.0	97.8
98.9	99.6	99.4	99.4
96.4	98.0	96.8	98.2
34.9	49.6	29.9	37.0
68.2	87.9	74.4	68.0
39.8	55.7	35.0	41.6

Table VII.

Parameter	Period 6	20	22
Usage ratio	2.71	2.95	2.73
Heating value, Btu/scf	935	926	911
Carbon recovery, %	82	87	90

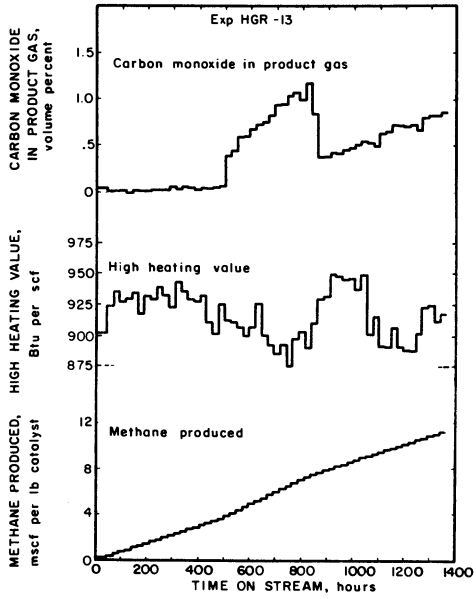

Figure 7. Product gas characteristics in experiment HGR-13

CO in product gas in periods 37 and 20: 0.4% *vs.* 0.1%). However, this activity loss is not evident in the heating values (933 and 926 Btu/scf for periods 37 and 20 respectively) because the product gas was less diluted with excess hydrogen in period 37 than in period 20. This is confirmed by the H_2/CO ratio in the fresh feed gas; it is 3.01 for period 37 and 3.24 for period 20.

X-ray diffraction analysis of the spent catalyst (Table VI) revealed that the nickel was present only in the metallic state. Chemical analyses demonstrated very little difference in catalyst composition at the gas inlet and outlet.

Experiment HGR-14. The reactor was packed with 2 ft of parallel plates sprayed with Raney nickel (Table I); catalyst spraying and activation were as described under catalyst preparation. Operating conditions were practically the same as in experiment HGR-13 except for the periodic changes in the CGR ratio (*see* Figure 8 for reactor conditions and Figure 9 for product gas characteristics).

Continued

Period			
34	*37*	*50*	*54*
2.91	2.94	3.10	3.09
890	933	888	925
80	78	70	63

At the start of the experiment, the CO concentration in the product gas was very low, < 0.01% (Table VIII). The unusually high value (0.71%) at 186 hrs stream time is the result of an analytical error. At the end of the experiment, after 2307 hrs stream time, CO in the product gas had increased to 0.93% (dry basis), and total methane produced per pound of catalyst was 32 mscf.

The CO concentration in the product gas was much less than that obtained in experiments HGR-10 and HGR-12. This improvement may be attributed mainly to the larger catalyst surface available per unit rate of feed gas or to the lower exposure velocity used in experiment HGR-14.

The average catalyst deactivation rate over the entire experiment was 0.0291%/mscf/lb. The rate of deactivation during the initial 462 hrs of operation at a fresh feed space velocity of about 2090/hr (216 scfh) was very low, 0.0017%/mscf/lb; from ~500 hrs to 841 hrs with ~2990/hr space velocity, the deactivation rate increased to 0.040%/mscf/lb. Catalyst deactivation rates were calculated (Table IX) for various operating periods and fresh feed space velocities.

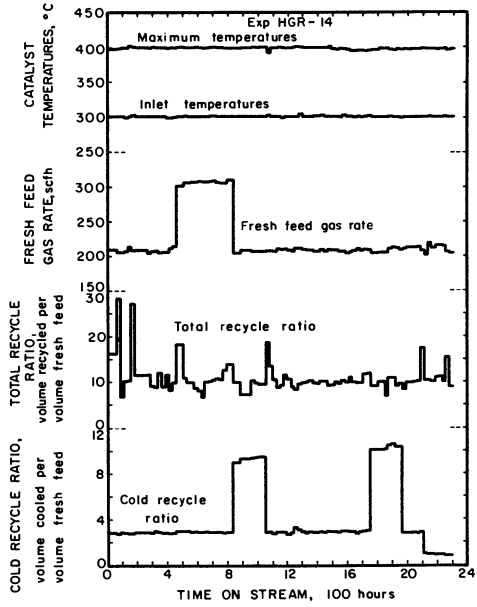

Figure 8. Reactor conditions for experiment HGR-14

Table VIII. Operating Data from

Parameter	*Period* 4	15	17
Time on stream, hrs	139	462	534
Fresh gas			
rate, scfh	207	214	306
H_2, vol %	75.8	75.4	75.3
CO, vol %	23.7	23.6	23.6
CO_2, vol %	0.1	0.1	0.3
N_2, vol %	0.4	0.9	0.7
CH_4, vol %	0	0	0.1
H_2O, vol %	0	0	0
H_2/CO	3.20	3.19	3.19
exposure velocity, scfh/ft^2	18.0	18.6	26.5
space velocity, hr^{-1}	2010	2090	2980
Mixed feed gas (wet)			
rate, scfh	2360	2400	3710
H_2, vol %	15.9	14.0	11.7
CO, vol %	2.1	2.1	2.0
CO_2, vol %	0.1	0.1	0.2
N_2, vol %	0.7	1.1	0.9
CH_4, vol %	76.4	78.0	80.6
H_2O, vol %	4.8	4.6	4.6
H_2/CO	7.68	6.63	5.88
inlet superficial velocity, ft/sec	1.25	1.27	1.97
inlet Reynolds number	546	563	882
exposure velocity, scfh/ft^2	37.2	34.0	44.5
space velocity, hr^{-1}	23,000	23,400	36,100
Total recycle/fresh gas, v/v	10.7	10.4	11.3
Cold recycle/fresh gas, v/v	2.95	2.93	3.12
Temperature			
gas inlet, °C	299	299	301
maximum catalyst, °C	400	400	400
Pressure, psig	300	300	300
Product gas (wet)			
rate, scfh	32.9	28.4	44.2
H_2, vol %	10.0	7.9	5.8
CO, vol %	0	0	0.1
CO_2, vol %	0.1	0.1	0.2
N_2, vol %	0.7	1.1	0.9
CH_4, vol %	81.9	83.9	86.1
H_2O, vol %	7.3	7.0	6.9
H_2/CO	—	785	117
Conversion			
H_2, % fresh feed	97.9	98.6	98.9
CO, % fresh feed	100	100	100
(H_2 + CO), % fresh feed	98.4	98.9	99.1
H_2, % mixed feed	40.4	47.0	52.2
CO, % mixed feed	100	99.6	97.8
(H_2 + CO), % mixed feed	47.3	53.9	58.9

Selected Periods in Experiment HGR-14

Period					
26	*34*	*37*	*62*	*64*	*76*
750	1058	1130	1732	1803	2091
307	207	207	210	203.5	213
74.6	75.1	75.4	75.1	74.7	75.4
24.4	22.9	23.6	24.0	24.8	24.1
0.2	0.1	0.1	0.1	0.1	0.1
0.8	1.8	0.8	0.8	0.3	0.4
0	0.1	0.1	0	0.1	0
0	0	0	0	0	0
3.06	3.28	3.19	3.13	3.01	3.13
26.6	17.8	17.9	18.2	17.7	18.6
2990	2020	2020	2050	1980	2080
3720	2240	2430	2760	2120	2430
8.8	11.8	11.1	10.1	10.4	13.8
2.2	2.2	2.2	2.1	2.9	2.9
1.5	0.2	0.4	0.7	0.4	0.7
1.1	1.3	0.9	1.1	1.1	1.2
81.9	84.3	80.7	81.4	85.2	76.9
4.5	0.2	4.7	4.6	0	4.5
4.00	5.38	5.10	4.84	3.64	4.77
1.97	1.19	1.29	1.46	1.12	1.29
898	532	582	666	512	570
35.8	27.5	28.2	29.6	24.8	35.6
36,200	21,800	23,700	26,900	20,700	23,700
11.3	10.1	11.0	12.4	9.66	10.6
3.01	9.59	2.93	3.13	10.2	2.94
300	300	300	300	299	299
400	401	400	395	397	398
300	300	300	300	300	300
45.4	27.3	27.6	43.9	44.7	40.6
2.8	5.3	5.0	4.7	3.5	7.8
0.2	0.1	0.2	0.3	0.5	0.9
1.6	0.2	0.5	0.7	0.5	0.7
1.1	1.2	0.9	1.1	1.2	1.3
87.6	90.7	86.3	86.5	91.8	82.5
6.7	2.5	7.1	6.7	2.5	6.8
14.1	58.3	27.7	16.2	6.68	9.14
99.4	99.1	99.1	98.7	99.0	97.9
99.9	99.9	99.9	99.7	99.5	99.2
99.5	99.3	99.3	98.9	99.1	98.2
69.5	57.7	57.0	55.4	67.8	46.5
91.5	96.2	92.2	86.8	82.6	72.1
73.9	63.7	62.7	60.8	71.0	50.9

Table VIII.

Parameter	Period 4	Period 15	Period 17
Usage ratio	3.10	3.13	3.14
Heating value, Btu/scf	930	941	957
Carbon recovery, %	83.1	74.2	79.0

As noted for experiment HGR-13, the deactivation rate increased significantly when the fresh feed space velocity was increased from 2000 to 3000/hr. During the period of 841–1058 hrs, the fresh feed space velocity was returned to 2000/hr and the CGR ratio was increased from ~3:1 to ~9:1 to give a low deactivation rate of 0.0027%/mscf/lb. When the CGR ratio was returned to ~3:1 at 1058–1760 hrs, the rate of catalyst deactivation increased to 0.0187%/mscf/lb. After 1760 hrs, the unit was shut down and put in standby condition under hydrogen. After the unit was restarted, the deactivation rate had increased greatly to 0.0821%/mscf/lb which indicates that the increase in deactivation rate was associated with this particular shutdown. Since this experiment had previously undergone three unscheduled shutdowns at 215, 798, and 894 hrs with no adverse effect on performance, some unknown factor unique to the shutdown at 1760 hrs was responsible for the subsequent rapid decline in activity.

From the operating data in Table VIII the following are points of special interest in the experiment: (a) period 4 represents performance at 2000/hr fresh gas space velocity and 3:1 CGR ratio when the catalyst is fresh; (b) period 15 represents performance at 2000/hr space velocity before changes to 3000/hr; (c) periods 17 and 26 represent the beginning and end of the 3000/hr space velocity operation; (d) period 34 represents operation at 2000/hr space velocity and a high CGR ratio (9.59:1); (e) periods 37 and 62 represent the beginning and end of an operating period later in the experiment at 2000/hr space velocity and 3:1 CGR

Table IX. Catalyst Deactivation Rates during Experiment HGR-14

Nominal Fresh Feed Space Velocity, hr^{-1}	Stream Period, hrs From	Stream Period, hrs To	Catalyst Deactivation Rate, %/mscf/lb
2000	0	462	0.00166
3000	462	841	0.0396
2000	841	1058	0.0027
2000	1058	1760	0.0187
2000	1760	2180	0.0821

Continued

Period					
26	*34*	*37*	*62*	*64*	*76*
3.04	3.23	3.15	3.09	2.99	3.08
962	961	960	956	967	927
78.5	94.5	98.3	94.4	89.4	86.5

ratio; (f) periods 62 and 64 provide further comparison of the effect of increasing the CGR ratio from 3:1 to 10:1; and (g) period 76 represents performance after a long period of operation (2207 hrs).

X-ray analysis of the spent catalyst (Table XI) revealed metallic nickel and nickel carbide, Ni_3C, in the catalyst near the gas inlet and only metallic nickel near the gas outlet.

Discussion of Results

Operability. All four series of experiments prove that HGR methanation is a usable and operable system. With a total gas recycle ratio of about 10:1 and with CO concentrations in the mixed feed entering the catalyst bed as high as 4.3% (wet basis), temperature control was excellent and no hot spots developed. It appears likely that lower recycle

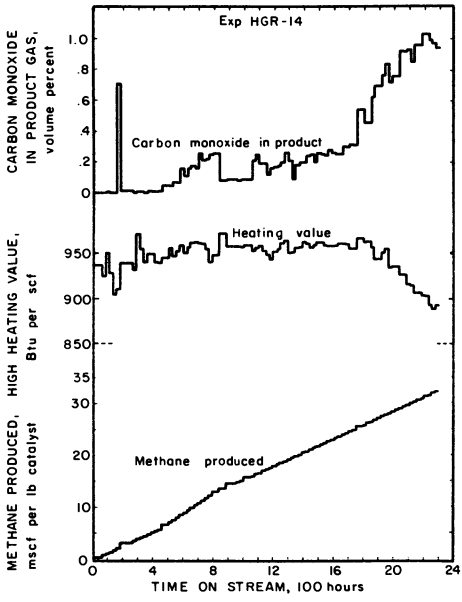

Figure 9. Product gas characteristics in experiment HGR-14

Table X. Pressure Drop across the Catalyst Bed[a]

Nominal Space Velocity, hr^{-1}		*Pressure Drop, in. water*	
Fresh Feed	*Total Feed*	*HGR-14*	*HGR-13*
2000	22,000	2.0	28
3000	33,000	2.7	49

[a] Experiment HGR-14: parallel plates, and experiment HGR-13: 0.25 in. pellets.

ratios, although how much lower it is not known, could be used successfully with attendant increases in inlet CO concentration and in temperature rise across the bed. Further testing is required to determine the limit in decreasing the total recycle ratio and the effect of such a decrease on the catalyst life.

Flame-Sprayed Raney Nickel Plates *vs.* Pellets of Precipitated Catalyst in a Packed Bed. Experiments HGR-13 and HGR-14 demonstrated that the performance of the plates sprayed with Raney nickel catalyst was significantly better than that of the precipitated nickel catalyst pellets. The sprayed plates yielded higher production of methane per pound of catalyst, longer catalyst life or lower rate of deactivation, lower CO concentration in the product gas, and lower pressure drop across the catalyst bed.

One of the reasons for developing the parallel plate catalyst was to reduce the pressure drop across the catalyst bed and consequently to reduce power costs for circulating the recycle gas. For pressure drop measurements across the 2-ft long catalyst beds, *see* Table X. These data show that the pressure drop across the parallel plates is about 1/15 of that across the pelleted catalyst bed.

The bed of parallel plates coated with Raney nickel catalyst was much more reactive than the bed of precipitated nickel. This was revealed by the generally lower CO concentration in the product gas during operation with the parallel plate bed; for example, after ~450 hrs stream time, it was 0.01% with the bed of sprayed Raney nickel (experiment HGR-14) and 0.05% with the bed of precipitated nickel catalyst (experiment HGR-13).

The higher reactivity of the Raney nickel coated plates is also illustrated by the plots of catalyst temperature *vs.* bed length (Figure 10). The maximum bed temperature (indicative of near-completion of methanation) was consistently reached within a shorter distance from the gas inlet, and the slopes of the curves are correspondingly steeper for the more reactive bed of parallel plates coated with Raney nickel.

The initial reactivities of the catalyst beds in experiments HGR-13 and HGR-14 are considered satisfactorily high; however, the overall rate of deactivation of the Raney nickel catalyst bed (0.029%/mscf/lb) was

much lower than that of the precipitated catalyst (0.076%/mscf/lb). Consequently, catalyst life was longer (2305 *vs.* 1368 hrs) and the yield of methane (32.0 *vs.* 11.5 mscf/lb catalyst) was higher with the Raney nickel catalyst.

Other precipitated nickel catalysts that were developed recently are reputedly superior to that used in experiment HGR-13. These catalysts will be evaluated in the near future as well as other forms of Raney nickel.

Effects of Cold Gas Recycle and Approach to Equilibrium. Product gases resulting from various CGR ratios were analyzed (Table XI). For the experiments tabulated, a decrease in the cold recycle ratio resulted consistently in increases in the product gas concentrations of water vapor, hydrogen, and carbon dioxide and a decrease in methane concentration. These trends may be noted in experiment HGR-12 as the CGR ratio decreased from 8.7:1 to 1.2:1, in experiment HGR-13 as it increased from 1.0:1 to 9.1:1, and in experiment HGR-14 as it decreased from 3.0:1 to 1.0:1. These trends indicate that the water–gas shift reaction ($CO + H_2O \rightarrow CO_2 + H_2$) was sustained to some degree. Except for the 462-hr period in experiment HGR-14, the apparent mass action constants for the water–gas shift reaction (based on the product gas compositions in Table XI) remained fairly constant at 0.57–1.6. These values are much lower than the value of 11.7 for equilibrium conversion at 400°C. In

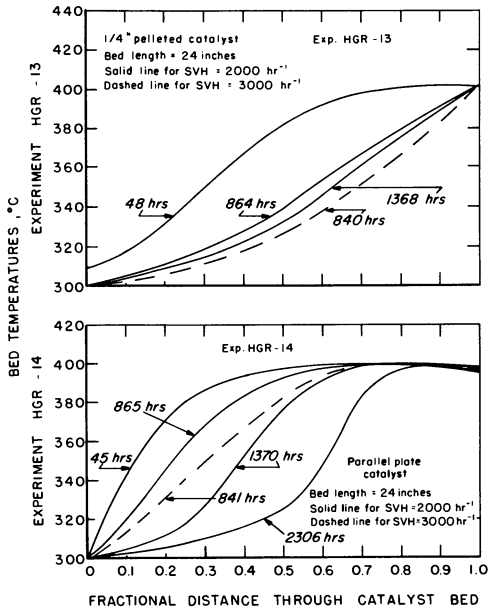

Figure 10. Axial temperature profiles during methanation
Top, experiment HGR-13; and bottom, experiment HGR-14

Table XI. Effect of Cold

Experiment	Stream Time, hrs	CGR Ratio	H_2O in Mixed Feed, %	Product Gas Analysis,[a] % H_2O	H_2	CO	CO_2	CH_4
HGR-12	1307	8.7:1	1.4	2.6	17.6	3.3	0.6	75.6
	1379	3.0:1	5.3	6.3	19.9	3.3	0.9	69.0
	1403	1.2:1	11.2	11.9	20.3	3.3	1.5	62.2
	539	3.0:1	5.4	6.6	13.0	1.6	0.5	77.5
HGR-13	1224	1.0:1	11.8	14.0	13.1	0.6	0.8	71.0
	1320	9.1:1	0.9	2.6	9.2	0.8	0.4	85.7
HGR-14	462	2.9:1	4.6	7.0	7.9	0.01	0.1	83.9
	2091	3.0:1	4.5	6.8	7.8	0.9	0.7	82.5
	2307	1.0:1	10.5	13.2	10.1	0.8	1.4	73.0

[a] On a wet basis.

experiment HGR-14, the apparent mass action constant for the shift reaction was 0.075 at 462 hrs, which represents a much greater departure from equilibrium than that encountered in the other periods included in this table. The apparent mass action constant for the methanation reaction ($3H_2 + CO \rightarrow CH_4 + H_2O$) at 462 hrs in experiment HGR-14 was 2650 which constitutes a much closer approach to the 400°C equilibrium value of 1.7×10^4 than that achieved by the other test periods. This greater dominance by the methanation reaction while the catalyst is still relatively fresh probably caused the greater departure from equilibrium observed in the shift reaction during the 462-hr period early in the experiment.

Catalyst Deactivation. In this series of HGR experiments, the sulfur content in the feed gas was very low, generally < 0.1 ppm. Catalyst deactivation caused by sulfur poisoning is therefore considered negligible. On the other hand, the iron deposited on the catalyst in experiment HGR-10 (and to a lesser extent in experiments HGR-12 and HGR-14) is suspected of promoting carbon formation and subsequent fouling and deactivation of the catalyst. Iron concentrations of 5 mg/mscf in the recycle stream indicate the presence of iron carbonyl. The iron:nickel ratio in fresh Raney nickel is about 2.4:1000, but the ratio is significantly higher in spent Raney nickel catalyst. The iron:nickel ratios in the spent Raney nickel catalysts from experiments HGR-12 and HGR-14 were 5.2:1000–14.8:1000, and the higher iron concentrations generally resulted in greater carbon deposition. The same trend was observed in experiment HGR-10.

Nickel carbide, detected on the catalyst in experiment HGR-14, is another compound suspected of deactivating Raney nickel catalyst. However, the shutdown involved purging with hydrogen while the catalyst

Gas Recycle on Product Gas

Apparent Mass Action Constant, k_p		
Shift Reaction	*Methanation Reaction*	*Maximum* T, °C
0.78	0.24	420
0.86	0.37	422
1.2	0.59	420
1.6	3.2	422
0.79	16.0	401
0.57	7.8	400
.075	2650	400
1.02	30.8	398
0.75	25.3	398

was hot, and the presence of nickel carbide is contrary to the findings of Steffgen and Hobbs (*3*) by TGA that nickel carbide is not stable under hydrogen at temperatures above 280°C. More information on nickel carbide formation is needed.

The metal surface area at the inlet end of the catalyst bed in experiment HGR-12 was smaller than that at the outlet end; this indicates that a decrease in nickel metal sites is part of the deactivation process. Sintering of the nickel is one possible mechanism, but carbon and carbide formation are suspected major causes. Loss of active Raney nickel sites could also conceivably result from diffusion of residual free aluminum from unleached catalyst and subsequent alloying with the free nickel to form an inactive material.

As was noted for experiments HGR-12, HGR-13, and HGR-14, the rate of catalyst deactivation increased as the fresh gas feed rate increased. It is possible that higher rates of carbon deposition and metal sintering occur at the higher feed rates with resultant higher deactivation rates.

The catalyst in an isothermal tube-wall reactor (experiment TWR-6 in Ref. 2) deactivated much more slowly than did the catalyst in the best test (experiment HGR-14) in an adiabatic HGR reactor (0.009 *vs.* 0.0291%/mscf/lb), and it also produced much more methane (177 *vs.* 32 mscf/lb catalyst). This indicates that adiabatic operation of a methanation catalyst between 300° and 400°C is not as efficient as isothermal operation at higher temperature (~400°C).

Another factor that may account for the relatively higher rate of deactivation with the HGR reactor system is the entrainment in the catalyst bed of oil vapors from the hot recycle gas compressor. This occurrence was evidenced by traces of heavy oil collected downstream of the HGR reactor. Such oil vapors would tend to decompose thermally

and subsequently foul the catalyst surface with carbon. In future HGR tests, efforts will be made to eliminate oil deposition on the catalyst bed.

Literature Cited

1. Forney, A. J., Demski, R. J., Bienstock, D., Field, J. H., "Recent Catalyst Developments in the Hot-Gas-Recycle Process," Bureau of Mines Rep. Invest. (1965) **6609**.
2. Haynes, W. P., Elliott, J. J., Forney, A. J., "Experience with Methanation Catalysts," *Amer. Chem. Soc., Fuels Div., Prepr.* **16** (2), 47–63 (Boston, April, 1972).
3. Steffgen, F. W., Hobbs, A. P., "Methanation of Synthesis Gas and the Nickel Carbide System," Pittsburgh Catal. Soc., Spring Symp., Pittsburgh, April, 1973.

RECEIVED October 4, 1974.

Effect of Certain Reaction Parameters on Methanation of Coal Gas to SNG

K.-H. EISENLOHR and F. W. MOELLER

Lurgi Mineraloeltechnik GmbH., Frankfurt/Main, Germany

M. DRY

South African Coal, Oil, and Gas Corp., Sasolburg, South Africa

Methanation of coal gas to specification grade substitute natural gas (SNG) has been investigated in two semicommercial pilot plants. One plant was operated with coal gas which was generated in a commercial Lurgi pressure gasification plant and purified in a commercial Rectisol unit. Thus, the overall scheme for producing SNG from coal has been demonstrated. In addition to long term test runs of 4000 and 5000 hrs that established a catalyst lifetime of > 16,000 hrs in a commercial plant, numerous tests demonstrated the effects of operating temperature and of steam in reactor feed gas on catalyst activity and catalyst deactivation. The effects of feed gas composition (e.g., H_2/CO *ratio,* CO_2 *content, trace components, and catalyst poisons) were also investigated.*

Converting coal to a gas which has the same characteristics as natural, pipeline quality gas and which is therefore known as substitute natural gas (SNG) is one promising possibility for meeting the increasing energy demand in the United States. Lurgi pressure gasification of coal and processes for treating and purifying the product gas used in 14 commercial plants are planned to serve as the basis for a processing scheme to convert coal into SNG (*1*, *2*, *3*). Four different steps are required in the Lurgi process (Figure 1): pressure gasification of coal, shift conversion of crude gas, gas purification by Rectisol, and methane synthesis. Since the methane synthesis process has not yet been applied

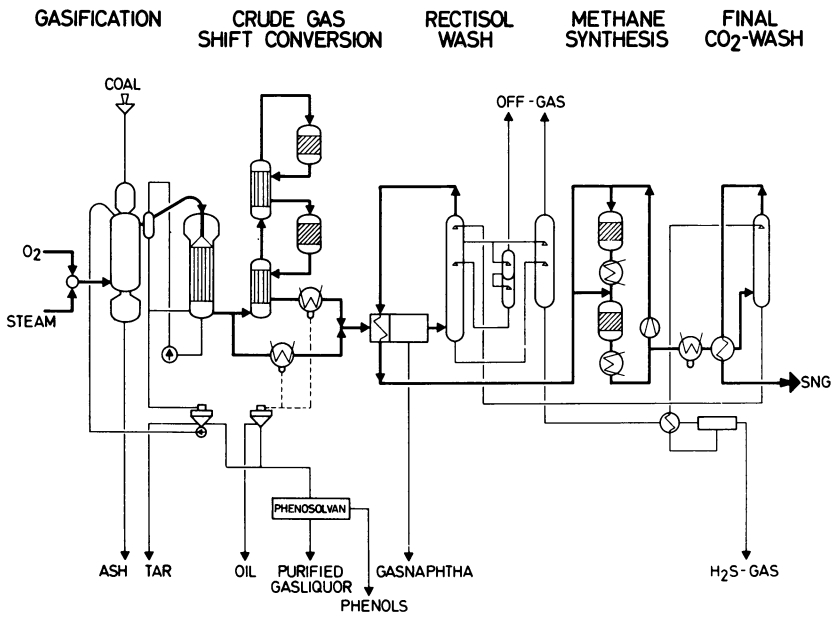

Figure 1. Lurgi process for producing SNG from coal

commercially, it is of significant importance to demonstrate its technical feasibility.

Consequently, two semicommercial pilot plants have been operated for 1.5 years. One plant, designed and erected by Lurgi and South African Coal, Oil, and Gas Corp. (SASOL), Sasolburg, South Africa, was operated as a sidestream plant to a commercial Fischer–Tropsch synthesis plant. Synthesis gas is produced in a commercial coal pressure gasification plant which includes Rectisol gas purification and shift conversion so the overall process scheme for producing SNG from coal could be demonstrated successfully. The other plant, a joint effort of Lurgi and El Paso Natural Gas Corp., was operated at the same time at Petrochemie Schwechat, near Vienna, Austria. Since the starting material was synthesis gas produced from naphtha, different reaction conditions from those of the SASOL plant have also been operated successfully.

The findings from two long term test runs in the SASOL plant relevant to catalyst life under design conditions in a commercial methane synthesis plant have already been published (3). This paper reports further test results from both demonstration units concerning the effect of certain reaction parameters which are the basis for flexibility and operability of the Lurgi methanation scheme.

Design of the Demonstration Plants

The scheme of commercial methane synthesis includes a multistage reaction system and recycle of product gas. Adiabatic reactors connected with waste heat boilers are used to remove the heat in the form of high pressure steam. In designing the pilot plants, major emphasis was placed on the design of the catalytic reactor system. Thermodynamic parameters (composition of feed gas, temperature, temperature rise, pressure, etc.) as well as hydrodynamic parameters (bed depth, linear velocity, catalyst pellet size, etc.) are identical to those in a commercial methanation plant. This permits direct upscaling of test results to commercial size reactors because radial gradients are not present in an adiabatic shift reactor.

Arrangement of the semicommercial pilot plants permitted supervision and operation of the plant from a central control panel. The installed safety control system was tested successfully during several emergency shutdowns with no effect on reactor material and catalyst.

The scheme of the methanation demonstration units is presented in Figure 2. Synthesis gas is heated in heater E1 and is then mixed with recycle gas. Zinc oxide reactor D1 serves as an emergency catchpot for sulfur breakthrough from the purification plant. The total feed is heated

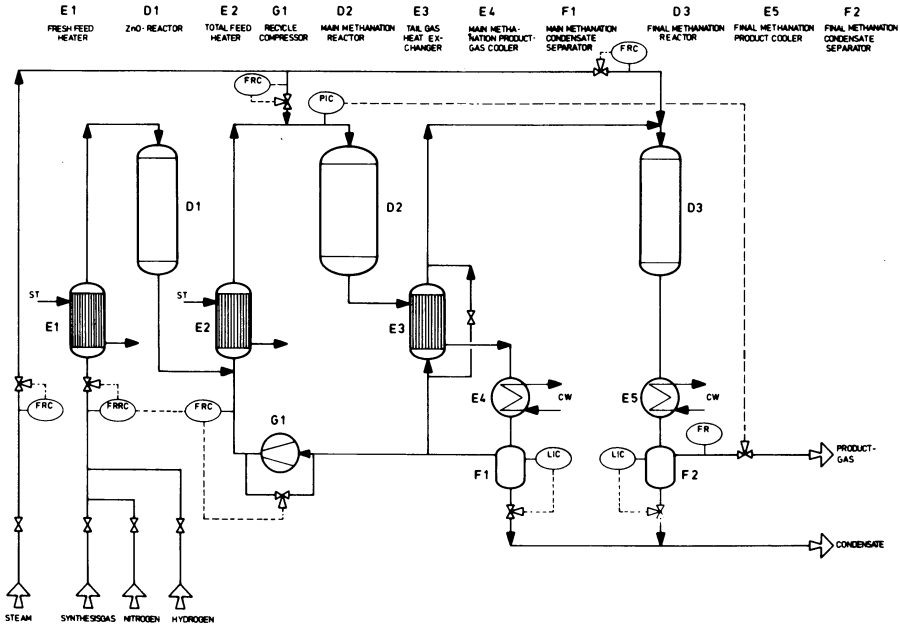

Figure 2. Scheme of methanation pilot plant

in heater E2 and then charged to main methanation reactor D2 with additional steam. Effluent gas from reactor D2 is cooled in heat exchanger E3 and in cooler E4, thereby condensing the steam. Part of the reactor effluent gas is recycled while the rest is reheated in E3 and fed to final or polishing methanation reactor D3. Product gas from D3 is cooled in E5.

All tests reported here were performed with a special methanation catalyst developed by BASF, Ludwigshafen, for the process. The catalyst had a relatively high nickel content on a carrier. It was charged to reactors D2 and D3 in unreduced form and had to be activated by reduction with hydrogen.

Effect of Synthesis Gas Composition

The effect of synthesis gas composition on conversion, catalyst life, carbon black formation, etc. was determined in numerous tests. Characteristic variables in the synthesis gas composition are the H_2/CO ratio, residual CO_2 content, and content of trace components in the form of higher hydrocarbons and catalyst poisons.

H_2/CO Ratio. In a commercial shift conversion plant, a change in throughput and conversion must be taken into account since it will affect

Table I. Effects of the H_2/CO Ratio in the Synthesis Gas

	H_2/CO = 5.8			*H_2/CO = 3.7*		
Variable	*Syn-gas*	*Feed to D2*	*D2 Effluent Gas*	*Syn-gas*	*Feed to D2*	*D2 Effluent Gas*
Pressure, kg/cm²	—	18.0	—	—	18.0	—
Temperature, °C	270	300	450	270	300	450
Gas composition						
CO_2, vol %	16.6	20.5	22.1	9.4	15.4	17.2
CO, vol %	10.7	3.4	0.4	16.6	4.1	0.4
H_2, vol %	62.0	23.9	8.7	62.0	20.6	8.4
CH_4, vol %	9.8	50.7	67.0	10.8	57.7	71.6
C_2^+, vol %	0.2	0.1	<0.1	0.2	0.1	<0.1
N_2, vol %	0.7	1.4	1.7	1.0	2.1	2.4
H_2O, Nm^3/Nm^3	—	0.417	0.584	—	0.387	0.501
Total conversion, %						
U_{CO_2}		48.3			23.7	
U_{CO}		98.4			99.0	
U_{H_2}		94.1			94.3	
Bed depth needed for total conversion, %						
500 hrs		20			20	
1000 hrs		22			22	

the H_2/CO ratio of the synthesis gas. Therefore the SASOL plant was operated in different test runs, each lasting more than 1000 hrs, with various H_2/CO ratios in the synthesis gas in order to determine if the H_2/CO ratio has any effect on the operability of methane synthesis. H_2/CO ratios of 5.8, 3.7, and even lower were adjusted by varying the mixing ratio of shifted and unshifted coal gas. The data obtained at a synthesis pressure of 18 kg/cm_2 are summarized in Table I. The expected equilibrium conversion was achieved in all test runs. A remarkable finding was that there was no difference in the axial temperature profile when the synthesis gas had a H_2/CO ratio of 3.7 or 5.8. In both cases, adiabatic end temperature was reached in 20% of the catalyst bed depth after 500 operating hours and in 22% of the catalyst bed depth after 1000 operating hours. Findings were similar during a long term test of 4000 operating hours when the H_2/CO ratio was decreased from 5.8 to 3.8 after 1500 hrs, and no change in the temperature profile or the deactivation rate was measurable (3).

In all tests, there was no sign of carbon black formation. Pressure drop over the reactor remained constant during the whole operating period, and there was no accumulation of free carbon on the catalyst. Analysis of the discharged catalyst for free carbon revealed that the carbon content was lower than the amount of carbon added to the catalyst as a pelletizing aid.

Finally, it can be stated that variation in the H_2/CO ratio will not affect operability of an SNG plant using a recycle system for methanation as demonstrated in the SASOL plant.

Residual CO_2 Content. The feed gas to Rectisol gas purification contains 29–36 vol % CO_2 depending on the rate of shift conversion. The rate of CO_2 to be washed out will be determined by the requirements of methane synthesis and by the need to minimize the cost of Rectisol purification.

For SNG manufacture, it is necessary to reduce the residual hydrogen to a minimum in order to achieve a high calorific value. This is best realized if the synthesis gas, instead of having a stoichiometric composition, contains a surplus of CO_2 which can be utilized to reduce the H_2 content by the CO_2 methanation reaction to less than 1% according to equilibrium conditions. The surplus CO_2 must be removed at the end of the process sequence. It is, of course, also possible to operate a methanation plant with synthesis gas of stoichiometric composition; then there is no need for a final CO_2 removal system. The residual H_2 content will be higher, and therefore the heating value will be lower (*cf.* the two long term runs in Table II).

Table II. A Comparison of SNG Production

	Sasol Plant				
	Main Methanation			*Final Methanation*	
Variable	*Syngas*	*Feed to D2*	*D2 Effluent Gas*	*Feed to D3*	*D3 Effluent Gas*
Pressure, kg/cm²	—	18.0	—	—	—
Temperature, °C	270	300	450	260	315
Gas composition					
CO_2, vol %	13.0	19.3	21.5	21.5	21.3
CO, vol %	15.5	4.3	0.4	0.4	<0.1
H_2, vol %	60.1	41.3	7.7	7.7	0.7
CH_4, vol %	10.3	53.3	68.4	68.4	75.9
C_2^+, vol %	0.2	0.1	<0.1	<0.1	<0.1
N_2, vol %	0.9	1.7	2.0	2.0	2.0
H_2O, Nm^3/Nm^3	—	0.37	0.50	0.04	0.08
Total conversion, %					
U_{CO_2}			33.4		
U_{CO}			99.9		
U_{H_2}			99.5		

The SASOL plant was operated with a surplus of CO_2 during a long term test of 4000 hrs. Of the CO_2 in the synthesis gas, 33.4% was methanated while the remaining 66.6% left the reaction system unconverted. Product gas from final methanation yielded specification grade SNG containing residual hydrogen of 0.7 vol % and residual CO of less than 0.1 vol %. The heating value was 973 Btu/standard cubic foot (scf) after CO_2 removal to 0.5 vol % (calc.).

The Schwechat plant was operated with a stoichiometric synthesis gas in a long term test of 5000 hrs. The residual hydrogen content could be decreased to 2.2 vol % which resulted in a heating value of 950 Btu/scf when about 1 vol % nitrogen was present in the synthesis gas.

No differences in operability and catalyst behavior (activity and deactivation) in the two plants were discernible. The expected catalyst lifetime in a commercial plant, calculated from the movement of the temperature profile down the catalyst bed with time, in both cases will be more than 16,000 hrs under the design conditions.

A significant feature of the operation of the two plants is that only a small deviation in feed gas composition is tolerable when using a stoichiometric gas. Greater deviations in the H_2/CO ratio and in the residual CO_2 content of the feed gas will cause serious problems regarding SNG specifications. Thus, methanation of a stoichiometric synthesis gas is reasonable only when there are no stringent requirements for SNG specification.

in the SASOL and Schwechat Plant

Schwechat Plant

Main Methanation			*Final Methanation*	
Syngas	*Feed to D2*	*D2 Effluent Gas*	*Feed to D3*	*D3 Effluent Gas*
—	16.3	—	—	—
—	290	440	283	345
5.1	4.4	4.1	4.1	1.8
14.4	4.0	0.1	0.1	<0.1
61.6	25.7	12.1	12.1	2.2
18.9	65.9	83.7	83.7	96.0
—	—	—	—	—
—	—	—	—	—
—	0.349	0.481	0.061	0.123
		86.1		
		99.9		
		98.6		

Content of Higher Hydrocarbons. After purification in a Rectisol unit, coal pressure gasification gas contains higher hydrocarbons in the C_2–C_3 range at 0.2–0.6 vol %. Analytical examination during all test runs demonstrated that the used nickel catalyst has good gasification or hydrogenation activity. Unsaturated hydrocarbons such as ethylene and propylene are hydrogenated completely while saturated hydrocarbons such as ethane and propane are converted to methane up to equilibrium concentrations of 50 ppm ethane and < 5 ppm propane.

Catalyst Poisons. It is well known that sulfur, chlorine, etc. are strong poisons for nickel catalyst. Chlorine was not detectable in the synthesis gas downstream of the Rectisol in the SASOL plant. The total sulfur content of this gas—in the form of H_2S, COS, and organic sulfur components—averaged 0.08 mg/m³ with maximum values of 0.2 mg total sulfur/m³.

The effect of sulfur contamination on catalyst activity was examined in a special test run in the SASOL plant. Conversion in 6.3 and 23.8% of the total catalyst bed, taken as an indirect criterion of catalyst activity, is plotted *vs.* operating time in Figure 3.

During the first operating period (750–950 hrs), the plant was run with the ZnO emergency catchpot on line. Sulfur content could be decreased to 0.04 mg total sulfur/m³ synthesis gas and 0.02 mg H_2S/m³. Conversion in the first 6.3% of the catalyst bed decreased from 50 to 46% while no change in conversion was detectable in the first 23.8% of the bed.

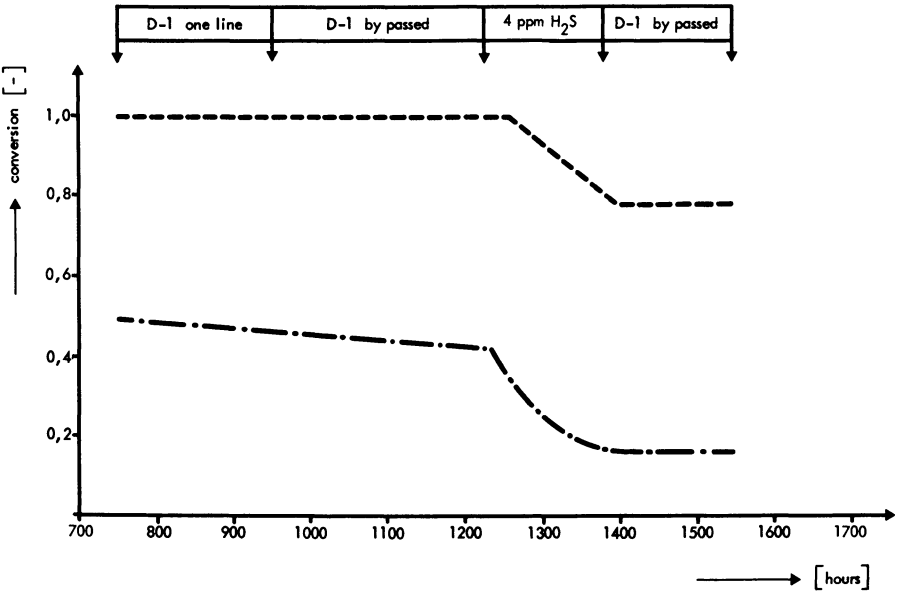

Figure 3. Effect of sulfur poisoning on conversion

No change in deactivation was measured during the second operating period (950–1230 hrs) when the ZnO reactor D1 was bypassed. Conversion in the first 6.3% of the catalyst bed decreased from 46 to 42%.

During the third operating period (1230–1380 hrs), a breakthrough of 4 mg H_2S/m^3 synthesis gas was simulated; this caused an enormous activity loss. The point in the catalyst bed where adiabatic end temperature was reached dropped from 22 to 44% of bed depth while conversion in the first 23.8% of the bed decreased from 100 to 78%.

These tests demonstrated that the Lurgi Rectisol process provides an extremely pure synthesis gas which can be charged directly to the methanation plant without problems of sulfur poisoning of the nickel catalyst. However, in order to cope with a sudden sulfur breakthrough from Rectisol as a result of maloperation, a commercial methanation plant should be operated with a ZnO emergency catchpot on line.

Effect of Temperature and Pressure on Catalyst Activity

The selection of optimum reactor inlet and outlet temperatures is affected by catalyst activity, and catalyst stability, and the need to minimize operating and investment costs. When the special BASF methanation catalyst is used, inlet temperatures of 260°–300°C or even lower are quite acceptable (*see* Table II). The final decision on design inlet temperature is affected by engineering requirements.

The long term tests in the SASOL plant as well as in the Schwechat plant were run with outlet temperatures of 450°C, but both plants were also operated with higher loads that caused reactor outlet temperatures of 470°C or even higher. In comparison with the test run at 450°C, only a slight increase in deactivation rate was detectable which demonstrates the thermostability of the catalyst. From the aspect of thermostability, outlet temperatures of 450°–470°C are acceptable. Further considerations including the possibility of overload operation, the SNG specification to be achieved in final methanation, end-of-run conditions, and cost of reactor material will affect the selection of optimum outlet temperature.

Because of the SNG specification a relatively high pressure is preferred, but compression of synthesis gas was uneconomical compared with final SNG compression. The pressure during methanation is governed by the pressure of gasification and the pressure drop across upstream plants.

Table III. Hydrogen Chemisorption as an Indicator of Catalytically Active Area

Catalyst	*H_2 Adsorption,[a] ml/g*
Fresh reduced	11.2
After H_2–H_2O Treatment	8.0
Used in main methanation	
1000 hrs	4.4 (top)
	6.4 (bottom)
4000 hrs	4.0 (top)
	6.2 (bottom)
Used in final methanation	
4000 hrs	11.0 (middle)

[a] Section of catalyst bed is indicated in parentheses.

Effect of Steam on Catalyst

In addition to actual synthesis tests, fresh and used catalysts were investigated extensively in order to determine the effect of steam on catalyst activity and catalyst stability. This was done by measurement of surface areas. Whereas the Brunauer–Emmett–Teller (BET) area (*4*) is a measure of the total surface area, the volume of chemisorbed hydrogen is a measure only of the exposed metallic nickel area and therefore should be a truer measure of the catalytically active area. The H_2 chemisorption measurement data are summarized in Table III. For fresh reduced catalyst, activity was equivalent to 11.2 ml/g. When this reduced catalyst was treated with a mixture of hydrogen and steam, it lost 27% of its activity. This activity loss is definitely caused by steam since a

catalyst treated with a nearly dry gas for 4000 hrs during final methanation showed no activity loss. In the first 1000 operating hrs, the catalyst again lost 33% of its activity in the top section and 16% in the bottom section of the reactor. This should be called loss of starting activity. In the next 3000 operating hrs, activity loss was extremely low; the catalyst had achieved its stabilized standard activity.

The activity loss measured here is caused by recrystallizations. This was demonstrated by using scanning electron microscopy to determine nickel crystallite size in the same catalyst samples. These tests revealed that the catalyst used in demonstration plants has only a slight tendency to recrystallize or sinter after steam formation and loss of starting activity.

Conclusion

These tests were performed to establish the limits in flexibility and operability of a methanation scheme. The two demonstration plants have been operated in order to determine the optimum design parameters as well as the possible variation range which can be tolerated without an effect on catalyst life and SNG specification. Using a recycle methanation system, the requirements for the synthesis gas concerning H_2/CO ratio, CO_2 content, and higher hydrocarbon content are not fixed to a small range; only the content of poisons should be kept to a minimum. The catalyst has proved thermostability and resistance to high steam content with a resultant expected life of more than 16,000 hrs.

Literature Cited

1. Rudolph, P. F., "The Lurgi Route to Substitute Natural Gas from Coal," Synthetic Pipeline Gas Symp., 4th, Chicago, October 1972.
2. Roger, A., "Supplementing the Natural Gas Supply," South Texas Sect. Mtg., Amer. Soc. Mech. Eng., Houston, April 1973.
3. Moeller, F. W., Roberts, H., Britz, B., "Methanation of Coal Gas for SNG," Hydrocarbon Processing (1974) **53** (4), 69.
4. Wallas, S. M., "Reaction Kinetics for Chemical Engineers," p. 153, McGraw–Hill, New York, 1959.

RECEIVED October 4, 1974.

Design and Operation of Catalytic Methanation in the HYGAS Pilot Plant

WILFORD G. BAIR, DENNIS LEPPIN, and ANTHONY L. LEE

Institute of Gas Technology, Chicago, Ill. 60616

The concept of the HYGAS process for producing a high-Btu pipeline quality gas includes a cold gas recycle methanation step. The overall process and equipment is described. Typical data from the 561 hours of operation are discussed. Space velocities of 3200–4400 scf/ft³ catalyst hr with an essentially sulfur-free feed gas with hydrogen:carbon monoxide ratios of 2.9–16.8 were used in the tests. Carbon monoxide conversion was complete in all tests. No significant deterioration of the Harshaw Ni-0104T catalyst with continued use was observed. The design conditions for subsequent operation of the pilot-plant methanation units, which have changed as a result of the recent steam–oxygen modification of the HYGAS plant, are presented.

The Institute of Gas Technology (IGT) HYGAS process for converting coals of any rank or sulfur content to a substitute natural gas has been under development at IGT since the mid-1950's (*1, 2, 3, 4*). Figure 1 is a simplified flow sheet that indicates the essential steps of the HYGAS process. The coal is first pulverized, dried to a preferred particle size ranging from −10 to +100 U.S. sieve size, and pretreated if necessary (if the coals are agglomerating, they are first pretreated in a low-temperature, atmospheric pressure, air oxidation reactor that eliminates the agglomerating tendencies of the coals). The coal is then passed into the main reactor vessel where it is contacted in a two-stage fluidized bed with synthesis gases of high hydrogen content. The volatile matter and much of the fixed carbon content of the coal is converted directly to methane. Raw product gas from the hydrogasifier contains carbon oxides, unreacted hydrogen, methane, and sulfur compounds (principally hydrogen sulfide) produced by direct hydrogenation of the sulfur in the feed coals.

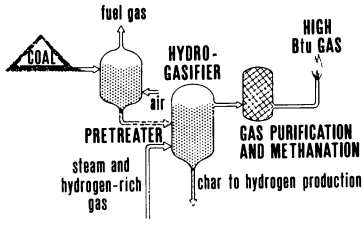

Figure 1. Schematic flow sheet of IGT HYGAS process

The hydrogasification reactor operates at pressures of 1000–1500 psig and at temperatures of 760°–982°C in order to obtain the proper reaction rates and yields of methane required for process optimization. About 50% of the feed carbon is converted to gases in the hydrogasifier.

The residual or ungasified char from the HYGAS process is used to produce hydrogen-rich synthesis gas by the steam–oxygen (5), electrothermal, or steam–iron process. (The first two processes utilize the steam–carbon reaction to produce a high hydrogen content gas.) Figure 2 is a schematic flow sheet of the essential HYGAS process steps incorporating a steam–oxygen gasification reactor that uses spent char from the hydrogasifier to produce synthesis gas.

Raw product gases from the hydrogasifier reactor must, of course, be purified before they can be upgraded to pipeline quality. Purified product gas from the hydrogasifier typically contains 17% carbon monoxide, 53% hydrogen, 30% methane, and traces of ethane, and it has a heating value of about 540 Btu/standard cubic foot (scf) (6). Although this gas would make a very useful gas for a variety of special applications, it does not have the same combustion characteristics as natural gas and cannot be substituted for or interchanged with the natural gas distributed today by long distance transmission lines. Therefore, it is necessary to upgrade this fuel gas to a high heating value, essentially pure methane product that can be interchanged with present day pipeline gas. This is accomplished in the HYGAS process with a cleanup methanation system. The HYGAS process produces approximately two-thirds of the total methane by hydrogenation and about one-third by cleanup methanation.

The methanation of synthesis gas occurs by Reactions 1 and 2 in the absence of carbon formation. With the given hydrogen:carbon monoxide

$$CO + 3H_2 \rightarrow CH_4 + H_2O \qquad \Delta H°_{298°K} = -88{,}700 \text{ Btu/lb mole} \qquad (1)$$

$$CO + H_2O \rightarrow CO_2 + H_2 \qquad \Delta H°_{298°K} = -17{,}700 \text{ Btu/lb mole} \qquad (2)$$

ratio and concentrations of water and carbon dioxide in the feed to the methanation reactors, very low concentrations of unreacted carbon monoxide and hydrogen can be obtained that meet pipeline gas standards. Carbon deposition is unlikely with a hydrogen:carbon monoxide ratio greater than two at temperatures of 288°–482°C although equilibrium calculations with carbon in the form of graphite place the value of the limiting ratio at approximately 2.6 (*7*, *8*, *9*). One of the principal problems in converting high concentrations of carbon monoxide and hydrogen to methane has been to control the exothermic heat of reaction to a useful and acceptable level.

Nickel catalysts were used in most of the methanation catalytic studies; they have a rather wide range of operating temperatures, approximately 260°–538°C. Operation of the catalytic reactors at 482°–538°C will ultimately result in carbon deposition and rapid deactivation of the catalysts (*10*). Reactions below 260°C will usually result in formation of nickel carbonyl and also in rapid deactivation of the catalysts. The best operating range for most fixed-bed nickel catalysts is 288°–482°C. Several schemes have been proposed to limit the maximum temperature in adiabatic catalytic reactors to 482°C, and IGT has developed a cold-gas recycle process that utilizes a series of fixed-bed adiabatic catalytic reactors to maintain this temperature control.

Description of the Cold-Gas Recycle Process and Pilot-Plant Equipment

The diagram of the IGT cold-gas recycle process includes four reactor stages in series (Figure 3). Note that the concept can be applied to any number of stages.

Fresh feed that has the proper hydrogen:carbon monoxide ratio (*i.e.*, slightly above the 3:1 minimum stoichiometric ratio) is mixed with recycle gas and sent through a heat exchanger and into the first catalyst bed, Stage I. The space velocity in Stage I is controlled so that all of the carbon monoxide fed to it is completely converted. The inlet gases are

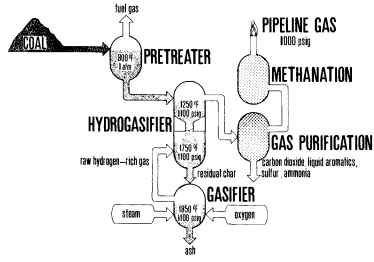

Figure 2. IGT HYGAS process —steam–oxygen gasification

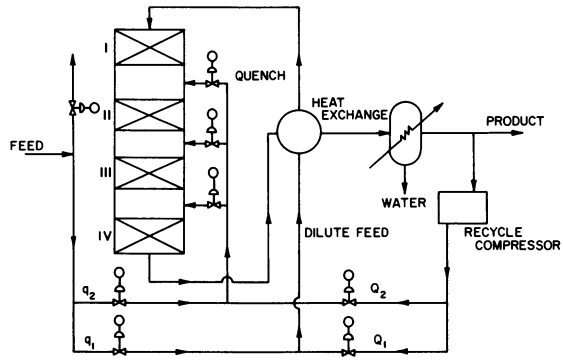

Figure 3. IGT cold-gas recycle methanation system

preheated to about 288°C before being introduced into Stage I, and the carbon monoxide concentration in the total feed to Stage I is controlled so that the outlet temperature is limited to a maximum of 482°C. Since the maximum reactor temperature is reached when all of the carbon monoxide is reacted, the temperature can be regulated by controlling the carbon monoxide concentration in the fresh feed gases to any stage of this multistage reactor system. All of the reaction products from Stage I are mixed at 482°C with fresh feed and recycle gas in the proper proportions so that (a) the temperature of the total gas mixture is reduced to about 288°C and (b) the carbon monoxide concentration in the feed gas to the second-stage reactor is limited to about 4–4.5 mole %.

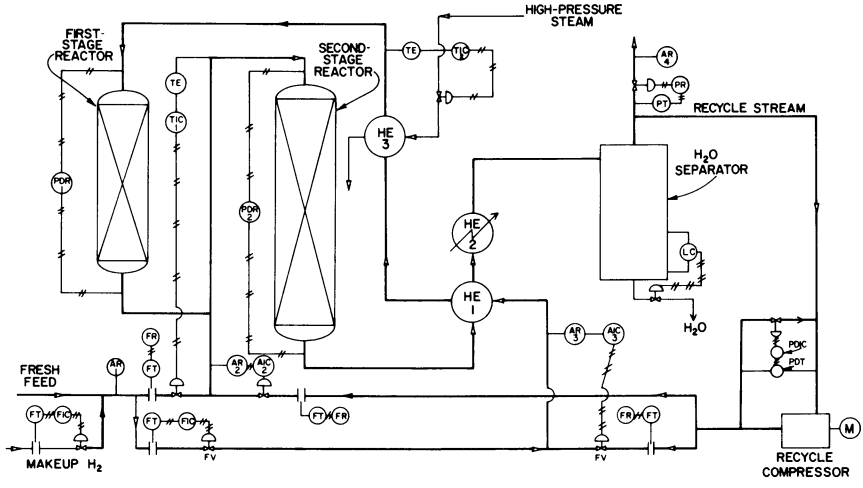

Figure 4. Diagram of methanation section of HYGAS pilot plant

The same ratio of fresh feed to recycle gas is used in all subsequent stages of the system. Note that although the ratio of fresh feed to recycle gas does not change for all succeeding stages, the amount of feed plus recycle gas to be added at interstage points increases geometrically (1:2:4:8:16 . . .) as stages are added to the process (*6*). Therefore, in order to maintain the same fresh feed space velocity for all stages or the same fresh feed plus recycle gas space velocity, the catalyst volume must be increased in the same ratio for all succeeding stages.

The IGT multistage cold-gas recycle methanation process has a built-in temperature control mechanism and a low recycle ratio. Much less recycle gas is used in this multistage operation than would be required if the same amount of conversion were achieved in a single vessel with all fresh feed and recycle gas added at the inlet to one large catalytic reactor.

Figure 4 is a schematic flow diagram of the methanation section of the HYGAS pilot plant in which there are two reactor stages in series. As was mentioned, any subsequent reactor stages require feed gases with identical hydrogen-to-carbon monoxide and recycle gas-to-fresh feed ratios. The HYGAS plant's methanation section was limited to two stages since additional ones would not alter the stoichiometry or process instru-

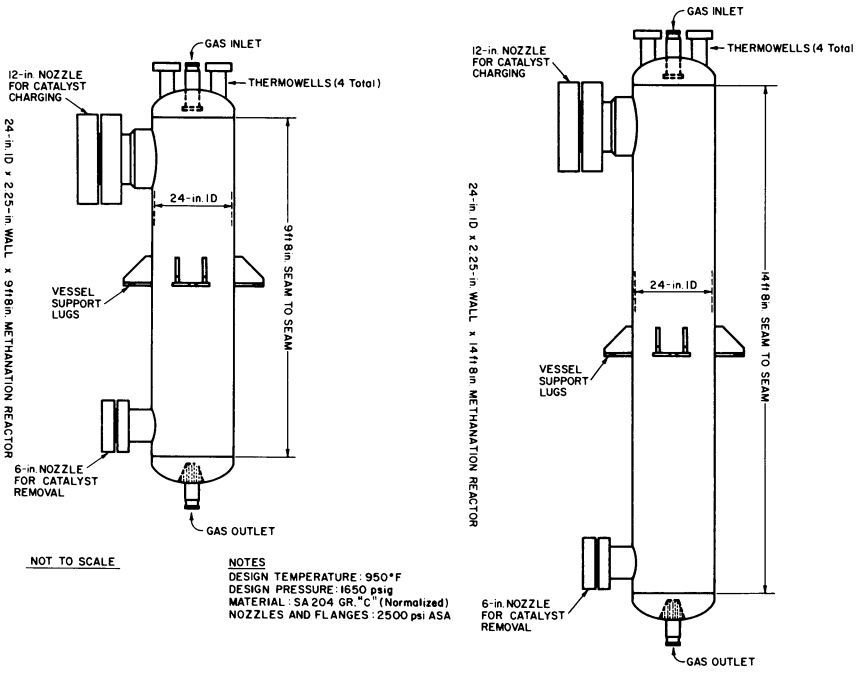

Figure 5. Details of HYGAS methanation reactor

mentation. Additional stages can be added in the future if necessary for our experimental program.

The two 24-in. i.d. catalytic reactors (Figure 5) were fabricated from type A204 grade C steel (carbon, 0.5% molybdenum alloy) which was selected for its resistance to hydrogen embrittlement at the operating temperatures and pressures. The reactors were constructed in accordance with Section VIII, Division 1 of the ASME code for unfired pressure vessels; they are designed for a pressure of 1650 psig at 510°C. The reactors are installed vertically in the pilot plant. There is a 6-in. handhole at the base of the vessel for removing the catalyst and catalyst support and a 12-in. handhole at the top of the reactor for charging catalysts and inert catalyst hold-down layers. The first-stage reactor was designed for a catalyst volume of 15.7 ft^3 which corresponds to a 5-ft bed depth at the full 24-in. i.d. The construction of the second-stage reactor is identical to that of the first except that it has a longer shell holding a 10-ft deep catalyst bed and twice the catalyst volume (31.4 ft^3) of the first-stage reactor.

Since temperature control was one of the primary experimental objectives of the cold-gas recycle deisgn test program, the reactors were completely instrumented to obtain temperature profiles. A total of 24 thermocouples are arranged in four thermowells that enter through the top of each reactor (Figure 6). The six thermocouples in each well are spaced vertically every 2.5 in. in the 5-ft-deep catalyst bed and every 5.0 in. in the 10-ft-deep catalyst bed. The thermocouple locations are arranged among the four thermowells to form a complete spiral ascending pattern. The catalyst charge is centered in each reactor by inert 0.75-in. diameter alumina balls located above and below the active catalyst bed that serve as gas distributors to ensure an even flow of gas to the catalyst bed and as a catalyst support. The catalyst used is a commercially available nickel-on-kieselguhr type (Ni-0104T) manufactured by Harshaw as ¼ × ¼ in. cylindrical pellets.

The schematic flow diagram (Figure 4) of the methanation system at the HYGAS plant includes the principal instrumentation and control systems. If the hydrogen:carbon monoxide ratio of the fresh feed gas is not at the proper stoichiometric ratio (minimum value, 3.1:1), then makeup hydrogen can be added from an outside source to adjust the hydrogen:carbon monoxide ratio to the desired level. The HYGAS pilot plant does not have a water–gas shift reactor to adjust the hydrogen:carbon monoxide ratio. The carbon monoxide content is first monitored at AR-1 by a continuous-recording IR analyzer; the flow is then split, a portion being directed as fresh feed to the first-stage reactor, and the remainder going as fresh feed to the second-stage reactor. The fresh feed to the first stage is metered and then mixed with recycle gas from

the recycle compressor. A continuous IR recorder controller, AR-3, controls the amount of recycle gas that is mixed with the fresh feed. AR-3 is set to maintain a 4–4.5% carbon monoxide content in the gases fed to the first-stage reactor. The total gas feed stream to the first stage is passed through an exchanger, HE-1, for preheating of the feed gases with the effluent gases from the second-stage reactor to a temperature of 288°C. HE-3 is a steam heater that is used for start-up only, before sufficient heat of reaction is developed for operation of the feed effluent exchanger HE-1.

The hot gas mixture passes to the first-stage reactor where carbon monoxide is completely converted to methane and water, and the temperature rise is controlled to stay below a maximum of 194°C. The product gases—methane, unreacted hydrogen, and water—exit from the base of the first-stage reactor; they are mixed with additional fresh feed plus recycle gases and sent to the second-stage reactor inlet. Hot product gases from the second-stage reactor (exiting at 482°C) go through the feed–effluent exchanger and then to HE-2, an aftercooler, to condense all the water vapor and to reduce the temperature of the final product gas to 66°C (150°F). In the HYGAS plant, HE-2 is an air-cooled heat

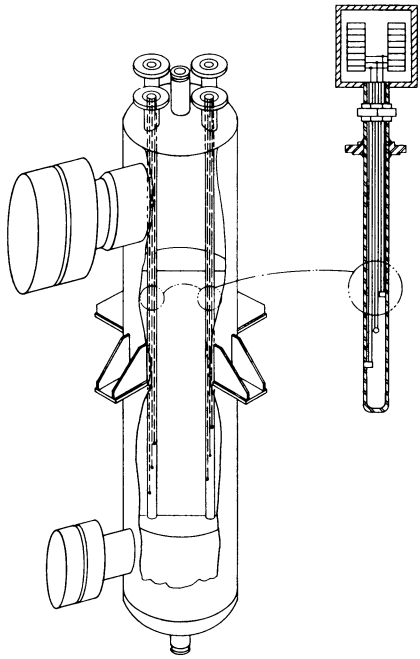

Figure 6. Details of thermowell of the HYGAS methanation reactors

Table I. Activity Tests for Harshaw

Variable	*Test Duration, hrs*					
	19	*80*	*217*	*288*	*421*	*464*
Pressure, psig	1000	1005	1003	1000	1006	1000
Temperature, °C						
preheater	346	338	333	329	319	224
1.5 in. from top	377	371	368	363	351	260
4 in. from top	457	471	468	465	476	449
product gas	335	335	333	326	319	304
furnace	307	304	302	288	232	257
Feed gas composition (dry), mole %						
CO	4.3	4.0	4.0	3.5	4.0	4.0
CO_2	1.5	1.4	1.4	1.0	0.8	0.8
H_2	18.8	19.4	19.4	18.8	20.1	20.1
CH_4	70.1	69.3	69.3	70.0	69.0	69.0
C_2H_6	2.7	2.7	2.7	3.4	3.7	3.7
N_2	2.62	3.22	3.22	3.25	2.39	2.39
Total	100.02	100.02	100.02	99.95	99.99	99.99
Space velocity, scf/ft³ hr	2539	2590	2599	2596	2619	4704
Feed rate, scf/hr	8.99	9.12	9.15	9.14	9.22	16.56
Product gas composition (dry), mole %						
CO	0.2	0.1	0.2	0.1	0.1	0.0
CO_2	0.9	1.0	1.0	0.8	0.6	0.1
H_2	1.8	1.8	1.7	1.4	1.5	1.6
CH_4	93.6	93.5	93.6	94.4	94.2	94.9
C_2H_6	0.2	0.1	0.2	0.2	0.2	0.1
N_2	3.34	3.53	3.33	3.12	3.4	3.29
Total	100.04	100.03	100.03	100.02	100.00	99.99
Product, scf/scf feed	0.77	0.77	0.77	0.78	0.78	0.82
Heating value, Btu/scf	942	940	941	948	950	955
Carbon recovery, %	90.8	92.1	92.6	92.6	92.2	96.3
Hydrogen recovery, %	91.3	91.5	92.0	90.9	91.5	96.3
Oxygen recovery, %	94.5	97.8	101.8	90.5	109.8	100.9
Total material recovery, %						
Water collected by condensate measurement, g/hr	10.40	9.88	10.37	7.26	10.24	19.62
CO conversion, %	96.3	98.0	96.1	97.7	98.0	100.0
CO_2 conversion, %	53.4	44.4	44.3	37.0	41.0	89.7
C_2H_6 conversion, %	94.2	97.1	94.2	95.3	95.7	97.7

[a] Run LT-H; catalyst volume, 0.00352 ft³.

exchanger specifically installed to determine operating limits and overall effectiveness of this type of equipment. After passing through the final product gas cooler, condensed water is separated, and the cooled, dry product gas is reduced in pressure through a pressure control valve and is sampled by a continuous IR analytical instrument (AR-4) that monitors the carbon monoxide content of the product gas. The high Btu product gas is then available for utilization in the HYGAS plant's fuel system, or it can be sent to the flare for disposal.

Experimental Test Operations of the HYGAS Methanation Units

Catalyst Section. The design criteria for the HYGAS plant methanation section were developed in the late 1960's (*10*). At that time, three commercially available nickel methanation catalysts and one ruthenium

Ni-0104T Methanation Catalyst[a]

Test Duration, hrs										
558	*653*	*771*	*820*	*986*	*1109*	*1152*	*1250*	*1320*	*1391*	*1420*
1000	1003	998	1014	1005	1003	1000	1006	1006	1000	1010
285	241	254	249	232	263	249	296	244	280	268
316	280	268	285	266	296	288	330	282	316	313
449	449	421	432	393	432	410	482	388	457	424
285	326	252	330	321	343	379	338	410	340	441
257	249	218	249	244	268	274	282	282	274	316
4.0	4.0	3.7	3.8	4.2	3.7	3.7	3.7	3.7	3.7	3.7
0.8	0.8	0.7	0.6	0.6	0.8	0.8	1.0	1.0	1.0	1.0
20.1	21.3	2.13	19.8	20.0	18.9	18.9	19.6	19.6	19.6	19.6
69.0	68.0	68.0	71.9	72.2	72.6	72.6	71.7	17.7	71.7	71.7
3.7	3.7	3.7	1.2	1.1	0.9	0.9	0.9	0.9	0.9	0.9
2.39	2.56	2.56	2.73	1.94	3.09	3.09	3.06	3.06	3.06	3.06
99.99	99.96	99.96	100.03	100.04	99.99	99.99	99.96	99.96	99.96	99.96
2551	4798	2619	4803	5284	4832	6852	4193	8664	4383	9130
8.34	16.89	9.24	16.91	18.60	17.01	24.12	14.76	30.50	15.43	32.14
0.1	0.1	0.1	0.1	0.1	0.00	0.1	0.1	0.1	0.1	0.1
0.2	0.1	0.1	0.00	0.00	0.1	0.1	0.1	0.3	0.2	0.5
1.5	2.1	3.3	2.8	4.2	3.0	3.3	2.6	3.3	2.4	4.0
95.0	94.3	92.9	93.9	92.5	93.3	92.9	93.4	92.6	93.3	91.5
0.1	0.1	0.4	0.00	0.00	0.00	0.00	0.1	0.00	0.00	0.00
3.07	3.25	3.17	3.16	3.16	3.55	3.56	3.66	3.74	4.03	3.89
99.97	99.95	99.97	99.96	99.96	99.95	99.96	99.96	100.04	100.03	99.99
0.64	0.80	0.88	0.86	0.84	0.82	0.82	0.82	0.80	0.83	0.80
957	947	949	952	940	949	944	941	932	938	922
76.6	97.6	103.7	103.4	98.6	98.1	97.6	99.3	95.9	100.3	94.4
76.3	94.0	102.9	101.8	97.7	96.8	96.5	96.9	94.2	97.5	93.0
81.7	105.7	114.5	105.5	78.8	84.9	90.5	67.3	81.5	65.0	89.8
			103.0	98.6	96.9	96.8	96.7	94.8	98.0	94.3
8.34	19.00	11.15	18.96	16.80	15.98	23.69	11.67	26.89	10.97	24.47
98.3	97.8	97.6	97.3	97.9	100.0	97.7	97.7	97.8	97.7	97.8
83.8	88.5	87.3	100.0	100.0	89.6	89.6	91.7	75.7	81.3	59.8
98.2	97.8	90.4	100.0	100.0	100.0	100.0	89.6	100.0	100.0	100.0

catalyst were evaluated on the basis of the effects of (a) activity; (b) upper and lower operating temperature limits; (c) pore diffusion; (d) hydrogen:carbon monoxide ratios; (e) presence of excess methane, benzene, carbon dioxide, and nitrogen; and (f) their resistance to poisons such as ammonia, hydrogen sulfide, ethyl mercaptan, thiophene, and carbonyl sulfide. The experimental procedures and the findings from these studies have been published (*11*, *12*).

IGT selected Harshaw Ni-0104T nickel-on-kieselghur catalyst formed in ¼ × ¼ in. cylindrical pellets for the initial catalyst charge to the methanation section of the HYGAS pilot plant. This selection was based on high activity over a range of temperatures (274°–516°C) and space velocities. Catalyst activity life tests were conducted for 1420 hrs without deterioration (Table I); consequently, we felt that suitable longevity could be obtained in the pilot-plant methanation reactors.

Table II. Typical Reformed Natural Gas

Component	*Content, mole %*
H_2	97.7
CO	1.6
N_2	0.6
CH_4	0.1
Total	100.0

The space velocity was varied from 2539 to 9130 scf/hr ft^3 catalyst. Carbon monoxide and ethane were at equilibrium conversion at all space velocities; however, some carbon dioxide breakthrough was noticed at the higher space velocities. A bed of activated carbon and zinc oxide at 149°C reduced the sulfur content of the feed gas from about 2 ppm to less than 0.1 ppm in order to avoid catalyst deactivation by sulfur poisoning. Subsequent tests have indicated that the catalyst is equally effective for feed gases containing up to 1 mole % benzene and 0.5 ppm sulfur (5). These are the maximum concentrations of impurities that can be present in methanation section feed gases.

Methanation Section Test Conditions. To date, the HYGAS pilot plant has been operated with Montana lignite coal feed. This lignite is a low sulfur (usually less than 1 wt %) coal which has good reactivity for hydrogasification. The coal is nonagglomerating (thus eliminating the need for pretreatment), and it represents the lowest rank of U. S. coals that are available for conversion to substitute natural gas.

In all operations to date, the HYGAS plant has used a synthesis gas made up of a mixture of reformed natural gas and steam. The reformed natural gas stream has been processed through a water–gas shift reactor and an amine–carbon dioxide removal step; it has a very high hydrogen content (Table II). In 27 experimental runs, this source of synthesis gas was used. Total operating time for coal feed was 2400 hrs, and approximately 2800 tons of coal were processed. During much of this operating time, primary attention has focused on the operation of the hydrogasifier itself and on solving throughput problems (3).

The methanation section was operated for a total of 561 hrs. The runs, test duration, and total coal feed during methanation testing are summarized in Table II.

Note that the methanation section is the last processing step in the HYGAS pilot plant, and it depends on the steady-state troublefree operation of the preceding steps (the gasification reactor, amine purification, and caustic wash sections for cleanup sulfur removal) before it can be brought on-line.

We have imposed an additional restriction on the operation of the pilot plant methanation section. We must have accurate and continuous

analysis of the total sulfur content of the feed-gas stream to the methanation section. This is effected with a specially developed, on-line gas chromatograph that analyzes for specific sulfur compounds in the parts per billion (ppb) concentration range (*13*). This chromatograph is used on the purified feed-gas stream to the methanation section; it automatically analyzes for total sulfur level as well as for several individual sulfur species. The feed gas to the methanation section normally contains 0.1–0.2 ppm total sulfur compounds. Gas feed to the section is interrupted if the total sulfur content of the feed gases exceeds 0.5 ppm. This latter condition might result from improper operation of the amine-type acid–gas removal system or the final sulfur cleanup section—a 10% caustic solution gas-scrubbing process. When the gas purification section is operating normally, the amine scrub will remove sulfur compounds to the 1.0–0.5 ppm level with the caustic wash section effecting removal to the 0.1–0.2 ppm level.

Pilot Plant Methanation Test Data. Detailed analysis of typical operating periods from four of the pilot plant runs are presented in Table IV. A relatively high hydrogen:carbon monoxide ratio has been typical with resultant high residual concentrations of hydrogen and therefore low product gas heating values. The carbon monoxide concentration was also low, which resulted in moderate temperature rises in the first-stage reactor and in even smaller temperature differences in the second-stage reactor. The low carbon monoxide concentrations are primarily the result of low solids feed rates, typically ⅓–½ of design (the design rate is 3 tons/hr). In run 19, the coal feed rate was near design conditions—the hydrogen:carbon monoxide ratio was 2.9:1, and a high-Btu gas was produced. The indicated nitrogen content of the product gas comes from an air–hydrogen auxiliary burner which was operated during most of the lignite coal tests to make up for the low temperature of the synthesis gas to the hydrogasifier. The nitrogen content of the combustion

Table III. Summary of Pilot Plant Methanation Operations

Run No.	*Total Time of Coal Slurry Feed, hrs*	*Total Coal Feed, tons*	*Methanation Section Operating Time, hrs*
15	66	87	49
16	138	181	132
17	86	89	5
19	159	285	130
23	93	81	84
24	132	165	24
27	433	680	137
Total	1107	1568	561

gases mingled with the raw product gases resulted in a high nitrogen content.

In all tests, the temperature in the first- and second-stage reactors was kept within the necessary temperature limits of 288°–482°C. Because the carbon monoxide concentration was low in many of the tests, the second stage was not used to full capacity as is indicated by the temperature rise in runs 23, 24, and 27. The temperature profile shows the characteristic rise to a steady value. With the space velocities used (<5000 ft^3/ft^3 hr), the temperature profile is fully developed in the first stage within 30.0 in. of the top of the catalyst bed. A characteristic dip in temperature was observed over the first 8–10 in. of the catalyst bed in all runs. This temperature profile may indicate the presence of deactivated catalyst in this region, but, until the catalyst can be removed for examination, the cause of the temperature drop cannot be determined. There is no evidence that this low temperature zone is becoming progressively deeper. It is possible that an unrecorded brief upset in the purification system may have poisoned some of the top catalyst layers.

In run 19, where considerable carbon monoxide conversion was obtained in both stages, the recycle ratio was 1.48 scf recycle gas per scf feed gas. Recycle ratios in the other tests varied from 1.14 to 1.30. The design recycle ratio is 1.67 for lignite coal feed with hydrogen/steam synthesis gas.

In all operations to date, carbon monoxide conversion has been

Table IV. Selected Operating Data from HYGAS Pilot Plant Methanation Tests

Variable	*Run Number*[a] *27*	*24*	*23*	*19*
Pressure, psig	982	978	1024	1013
First-stage reactor conditions				
space velocity, vol/vol hr	4397	3288	4380	3220
feed gas flow rate, lb/hr	745	753	1024	633
recycle flow rate, lb/hr	1369	1305	1376	1674
recycle molecular weight	11.8	15.9	14.1	18.7
reactor temperatures, °C				
in (total feed)	289	293	292	287
out (effluent)	370	397	419	432
ΔT across reactor	81	104	127	145
maximum temperature observed (average)	387	402	431	454
depth of maximum temperature, ft	2.5	1.7	1.7	1.0
average catalyst temperature (after maximum is reached)	374	397	419	443
bed pressure drop, in. H_2O/ft depth	0.76	—	0.99	1.11

Variable	*Run Number*[a] *27*	*24*	*23*	*19*
Second-stage reactor conditions				
space velocity, vol/vol hr	2554	2024	2732	1720
feed gas flow rate, lb/hr	383	333	587	428
recycle flow rate, lb/hr	—	125	255	367
recycle molecular weight	—	15.9	14.1	18.7
reactor temperatures, °C				
in (total feed)	278	295	292	283
out (effluent)	296	332	359	382
ΔT across reactor	18	37	67	99
bed pressure drop, in. H_2O/ft depth	0.74	1.03	1.22	1.31
Overall results				
CO conversion, total moles/hr	3.7	3.9	6.6	8.8
H_2 CO ratio in feed	16.8	8.4	9.6	2.9[b]
product gas heating value, Btu/scf[c]	485	677	575	916
recycle ratio, ft^3 recycle/ft^3 feed	1.14	1.15	1.30	1.48
feed gas composition,[d] mole %				
H_2	60.00	43.13	50.45	34.57
C_2H_6	0.17	0.62	0.59	—
Ar	0.27	0.33	0.32	0.15
N_2	25.96	30.16	26.19	22.66
CH_4	10.02	20.62	17.10	30.72
CO	3.58	5.14	5.27	11.90
molecular weight	11.25	14.38	12.91	15.36
product gas composition,[d] mole %				
H_2	54.77	31.34	40.52	7.68
C_2H_6	0.01	—	—	—
Ar	0.29	0.39	0.44	0.23
N_2	28.20	34.98	30.64	30.56
CH_4	16.74	33.29	28.41	61.56
molecular weight	11.80	15.93	14.13	18.67
product gas pressure, psig	901	857	879	895

[a] Run 27: 3/19/74 (2207)–3/20/74 (0294); run 24: 10/31/73 (1205–1997); run 23: 10/13/73 (0804–1996); run 19: 6/28/73 (0766–1219).
[b] Before hydrogen addition to ensure complete carbon monoxide conversion.
[c] Saturated at 30 in. mercury and 15.6° C; nitrogen-free basis.
[d] Total gas composition = 100.00%.

complete. The gases were analyzed with an on-line gas chromatograph which can detect 0.05 mole % carbon monoxide.

The automatic controls, which split the feed and recycle to the two reactors so that the temperature reached in each stage does not exceed 482°C, were operated for a considerable portion of the total on-stream time of the methanation section. They performed quite satisfactorily.

To summarize the test results, the HYGAS methanation section has operated satisfactorily. Carbon monoxide conversion has been complete. The cold-gas recycle system was completely adequate for temperature

control, and there was no indication of a continued trend of loss of catalytic activity.

Steam–Oxygen Modification of the HYGAS Plant

The HYGAS plant was recently modified to conduct nonslagging steam–oxygen gasification for synthesis gas production. A 30% carbon monoxide concentration and a hydrogen:carbon monoxide ratio of 1.7 are expected in the purified product gas. Because the plant was not built with a shift converter, process hydrogen from the natural gas reformer will be added to bring the hydrogen:carbon monoxide ratio to the design value for feed to the methanation section. The steam–oxygen modification has obviated the need for an air–hydrogen auxiliary heater, which previously accounted for the large percentage of nitrogen (>20%) in the methanation feed. The design conditions for this mode of operation of the methanation section are listed in Table V.

The objective of this phase of the methanation system's operation is to determine space velocity requirements, recycle ratio, and analytical and control systems.

Table V. HYGAS Methanation Pilot Plant Design Conditions[a]

Stream Description	*Flow, scf/hr*	*Molecular Weight*	*Nominal Constituents,[b] mole fraction*		
			CO	H_2	CH_4
Total feed from caustic scrubber	20,395	12.51	0.294	0.503	0.203
Hydrogen addition	9,320	2.28	0.01	0.99	—
First-stage fresh feed	10,348	9.30	0.205	0.656	0.139
First-stage recycle	36,776	14.55	—	0.106	0.894
Second-stage fresh feed	19,367	9.30	0.205	0.656	0.139
Second-stage recycle	25,945	14.55	—	0.106	0.894
Product gas	11,446	14.55	—	0.106	0.894
Water from knockout drum	289.2[c]	—	—	—	—

[a] Lignite/steam–oxygen case with H_2:CO = 3.2; space velocity = 3000 scf/ft³ catalyst hr.
[b] Trace quantities of CO_2, C_6H_6, C_2H_6 have not been included in this material balance.
[c] In lbs.

Acknowledgment

The methanation system tests described here were done under a development program sponsored by the Energy Research and Development Administration and the American Gas Association.

Literature Cited

1. "HYGAS: 1964 to 1972, Pipeline Gas From Coal Hydrogasification (IGT Hydrogasification Process)," Final Report HYGAS 381, Washington, D.C.
2. Institute of Gas Technology, "Production of Pipeline Gas by Hydrogasification of Coal," *Inst. Gas Technol. Res. Bull.* (1972) **39.**
3. Lee, B. S., Lau, F. S., "Results from HYGAS Development," Amer. Inst. Chem. Eng., Nat. Mtg., 77th, Pittsburgh, June, 1974.
4. Lee, B. S., "Status of HYGAS Process—Operating Results," Amer. Gas Ass., Synthetic Gas Pipeline Symp., 5th, Chicago, October, 1973.
5. Punwani, D., Pyrcioch, E. J., Johnson, J. L., Tarman, P. B., "Steam–Oxygen–Char Gasification in a Non-Slagging Fluid Bed., Joint Amer. Inst. Chem. Eng.–Gesellschaft Verfahrenstech. Chemieing. Mtg., Munich, September, 1974.
6. Schora, F. C., Matthews, C. W., "Analysis of a HYGAS Coal Gasification Plant Design," Amer. Inst. Chem. Eng., Ann. Mtg., New York, November, 1972.
7. Dent, F. J., *et al.*, "An Investigation into the Catalytic Synthesis of Methane for Town Gas Manufacture," *Gas Res. Board Commun.* (1948) **GRB 20/10.1.**
8. Dirksen, H. A., Linden, H. R., "Pipeline Gas From Coal by Methanation of Synthesis Gas," *Inst. Gas Technol. Res. Bull.* (1963) **31.**
9. Greyson, M., *et al.*, "Synthesis of Methane," *U.S. Bur. Mines Bull.* (1955) **RI 5137.**
10. Lee, A. L., "Methanation for Coal Gasification," Clean Fuels from Coal Symp., Chicago, September, 1973.
11. Lee, A. L., Feldkirchner, H. L., Tajbl, D. G., "Methanation for Coal Hydrogasification," Amer. Chem. Soc., Fuel Chem. and Div. Petrol. Chem., Joint Mtg., Chicago, September, 1970.
12. Tajbl, D. G., Feldkirchner, H. L., Lee, A. L., "Cleanup Methanation for Hydrogasification Process," *Amer. Chem. Soc., Div. Fuel Chem. Prepr.* **10,** 235–245 (1966) September.
13. Anderson, G. L., Olson, D. P., unpublished data.

RECEIVED October 4, 1974. The methanation system tests described here were done under a development program sponsored by the Energy Research and Development Administration and the American Gas Association.

8

The RMProcess

G. A. WHITE, T. R. ROSZKOWSKI, and D. W. STANBRIDGE

The Ralph M. Parsons Co., Pasadena, Calif. 91124

The RMProcess is a methanation scheme which catalytically converts mixtures of carbon oxides to methane at high temperatures without recycle. Syngas mixed with steam is directed over methanation catalysts contained in a series of adiabatic fixed bed reactors at progressively lower temperatures. Shift conversion occurs simultaneously with methanation, thereby eliminating the need for any pretreatment to achieve a stoichiometric feedstock mix and permitting removal of carbon dioxide in a single stage. Carbon formation is avoided completely by using steam and operating at high temperatures. This methanation process was developed to allow direct handling of gases high in CO content, e.g. *those generated by coal or heavy oil gasification, at pressures ranging from atmospheric to > 1000 psig.*

Current specifications for pipeline gas dictate that most gasification processes upgrade their crude syngas by a methanation stage. Upgrading reduces the concentrations of hydrogen and carbon monoxide while increasing the heating value of each cubic foot of gas. The RMProcess has the unusual capability of upgrading by methanation, without recycle, a crude syngas consisting of approximately 50% hydrogen, 50% carbon monoxide, and < 1% methane. The process has exceptionally wide applicability for gases produced by any coal gasification system at pressures from near atmospheric to > 1000 psig.

Process Description

Desulfurized syngas flows through a series of fixed-bed, adiabatic catalytic reactors. Between reactors, heat is removed from the system by the generation of high pressure steam in conventional heat-exchange equipment. As the flow progresses through the series of reactors and exchangers and the bulk of the syngas is methanated, the temperature of

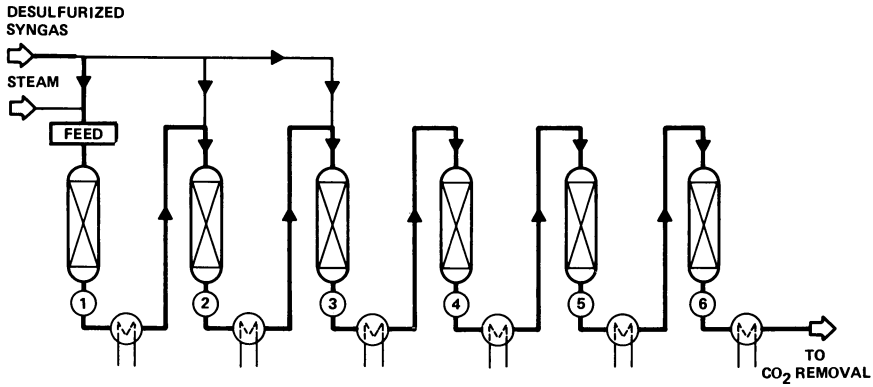

Figure 1. Bulk methanation

the process gas is progressively lowered until it finally reaches an adequately reduced level that is favorable for high efficiency conversion of hydrogen and carbon oxides to methane.

The series of reactors and exchangers which methanates a raw syngas without pretreatment other than desulfurization is collectively termed bulk methanation. The chemical reactions which occur in bulk methanation, including both shift conversion and methanation, are moderated by the addition of steam which establishes the thermodynamic limits for these reactions and thereby controls operating temperatures. The flow sequence through bulk methanation is shown in Figure 1.

Example at 400 psia

The conditions selected for this illustration include desulfurized syngas available at 371°C and 400 psia that consists of 49.8% hydrogen, 49.8% carbon monoxide, 0.1% carbon dioxide, and 0.3% methane. Forty percent of this syngas is mixed with superheated steam and the mixture enters the first bulk methanator at 482°C. The principal reaction occurring in this reactor is shift conversion with only a minor degree of methanation. The first reactor effluent is cooled and mixed with an additional 30% of the syngas to give a temperature of 538°C into the second bulk-methanation reactor. The second reactor effluent is cooled by steam generation; then it is mixed with the remaining 30% of the syngas to give a temperature of 538°C to the feed to the third reactor. In the fourth, fifth, and sixth reactors, the inlet temperatures are controlled at 538°, 316°, and 260°C respectively which results in a bulk-methanated product gas. *See* Table I for product gas composition and the operating temperatures and pressures for each reactor in bulk methanation. The residual hydrogen content of the effluent from the sixth reactor is $<$ 10 vol % on

Table I. Methane Production at 400 psia

	Feed to Reactor	*Effluent at Outlet of Reactor*					
	1	*1*	*2*	*3*	*4*	*5*	*6*
Composition,[a] vol %							
H_2	49.80	54.53	48.07	43.09	36.90	22.86	9.29
CO	49.80	13.97	18.46	20.63	15.25	5.64	.87
CO_2	0.10	25.80	24.04	23.64	29.21	39.90	46.84
CH_4	0.30	5.70	9.43	12.64	18.64	31.60	43.00
Steam/gas	1.20	0.88	0.56	0.43	0.50	0.65	0.83
Pressure, psia	397	387	372	357	342	327	312
Temperature, °C	482	773	779	773	717	604	472

[a] Total = 100.00%.

a dry basis. Such a gas can then be methanated in a final dry stage after carbon dioxide removal to reduce the hydrogen content to $< 3\%$ with $< 0.1\%$ carbon monoxide.

Example at Low Pressure

Data for the RMProcess operating at near atmospheric pressure are presented in Table II. Inlet pressure to the first bulk-methanation reactor is 65 psia, and the outlet pressure from the sixth reactor is 22 psia. In this case, all the syngas is introduced into the first bulk-methanation reactor together with all the steam. Because the driving force for methanation is proportionately lower at the lower pressure, the outlet temperature of even the first reactor is $< 760°C$. Significantly, the effluent gas from the sixth reactor has a hydrogen content on a dry basis of only 12.1% at 22 psia compared with 9.3% when operation is at 312 psia. This relatively small difference is not entirely surprising in view of the lower operating temperature and the large excess of carbon dioxide present in each case which tends to mask the difference in operating pressure.

Design Features

Whether operation is at high or low pressures, reactor outlet and inlet temperatures are all conveniently high for the economical generation of 1500 psig steam in conventional heat-exchange equipment. Of the total steam produced, approximately one-third is used in the RMProcess to effect shift conversion, methanation, and carbon dioxide regeneration. The mechanical energy of even the portion of produced steam that is needed for operating the process will provide part of the total power requirement of a coal gasification complex by using back-pressure turbines. The bulk of the steam produced, approximately two-

thirds of the methanation heat, is available as export steam at 1500 psig for any services within the complex.

There is no separate shift conversion system and no recycle of product gas for temperature control (*see* Figure 1). Rather, this system is designed to operate adiabatically at elevated temperatures with sufficient steam addition to cause the shift reaction to occur over a nickel catalyst while avoiding carbon formation. The refractory lined reactors contain fixed catalyst beds and are of conventional design. The reactors can be of the minimum diameter for a given plant capacity since the process gas passes through once only with no recycle. Less steam is used than is conventional for shift conversion alone, and the catalyst is of standard ring size (⅝ × ¼ in).

Avoiding Zones of Carbon Formation

Various design and operating problems have been experienced by most developers of methanation systems. Specifically, carbon formation and catalyst sintering are two of the more common problems in methanation processes. Carbon formation refers to the potential production of carbon from carbon oxides and methane by the following reactions.

$$2CO \longrightarrow CO_2 + C$$
$$CO + H_2 \longrightarrow H_2O + C$$
$$CO_2 + 2H_2 \longrightarrow 2H_2O + C$$
$$CH_4 \longrightarrow 2H_2 + C$$

The conditions favorable for carbon formation from these sources can be predicted by straightforward thermodynamic calculations. However, because a number of other chemical reactions can occur simultaneously and

Table II. Methane Production at 65 psia

	Feed to Reactor	*Effluent at Outlet of Reactor*					
	1	*1*	*2*	*3*	*4*	*5*	*6*
Composition,[a] vol %							
H_2	49.80	54.38	50.36	46.50	36.29	24.00	12.05
CO	49.80	25.37	20.42	16.27	8.24	2.69	0.49
CO_2	0.10	17.29	21.99	26.06	34.62	41.83	46.45
CH_4	0.30	2.96	7.23	11.17	20.85	31.48	41.01
Steam/gas	0.48	0.29	0.33	0.36	0.47	0.62	0.78
Pressure, psia	62	57	50	43	36	29	22
Temperature, °C	482	745	682	638	558	473	381

[a] Total = 100.00%.

the relative reaction rates are not well known, it is useful to know whether a specified mixture of syngas and steam would have the thermodynamic potential for carbon formation when it is at chemical equilibrium.

To assist in proper visualization of the multiple chemical reactions that occur simultaneously, we developed a ternary diagram that is simplified by considering only the concentration levels of the principal chemical elements present in mixtures of syngas and steam. Carbon, hydrogen, and oxygen are used as the identifying elements in our systems; these elements are located at the three apexes of the ternary diagram in Figure 2. A number of chemical compounds are shown on this figure when the elements are appropriately balanced with one another. Hydrocarbons such as methane and butane are on the left of the figure, carbon oxides on the right, and water on the base line connecting hydrogen and oxygen.

Carbon isotherms for a pressure of 30 psia are superimposed on the ternary (Figure 3). Interpretation of the isotherms reveals that mixtures of the elements which fall above the curves are in the carbon-forming region when at chemical equilibrium. Mixtures of the elements which

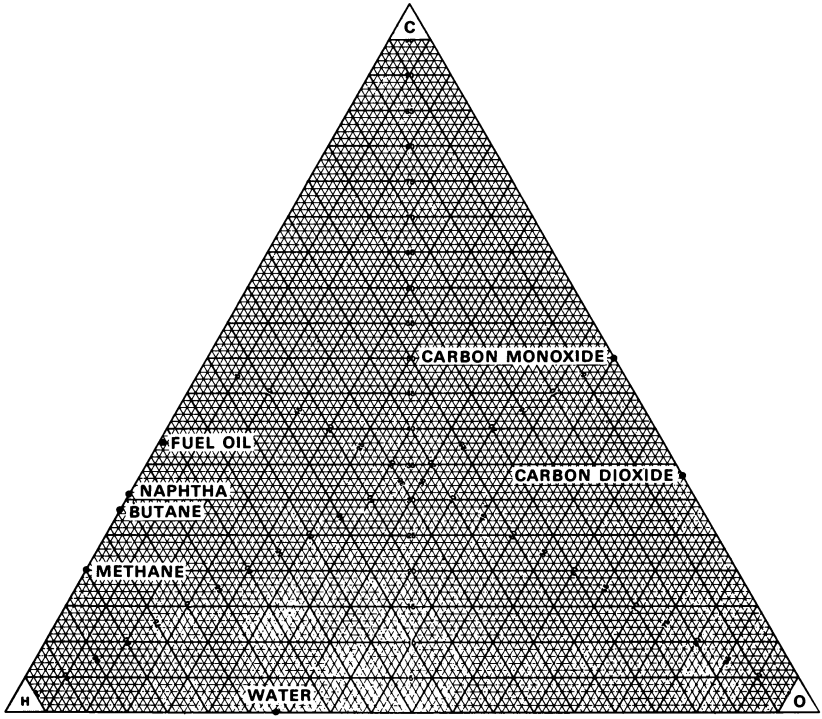

Figure 2. Element coordinates
Raw materials, intermediates, and products

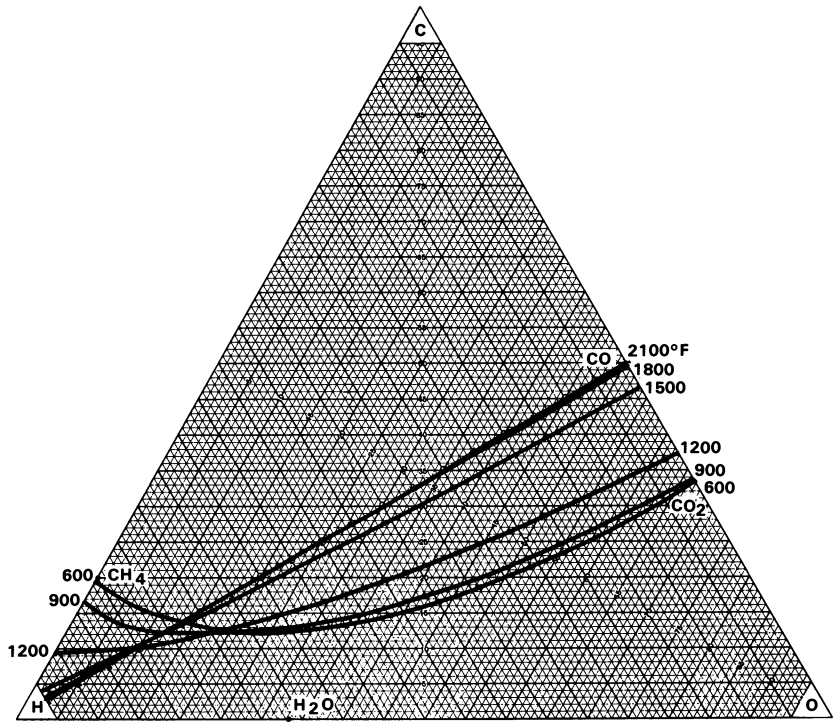

Figure 3. Carbon formation
Equilibrium isotherms (°F) at 30 psia

fall below the curves are outside the carbon-forming region at equilibrium. Gas mixtures falling within the family of curves should be at an operating temperature that will carry the specified concentration of carbon in the vapor phase.

Figure 4 represents a family of carbon isotherms at 400 psia. In certain areas of the diagram, elevated temperatures support higher concentrations of carbon in the vapor phase whereas in other areas lower temperatures favor higher carbon concentrations. Therefore, depending on the element mix of gases feeding a methanation reactor, an increase in temperature could cause the mixture to approach a condition under which carbon could theoretically be formed. Inasmuch as these figures are based on equilibrium concentrations of chemical compounds, temperature excursions into the carbon formation region may not result automatically in the formation of solid carbon since these reactions may occur at such a slow rate as to be negligible. On the other hand, it is not good practice to design a system that normally operates under conditions that are theoretically favorable for carbon formation and that depend on kinetics to keep the operation trouble free.

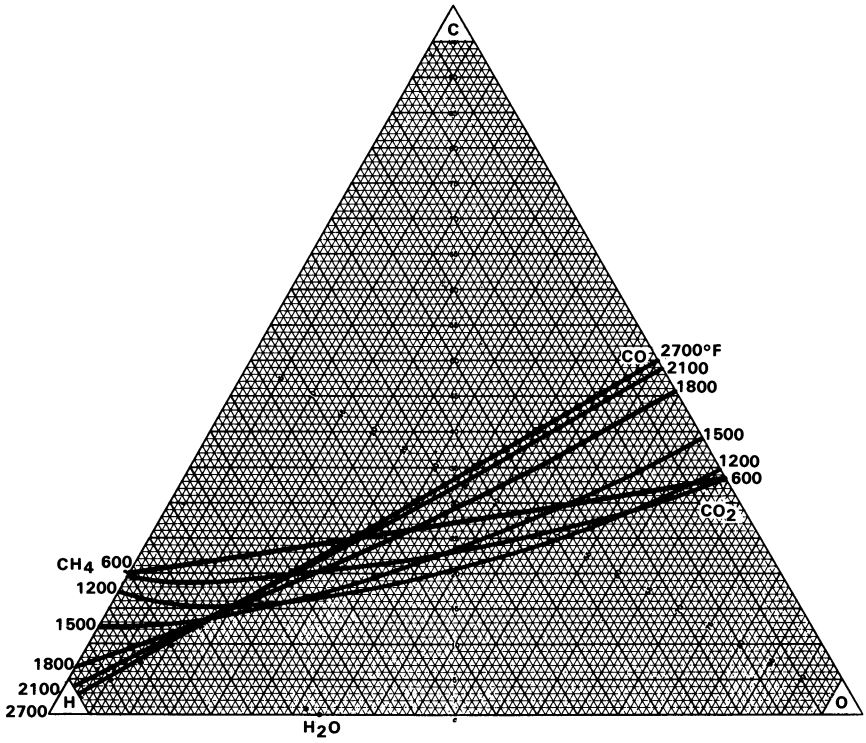

Figure 4. Carbon formation
Equilibrium isotherms (°F) at 400 psia total pressure

The mathematical properties of the set of equations describing chemical equilibrium in the synthesis gas system indicate that the carbon-producing regions are defined solely by pressure, temperature, and elemental analysis. Once a safe blend of reactants is determined from the ternary, the same set of equations which was used to derive the ternary may be used to determine the gas composition.

The gas compositions which represent proposed operating conditions at the pilot plant are given in Table I. Figure 5 shows the location of two compositions on the ternary diagram relative to the potential for carbon formation: (a) the feed gas composition to the first bulk-methanation reactor, and (b) the product composition from the third reactor which then remains a fixed point throughout the remaining reactors since no gas is added beyond the third reactor. From this figure, it is clear that sufficient steam has been added to move the mixture well outside the carbon formation region. Even after the total syngas is added to the system, it is not theoretically possible to form carbon when the system is at chemical equilibrium.

Feed gases to most, if not all, methanation systems for substitute natural gas (SNG) production are theoretically capable of forming carbon. This potential also exists for feed gases to all first-stage shift converters operating in ammonia plants and in hydrogen production plants. However, it has been demonstrated commercially over a period of many years that carbon formation at inlet temperatures in shift converters is a relatively slow reaction and that, once shifted, the gas loses its potential for carbon formation. Carbon formation has not been a common problem at the inlet to shift converters. It has been no problem at all in our bench-scale work, and it is not expected to be a problem in our pilot plant operations.

For a clearer understanding of the behavior of syngases in a shift converter, we established another set of carbon isotherms when considering the shift reaction only (without methanation) in addition to the carbon-forming reactions. Figure 6 shows isotherms at a partial pressure of 270 psia for all components of a gas mixture, but excluding methane.

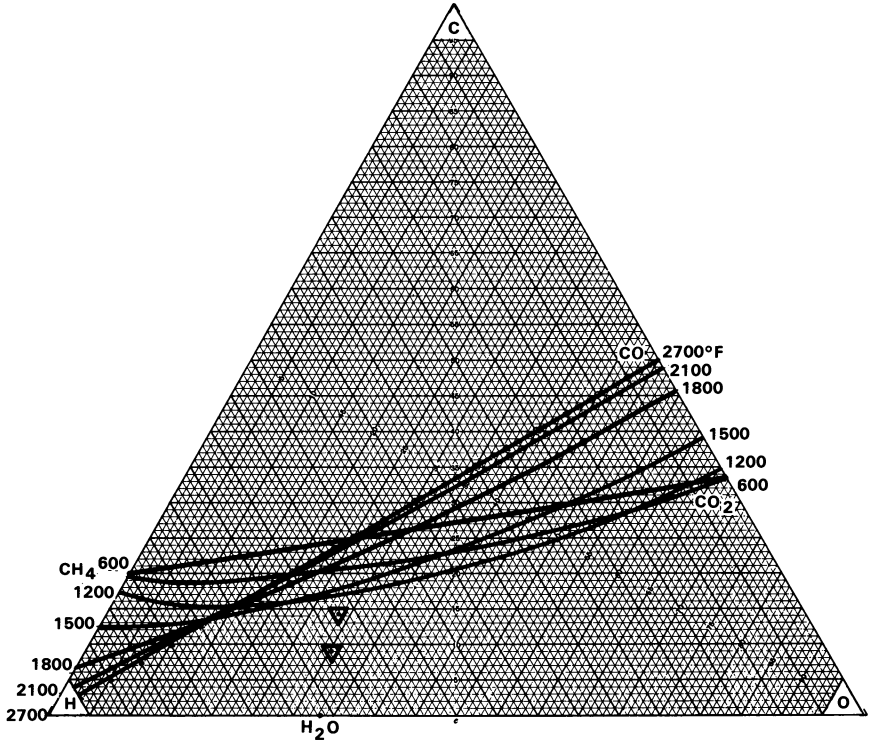

Figure 5. Carbon formation
Same as Figure 4; ▽, RMProcess

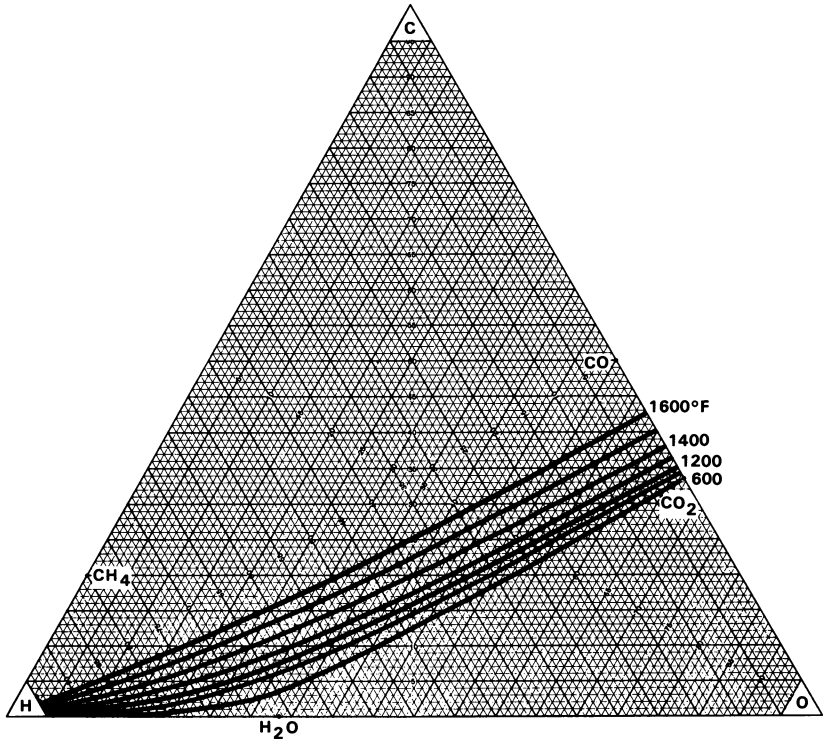

Figure 6. Carbon formation
Partial equilibrium isotherms (°F) at 270 psia partial pressure of hydrogen, carbon monoxide, carbon dioxide, and steam

Figures such as this are helpful when establishing inlet conditions to reactors since operating data from commercial plants can be used as points of reference.

Clean-Up Methanation

Figure 7 depicts a system wherein final methanation occurs following gas cooling and steam removal and a reduction of carbon dioxide to approximately 4%. Under these conditions and at a pressure of 300 psia, residual hydrogen is $< 3\%$ and carbon dioxide is < 2 vol % of the dry product gas after methanation. When the plant is operating at near atmospheric pressure, reduction of steam and carbon dioxide are followed by compression to either an interstage level or to delivery pressure for the final stage of methanation. For all pressure levels, the final methanation stage is outside the region of carbon formation.

Carbon dioxide can be removed from the effluent gas from bulk methanation by any of several conventional absorption systems. At this

point in the process, the volume of gas that must be treated for carbon dioxide removal is less than half that of a shifted gas from which carbon dioxide is normally removed when preparing a syngas to approach stoichiometric concentrations of reactants for methanation. Finally, the gas would be dried to a nominal 7 lbs of water per million standard cubic feet (scf) of gas.

Catalysts

Catalysts used in the process are of a proprietary nature. We hope to present details in another paper in the near future.

Conclusions

Advantages of the RMProcess are related particularly to cost savings in both capital equipment and operating requirements.

Shift Conversion. The shift reaction and methanation proceed concurrently without interference over bulk methanation catalyst thereby eliminating the need for a separate shift conversion operation.

Steam Utilization. Less steam is used in the RMProcess than is required for conventional shift conversion even though in other methanation processes as little as one-half of the total syngas is processed through shift conversion in order to achieve a near-stoichiometric balance of hydrogen and carbon monoxide for methanation.

Temperature Control. Temperature is controlled by steam addition. There is no gas recycle and therefore no recycle compressor.

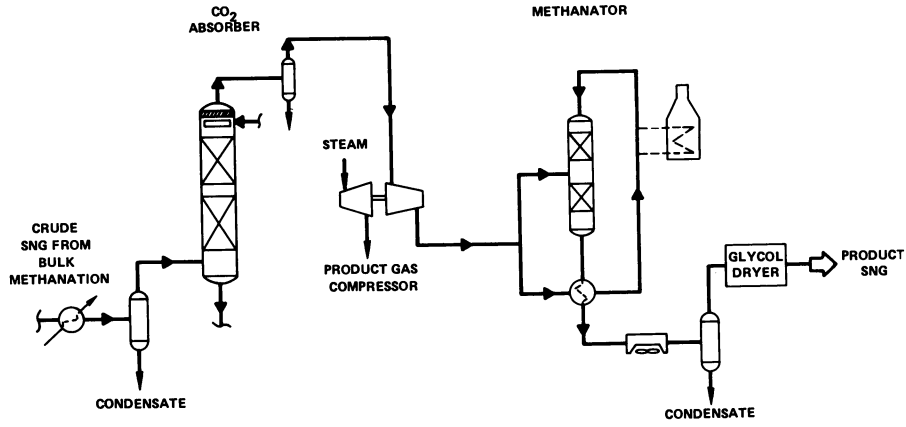

Figure 7. Final stage of methanation

Steam Production. The RMProcess operates at temperatures generally > 538°C which provide a large temperature difference for the production of high-pressure steam. Because of this, we can produce more steam and produce it at a higher pressure with less heat transfer surface than other processes.

Carbon Dioxide Removal. Aside from contained carbon dioxide which is removed from syngas when absorbing hydrogen sulfide, the total carbon dioxide produced in the methanation system is removed by conventional absorption in a single-stage operation in which the volume of gas to be treated is minimum and the partial pressure of the carbon dioxide is maximum.

Low Pressure Operation. By using the driving force of a large excess of carbon dioxide for methanation with operation at low pressures, bulk methanation can effect a high degree of syngas conversion thereby requiring only a single stage of final methanation after compression to meet pipeline SNG specifications. Such an operation reduces the compression duty by reducing the syngas to a fraction of its original volume while it is still at low pressure.

Space Velocity. Most of our experimental data were developed with operation at a wet outlet space velocity of approximately 10,000 vol/vol hour. However, we do have data at space velocities of up to 25,000/hr. The pilot plant will operate at a space velocity of 5,000/hr while processing 1 million scf raw syngas/day. With operation on a once-through basis without recycle and at the indicated space velocities, catalyst volumes are minimum compared with other processes when identical over-design factors are used.

Acknowledgment

Acknowledgment is sincerely made to Catalyst Consulting Services, Inc. of Louisville, Ky., in particular to Harold W. Fleming, for unusual services of the highest quality while directing the bench-scale experimental program which provides the technical basis and support for the RMProcess.

RECEIVED October 4, 1974.

Liquid-Phase Methanation of High Concentration CO Synthesis Gas

DAVID B. BLUM, MARTIN B. SHERWIN, and MARSHALL E. FRANK

Chem Systems, Inc., Research Center, 275 Hudson St., Hackensack, N. J. 07061

Chem Systems is conducting a development program for the methanation of synthesis gases as part of a joint program of the United States Office of Coal Research and the American Gas Association. The objective is to develop practical methods for producing substitute natural gas from coal. Chem Systems' process involves the reaction of CO and H_2 in a liquid–fluidized catalyst system which is a novel way of effecting highly exothermic gas–gas reactions that offers several advantages over present technology. Experimental data were obtained on both bench-scale and process development units. Process variables are examined, and a kinetic model is developed to define the reaction mechanism.

Development work on the liquid-phase methanation (LPM) process commenced in April 1972 and was first reviewed in October 1972 at the Fourth Annual Pipeline Gas Symposium. The development has been very successful. Prior to a review of recent accomplishments, the basic process and program background are reviewed briefly.

Process Background

The LPM process is ideally suited to the safe and reliable conversion of high concentration carbon monoxide streams to methane. The exothermic heat of reaction, which under adiabatic conditions could theoretically cause temperatures rises of ~950°C in a nonrecycle situation, is easily removed by the inert fluidizing liquid in a near-isothermal system. This is achievable by effecting the heterogeneously catalyzed reaction of the feed gases in the presence of an inert liquid phase which absorbs the large exothermic heat of reaction. The reaction proceeds to near-completion in a single pass. Economic studies will determine whether

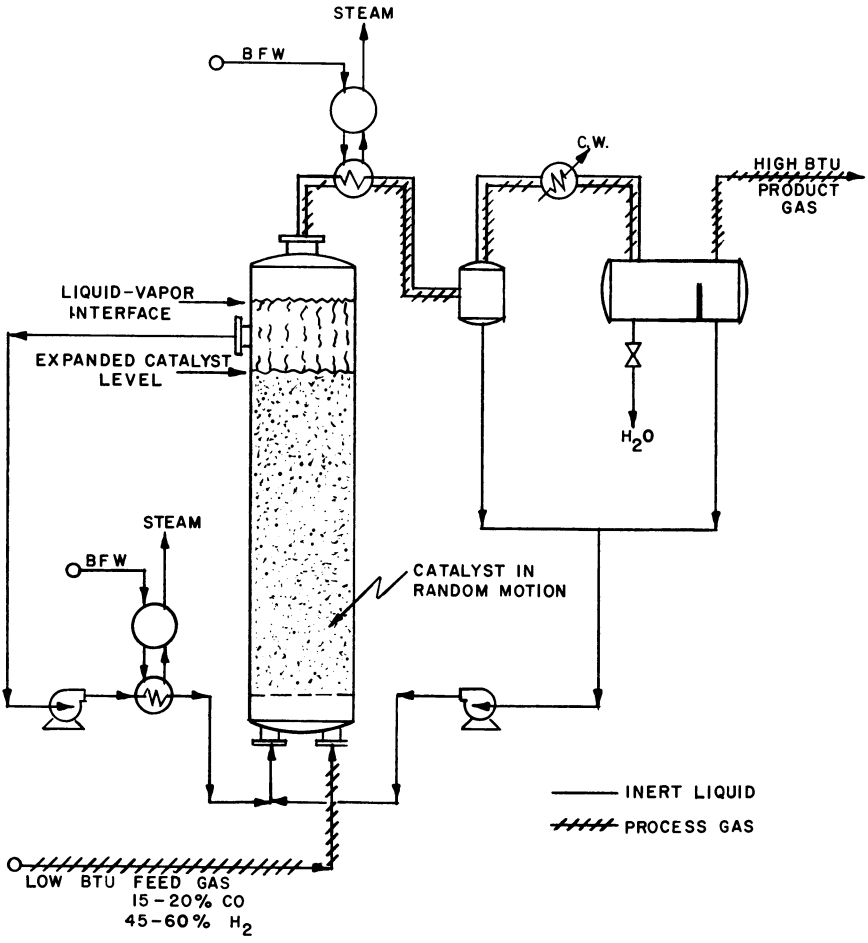

Figure 1. Schematic of liquid-phase methanation process

a single-stage reactor may be used or whether a polishing reactor should be utilized in the final design.

Figure 1 illustrates the process in more detail. The inert liquid is pumped upflow through the reactor at a velocity sufficient to fluidize the catalyst and to remove the reaction heat. The low Btu feed gas is passed simultaneously up the reactor where it is catalytically converted to a high concentration methane stream. The exothermic reaction heat is taken up by the liquid mainly as sensible heat and partly by vaporization (depending on the volatility of the liquid). The overhead product gases are condensed to remove the product water and to recover any vaporized liquid for recycle. The main liquid flow is circulated through a heat

exchanger where the heat of reaction is removed by generation of high-pressure steam. This also provides excellent temperature control for the system.

Project Background

Development of the LPM process is included within the American Gas Association–United States Office of Coal Research joint program on producing substitute natural gas (SNG) from coal. The development program consists of three phases which are proceeding in an overlapping manner. These are reviewed in Table I. Completion of the program is scheduled for June 30, 1975.

Table I. Program for Developing the LPM Process

Phase	*Objective*	*Completion, %*
I	exploratory research and development	100
II	operation of a larger scale process development unit	90
III	design of a full-scale integrated pilot plant	40

Description of Equipment

Bench-Scale Reactor. The bench-scale reactor is 0.81 in. i.d. and 48 in. long. The nominal feed gas rate for this unit is 30 standard cubic feet per hour (scfh); the feed gas is supplied from premixed, high-pressure gas cylinders. Except for reaction temperature, the bench-scale unit is substantially manually operated and controlled. The catalysts used in these studies were standard commercial methanation catalysts ground to a 16–20 mesh size which is compatible with the small reactor diameter.

Process Development Unit (PDU). The nominal feed gas rate for the PDU is 1500 scfh which is a 50–100-fold scale-up of the bench-scale unit. The methanation reactor is 3.62 in. i.d. and 84 in. high; the catalyst bed height can be varied from two to seven feet. The basic design and flow scheme of the PDU is similar to that of the bench-scale unit. After analysis, the product gases are sent to an incinerator where they are thermally oxidized to carbon dioxide and water prior to discharge into the atmosphere. Instrumentation is sufficient for complete automatic control and monitoring from a remote-control room. The reactor is fitted with movable gamma-ray detector which is used to measure density differences between the source (radioactive material) and the detector. In this manner we are able to determine accurately the height of the fluidized catalyst bed under varying reaction conditions.

The overall objectives of this phase of the program are: (a) to determine the effects of all process variables for optimum performance; (b) to

determine the data needed for reliable engineering design and cost estimates of larger plants; (c) to determine catalyst life, recovery, and regeneration methods; (d) to determine liquid life and effectiveness; and (e) to determine whether reaction model correlation is valid for PDU performance.

Pilot Plant. The third phase of the LPM project is the design, construction, and operation of a large pilot plant. The basic objectives are to demonstrate the process on a synthesis gas actually produced by coal gasification and to obtain the necessary design and performance data so that the design and engineering can be detailed for a full-size (*ca.* 250,000,000 scfd) coal gasification plant. The pilot-plant reactor has a 2-ft diameter and a 15-ft length. We feel this is large enough to provide adequate scale-up information for commercial-sized reactors. Again, the design is basically the same as for the PDU and the bench-scale unit, but it was obviously modified and adapted for the larger capacity. The scheduled start-up of the pilot plant is June 1975.

The pilot plant will be located at the site of an operating coal gasification plant. At this time, the two most logical places are the Institute of Gas Technology (IGT) plant in Chicago or the CO_2 Acceptor plant in Rapid City, South Dakota. The design concept is to build a skid-mounted unit that could be located at either place or at other locations where coal gasification plants are under construction. A skid-mounted unit could be operated at one site for a period of time and then moved to another location for testing with synthesis gas from another coal gasification process. The design of the unit is such that it can accommodate synthesis gas feed from any of a number of processes. The unit will be designed to handle a maximum feed gas of 2,000,000 scfd at 1100 psig. This is the maximum output of the IGT Hygas plant. The LPM process can also operate at lower pressure, and at Rapid City it would handle feed gas at lower pressure since the synthesis gas feed there is only 600,000 scfd available at 100 psig.

Reaction Correlating Model

One goal of our experimental program with the bench-scale unit was to develop the necessary correlations for use in the ultimate design of large commercial plants. Because of the complexity inherent in the three-phase gas–liquid–solid reaction systems, many models can be postulated. In order to provide a background for the final selection of the reaction model, we shall first review briefly the three-phase system.

(a) After entering the reactor, the gas bubbles rise by convection and buoyancy. At the same time, a solid phase retards the upward bubble motion with retardation dependent on void spacing and particle size.

(b) The reactants are transferred from the gas bubbles to the bulk liquid through the gas–liquid interface. Consideration of the relative resistances reveals that the liquid film coefficient at the gas–liquid interface should be the least efficient mass transfer step and that the liquid phase concentration at the gas–liquid interface is governed by Henry's Law.

(c) After diffusing from the gas–liquid interface to the bulk liquid, the reactants are convected by the fluid motion to the liquid–catalyst interface.

(d) Mass transfer of the reactants from the bulk liquid across the liquid–catalyst interface should again be governed by the liquid film coefficient.

(e) After absorbing onto the catalyst surface, the reactants undergo a catalytic surface reaction.

(f) The reaction products desorb and are transferred back to the gas bubbles *via* steps 4, 3, 2, and 1.

As our first approach to the model, we considered the controlling step to be the mass transfer from gas to liquid, the mass transfer from liquid to catalyst, or the catalytic surface reaction step. The other steps were eliminated since convective transport with small catalyst particles and high local mixing should offer virtually no resistance to the overall reaction scheme. Mathematical models were constructed for each of these three steps.

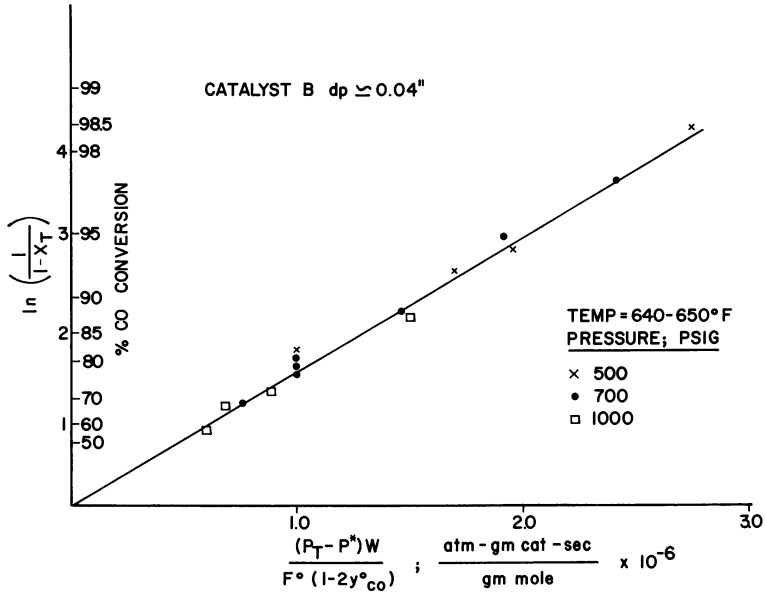

Figure 2. Conversion vs. *contact time with bench-scale unit*

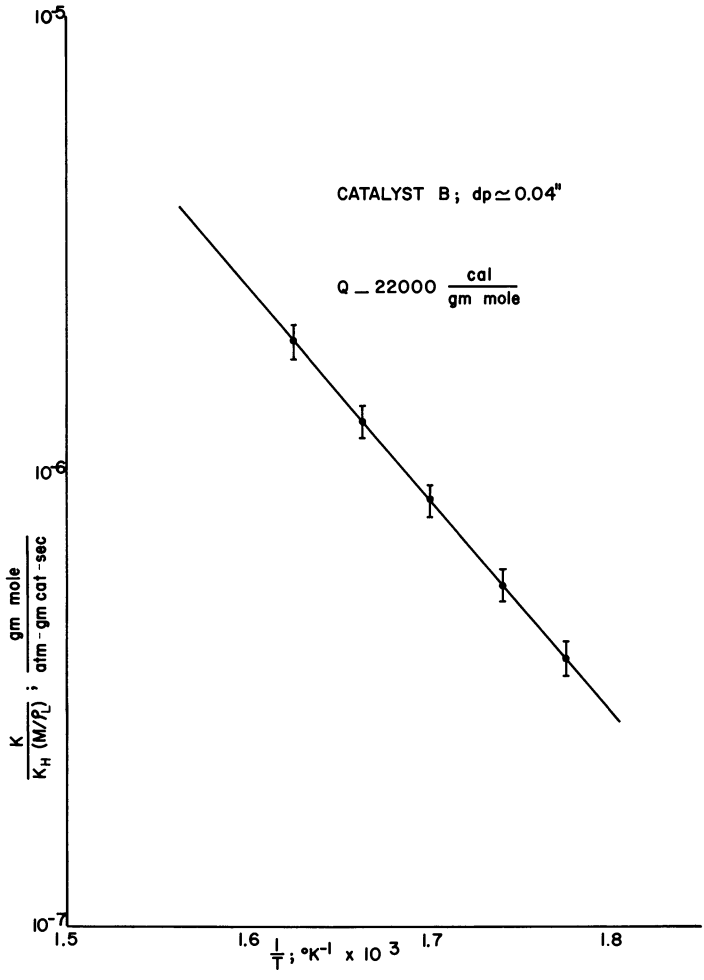

Figure 3. Effect of temperature on kinetic rate constant with bench-scaleunit

Our initial experimental results indicated that the kinetic model—first order in liquid phase CO concentration—was the leading candidate. We designed an experimental program specifically for this reaction model. The integrated rate expression (*see* Appendix for nomenclature) can be written as:

$$\ln\left(\frac{1}{1-X_T}\right) = \frac{K(P_T - P^*)\cdot W}{K_{HCO}(M/\rho_L)\cdot(1 - 2Y^\circ_{CO})\cdot F^\circ}$$

Therefore a plot of:

$$\ln\left(\frac{1}{1-X_T}\right) \text{ vs. } \frac{(P_T - P^*)\cdot W}{F^\circ(1 - 2Y^\circ_{CO})}$$

should result in a straight line through the origin with the slope $K/K_H(M/\rho_L)$ a direct measure of the catalyst–liquid pair productivity.

Findings with Bench-Scale Unit. We performed this type of process variable scan for several sets of catalyst–liquid pairs (*e.g.*, Figure 2). In all cases, the data supported the proposed mechanism. Examination of the effect of temperature on the kinetic rate constant produced a typical Arrhenius plot (Figure 3). The activation energy calculated for all of the systems run in the bench-scale unit was 18,000–24,000 cal/g mole.

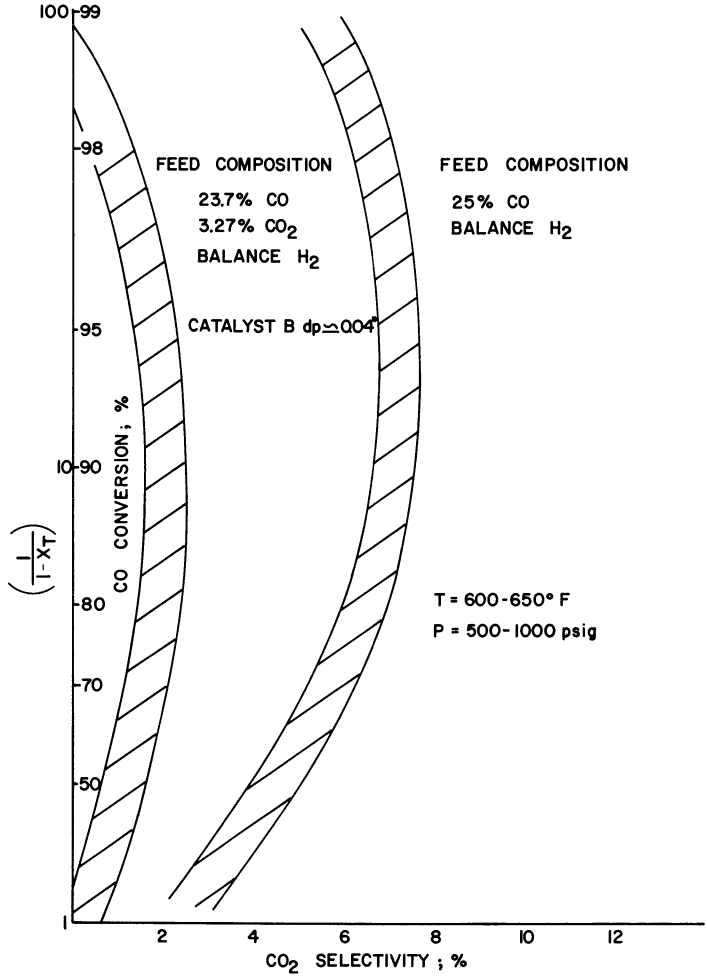

Figure 4. CO_2 selectivity vs. *CO conversion*

Data collected during these process variable scans indicate that more CO_2 than expected was being formed (Figure 4). Selectivity to CO_2 reached a maximum of 5–10% at about 90–95% conversion. At higher conversions, the CO_2 level is reduced by reverse shift and subsequent methanation of CO or by direct methanation of CO_2. This selectivity to CO_2 can be eliminated by cofeeding small amounts of CO_2 (3–5%). Since multiple CO_2 absorbers are required in the commercial SNG plant, one or more could be relocated downstream of the methanation step. This could offer some economic advantages since CO_2 absorption would now occur at higher concentration and pressure and at lower total gas flow.

Findings with PDU. Work with the PDU largely paralleled the bench-scale reactor tests; there was one important addition—extensive three-phase fluidization studies. As was mentioned, the PDU is equipped with a traversing gamma-ray density detector that is capable of measuring bed density to within ±0.01 specific gravity units. Thus, we could measure and correlate fluidized bed expansion as a function of liquid and gas velocities and physical properties, and could also determine the

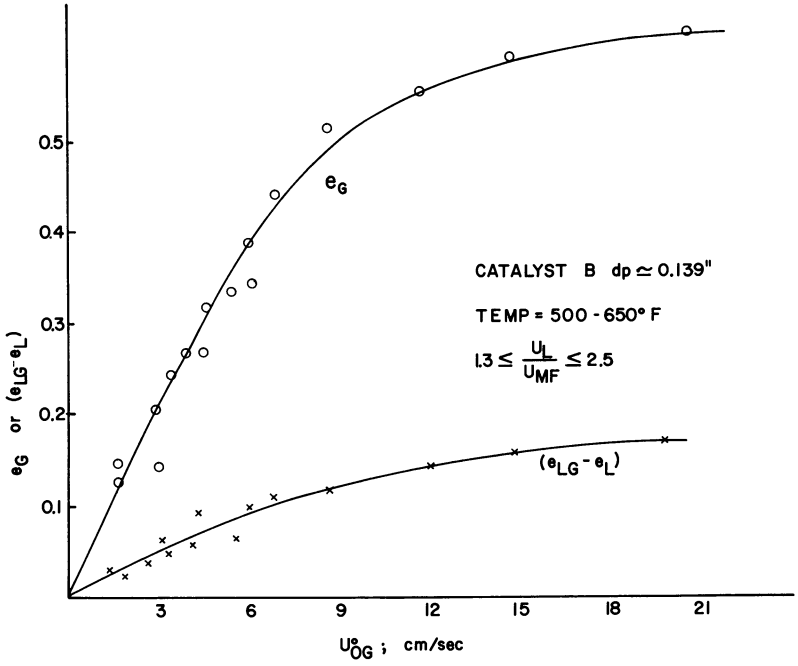

Figure 5. Gas holdup (e_G) and incremental bed porosity ($e_{LG} - e_L$) vs. superficial gas velocity with process development unit (PDU)

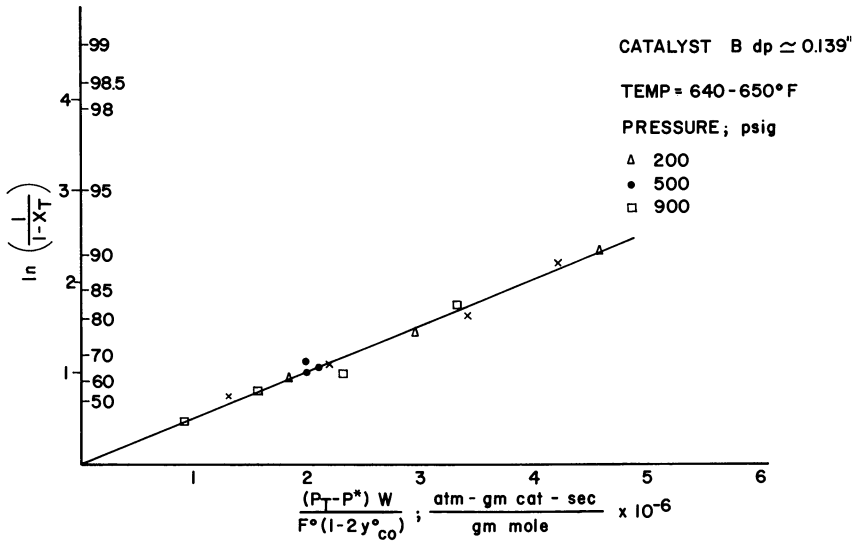

Figure 6. Conversion vs. *contact time with PDU*

individual phase volume fractions. The two major findings of this work (*see* Figure 5) were: (a) the absolute values for the gas holdup are 3–4 times greater than the incremental porosity increase because of the gas flow at constant liquid flow, and (b) the gas holdup is essentially independent of liquid velocity for 1.3 $U_{mf} < U_L < 2.5\ U_{mf}$. In addition, data for all the catalysts indicate that the maximum gas volume fraction obtainable was on the order of 0.5–0.6.

Reaction studies were made in the PDU in order to verify the correlating model developed in the bench-scale unit. This provided data that are applicable to the scale-up design required for the pilot plant and, ultimately, the commercial unit. In the initial PDU work, particles were much larger (1/8–3/16 in.) than those used in the bench-scale unit (<1/32 in.), and the reaction rates for these larger particles were about one-third those obtained with the smaller particles (*cf.* Figures 2 and 6). In addition, the activation energy derived from these data was on the order of 11,000 cal/g mole which is just about one-half the value obtained with the bench unit (*cf.* Figures 3 and 7). These findings suggest that we were encountering pore diffusion limitations; we attempted to verify this by investigating still smaller particles (1/16 in.). While the reaction rates did increase significantly, as they should, the activation energy remained essentially unchanged which indicated that we were still in the pore diffusion regime. Therefore, we can increase productivity still further simply by reducing particle size. This should not be too difficult since 1/32-in. particles are already being used in analogous

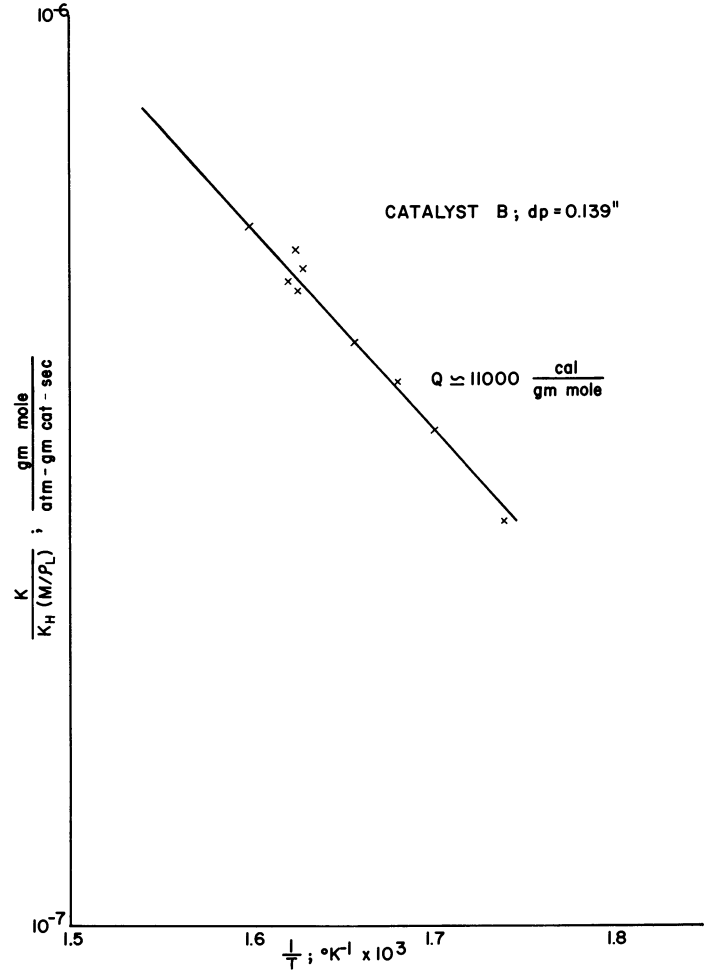

Figure 7. Effect of temperature on kinetic rate constant with PDU

commercial systems. The ultimate obtainable productivity has not yet been accurately defined although we are confident that a vapor hourly space velocity (VHSV) of 4000/hr at 1000 psig and 343°C with a feed containing 20% CO, 60% H_2, and 20% CH_4 should result in CO conversion of 95–98%. These findings do in fact confirm the first-order reaction rate model proposed as a result of the earlier bench-scale work. Future study will concentrate on the effect of axial dispersion arising from the varying geometries encountered during scale-up and on determining optimum particle size for the commercial unit.

In an attempt to define useful catalyst life, we conducted continuous runs of 2- and 4-wk duration. The results were encouraging; after an

initial period of deactivation over the first 50–100 hrs (which is common with nickel hydrogenation catalysts), the catalyst reached an equilibrium productivity that exceeded our original design basis of a VHSV equal to 4000/hr at 1000 psig and 343°C. Considering these findings as well as our substantial experience with all types of catalysts, we have every reason to believe that a catalyst life of more than one year can be achieved with catalyst replacement costs then insignificant in the overall SNG economics.

Conclusions

On the basis of this past work and ongoing experiments, we feel that the liquid-phase methanation process promises to become an economic, reliable, and versatile means of converting synthesis gas mixtures to high Btu gas. Chem Systems believes that this technology is a key step in the transformation of fossil feeds into pipeline gas, and we look forward to its successful application in commercial coal gasification plants.

Appendix—Nomenclature

e_G = volume fraction of gas phase
e_L = bed porosity with liquid only fluidizing
e_{LG} = bed porosity with liquid and gas fluidizing
F = gas flow rate at any position, g moles/sec
K = reaction rate constant, g moles/sec g catalyst (g mole/cm^3)
K_H = Henry's Law coefficient, atm/mole fraction
M = molecular weight of liquid phase, g/g mole
P_T = total pressure, atm
P^* = vapor pressure of liquid phase, atm
T = temperature, °K
U_{mf} = minimum fluidization velocity, cm/sec
U_{OG} = superficial gas velocity at reactor T and P_T, cm/sec
W = weight of catalyst, g
X_T = fraction of CO converted
Y = mole fraction of component bulk gas phase

Greek

ρ_L = density of liquid phase, g/cm^3

Superscript

° = initial condition

RECEIVED October 4, 1974.

10

Discussion

R. T. Eddinger (Cogas Development Co.): Considering the cost and thermal inefficiency of methanation, is it realistic to consider methanation as the long-term competitor of moderate Btu gas having a heating value of 300–500 Btu?

Wm. Bair: As one of the leading exponents of high Btu gas, I suppose that I should rise to the occasion. I think that, for certain selected loads and for certain selected geographical locations, the low Btu gas is certainly in the picture. For long distance transmission to replace existing high Btu natural gas supplies, I don't think anyone is interested in going through either the toxic problem of high CO concentrations or the conversion of some 60 million domestic residential appliances.

G. A. White: I think I would take exception to the premise that methanation is a low thermal efficiency operation. If you look in some of the publications on methanation as a part of the total project, you will find that the majority of processes turn around and produce steam by burning coal or product gas or something else. So, if you define thermal efficiency by reduction in heating value, I would certainly agree with that. But if you then have to utilize, or you can utilize, this energy in the form of steam, I don't see that methanation represents a thermal loss. If in fact you don't produce steam in excess of what is required in the process, then it should be incorporated in the calculation of thermal efficiency.

R. McClelland: I might add a couple of comments to that. Certainly, Consolidated Natural Gas as well as a number of other mid-Western utilities are looking at medium Btu gas for some applications. But these are typically in locations where you have a high density of large commercial or industrial consumers that can burn low Btu gas. Certainly, from the comments that I have heard in the utility industry, I think Bill Bair is right. For residential and commercial applications, to the extent the gas industry has to increase supplies beyond that which might be displaced by medium Btu industrial gas substitution, we will certainly need methanation.

Wm. Haynes: There may also be problems with carbonyl formation if you try to handle medium Btu gas in the present high pressure gas transmission system.

C. Woodward: May I add one thing for the record? I must take issue with the comment that the conversion of 60 million domestic

appliances couldn't be done. Britain has just converted, in the opposite direction actually, from roughly 500-Btu gas to North Sea gas of about 1000 Btu. It was done with remarkable efficiency, and remarkably quickly considering the magnitude of the job. It can be done!

L. Seglin (*Chairman*): I agree. We experienced the same conversion here in the northeastern United States back in the '50s. The question might be: if it's so easy to convert in one direction, wouldn't it be easy to do so in the other?

P. Shimizu (LaPorte–Davison, Inc.): What are the important and likely areas of future R & D work on methanation *vis a vis* catalyst development, process development, or whatever?

Dr. Woodward: I tried to indicate in my paper that in ammonia–hydrogen plant operation, in comparison with several other catalysts in such plants, the methanation catalyst situation is really well under control. Speaking for our company, and I would guess others, it's not a particularly active research area because we have higher priorities in catalyst development. As regards methanation catalysts for SNG, I did not discuss that today and perhaps I should let some other fellows answer first. Sulfur tolerance is one area for future development.

A. Hausberger: Probably one of the biggest areas for improvement would be a catalyst that is stable in the higher temperature ranges, such as those required by the RMProcess of Parsons, because, if you can take higher temperatures, you can take a considerably larger temperature rise and hence less gas recycle.

L. Seglin: We have heard today two rather novel approaches to methanation: the steam-moderated RMProcess and the slurry methanation process. These are the results of new or recent R & D. What can we visualize beyond that? Would it be some other exotic process?

Dr. Woodward: If you want to look at the ideal, there is a limit to hiw much conversion you can do when starting with a high CO–high hydrogen mixture. For equilibrium reasons, you cannot convert it all to methane in one step. The Parsons process, as I understood it, is endeavoring to do it in several stages, keeping the temperature rise in each stage within reason. It would, I suggest, perhaps be advantageous if all the methanation could be done in one or two reactors, rather than in six. So the requirement for future work may be a catalyst which has sufficient activity at a respectably low inlet temperature and sufficient stability at a high temperature.

G. A. White: We are of course looking for catalyst manufacturers to develop catalysts that we can test. We are not in the catalyst manufacturing business. If ICI or Badische or anybody else has catalysts they would like us to test, we would be very happy to do so. We do this testing on a non-analysis, confidential basis, and their catalyst is theirs.

But, so far as the number of reactors are concerned, I indicated that we have six. That's the maximum number that we require regardless of the quality of the syngas that we process. When we took the Lurgi gas and methanated it, starting with 38% methane already there, we required only four reactors. As a matter of fact, we could have gotten by with three. So it is really a question of how much work you have to do that determines the number of reactors that you would install in the system.

D. Blum: Just going a bit further, the liquid-phase methanation process now uses one reactor. You can or you cannot use a polishing reactor as the economics dictate. You can actually go right to pipeline quality gas in one reactor, which is equivalent to about 99.8% conversion of a 20% CO feed gas. We envision at this moment that combined shift–methanation could be done in the same single reactor. It would obviously require lower feed gas rates so you may need two of these reactors. We don't exactly have the numbers yet. I think that's one of the areas that deserves future work.

A. Vannice (Exxon Research and Engineering Co.): Would a more sulfur-tolerant catalyst be a significant improvement in the overall methanation process? If so, what would be the maximum tolerable sulfur concentrations in the feed stream?

D. Newsome (Virginia Polytechnic Institute and State University): Almost all the talks today are concerned with nickel catalyst. Is there any place for a somewhat less active but sulfur-tolerant catalyst?

A. Hausberger: I think a sulfur-tolerant catalyst would definitely be an advantage in that the requirement for critical control of the sulfur removal system would be eliminated. If you can allow some sulfur to pass on through the methanator into the product gas, the amount of reagent or regeneration cost of the sulfur removal system would be reduced. As to what level of sulfur could be tolerated, that is a hard question to answer since I don't think that there is a sulfur-tolerant catalyst.

F. Moeller: If you want to realize a catalyst which can hold some ppm's of sulfur, you should realize that you need not just one catalyst. You need a catalyst which does the job at all temperatures. We know of catalysts that can have some sulfur in the feed gas at relatively high temperature levels. That's no problem. But if you go to the low temperatures that you need to get specification SNG so that you can put your gas into your pipeline, then you have a real problem. So if you look for a sulfur-resistant catalyst, it must be resistant over the whole process sequence. Personally, I cannot foresee a catalyst which will work at lof temperature and be insensitive to sulfur.

Anonymous: What else can we say about the poisoning of methanation catalysts by materials other than sulfur, *e.g.*, any information in

that regards about the permanency of poisoning and allowable concentrations?

A. Hausberger: As we mentioned earlier, the light hydrocarbons do not seem to affect catalyst activity, and they do reform into methane. However, you can increase the hydrocarbon content to levels where they do depress the methanation activity. If the hydrocarbons are high enough in unsaturation, they will form carbon when they get to a certain level. As far as hydrogen cyanide and ammonia are concerned, we don't expect them to affect the nickel methanation catalyst.

Dr. Moeller: We have made an intensive, chemical, analytical examination of possible trace components in the coal gas. At the SASOL plant, we have typical coal gas available which has been cleaned in a Rectisol wash unit. We have detected in the unwashed raw gas possible catalyst poisons besides sulfur and chloride. We haven't found any chloride in the gas downstream of the Rectisol unit. So, I cannot say anything about methanation of coal gas with chloride. We know that chloride is an extreme poison. On the other side, we have done investigations on nitrogen oxide, ammonia, hydrogen cyanide, and organic cyanides. We found that in normal operation of the Rectisol unit there were no measurable changes in deactivation rate in comparison with the plant we are running in Schwechat, where we used a gas which was formed from naphtha and which definitely did not have these components. Nitrogen oxides at a very low level are not poisons. I cannot confirm this for nitrogen oxides at levels of 5–10 ppm which might result from using another wash system. Nor, can I say anything about hydrogen cyanide at high concentration levels. In summary, we found that these components, at the concentrations left in the syngas after the Rectisol wash, and cyanide are not poisonous to the nickel catalyst.

L. Winsor (Bechtel Associates Professional Corp.): Can carbon lay-down be avoided dependably by catalyst formulation ?

A. Hausberger: I am not sure that this is a factor because most of the systems that have been discussed today are actually operating outside the carbon deposition range, even outside the graphite range. You can, however, formulate catalysts that will operate in the graphite range, in other words, between graphite and the Dent range. I think it has been proven by Dent and by others.

L. Seglin: I would like to take exception to that. If you look at the composition, not the equilibrium composition, but the composition of the feed gas in practically any of the methanation schemes I have seen around, there is enough CO to lay down carbon. You have a situation where at the feed point you can potentially lay down carbon. At the exit you are outside carbon laydown. So, some place in-between, for some significant space, there is sufficient carbon monoxide to form

carbon according to the Boudouard reaction and lay carbon down irreversibly.

Dr. Moeller: I must say you can handle the carbon black formation with the structure of your catalyst. You can produce a catalyst with which you can go farther into the region of carbon black formation than when using a different catalyst. I think these results are published, especially those from ICl. We had the same experience when we developed our catalyst together with Badische. You can go farther into the carbon black region. But, on the other hand, you can adjust your system so that there is no need to go into the carbon black region.

G. A. White: We have done some experimental work on impregnating catalyst with potash, and, in fact, potash has been used in related fields to inhibit carbon formation primarily from hydrocarbons. We find that the mechanism of carbon formation from hydrocarbons is quite different from that from syngas. So an agent that is effective in reducing the formation of carbon from one source can be quite different with that from another source. You have to be a little bit specific in terms of the feed material from which you are trying to prevent carbon formation.

Dr. Woodward: May I just make one comment to emphasize and to repeat what was said earlier? Thermodynamics and kinetics. Yes, under the inlet conditions of several SNG processes, and also of methanation in ammonia and hydrogen processes, thermodynamically they are inside the carbon-forming region. At the exit they tend not to be. In practice, carbon is not formed. One could, therefore, conclude very simply that kinetics outweighs thermodynamics.

L. Seglin: This in turn is a function of the catalyst. We have, for example, Bill Haynes' paper, where Raney nickel was used and where quite a bit of carbon was deposited.

Wm. Haynes: we are not sure, though, whether the carbon formation was because of the iron in our system. We feel that much of this carbon formation that we ran into will possibly be eliminated if we eliminate the iron from the system.

Dr. Woodward: May I ask a question of some of our colleagues here as a point of information? You use the phrase "irreversible carbon laydown," yet the equation for carbon plus steam has arrows going in both directions. I wonder if anybody has any comments on whether it is irreversible or, if you inadvertently start to get some carbon down, is it reversible? Can you steam it out?

L. Seglin: Steam–carbon reaction is rather slow at the temperatures at which methanation takes place so, once you lay carbon down, I think you have a deuce of a time getting rid of it. Thatis way I loosely used "irreversible."

Anonymous: We have heard of carbon laydown as being a problem. Is the formation of metal carbides of concern, and can it be reversed?

Wm. Haynes: The nickel carbide formation has been reversed. That is,nickel carbide has been eliminated by hydrogen treatment in some of the laboratory tests at the Bureau of Mines, and catalyst activity has been restored that way. In the pilot plant, however, we have not been able to achieve any such regeneration of the catalyst.

Dr. Moeller: We have done this, and we compared an iron catalyst used for the Fischer–Tropsch plant and a nickel catalyst used in the methanation plant. By the same x-ray techniques, we found no nickel carbide on the used methanation catalyst, but we did find iron carbide on the used Fischer–Tropsch catalyst.

Anonymous: One of the speakers mentioned that carbonyls are very poisonous. Isn't it believed that carbonyls are being formed all the time during methanation?

G. A. White: Well, of course, we have no way of knowing if carbonyls are made continuously. But, I would suspect that, if in fact you do form the carbonyls, they are likely to be formed from the most active sites that you have in your catalyst. You would be very fortunate, it would seem to me, if in fact the redeposition of that carbonyl in the form of nickel would be equally active. So I would suspect that perhaps you are not forming carbonyls. Our experience has been when we have formed them and have known that we formed them, that our catalyst has lost substantial activity.

Anonymous: Several speakers found iron deposited on the nickel catalyst. Where is the iron believed to come from, and what steps will be taken to prevent the deposition?

Wm. Haynes: Well, we suspect that the carbonyl is formed in almost any part of the system that is composed of carbon steel, which has a temperature of about 100°C, and which is under a high pressure of CO. So, we feel that parts of the system that would be operating under these conditions would have to be lined with copper or a relatively inert material like that. In fact, it is the practice in the methanol industry to have the vessels copper lined.

Dr. Moeller: In our plant, we investigated our catalyst after 4000 and 5000 hrs of operation and we found no trace of iron on our catalysts. But we know that if you take no precautions against iron carbonyl formation, then you will destroy some part of your activity by iron deposition on your catalyst. And we found that the iron carbonyl is formed mainly at the mild steel tube walls or at the tube in the temperature range of 150°–200°C. So, if you enter this range and you have to heat up your gas, which has a high CO content and steam in it, you have to

take precautions against this. This is a problem in methanation and in methanol plants. If you design with this in mind, there should be no problem of iron fouling the catalyst.

L. Winsor: What are the estimated potential advantages of steam-moderated methanation over hot or cold gas recycle processes?

G. A. White: I really do not know. As a matter of fact, it is very difficult to predict or to say what differences there might be because we are not up-to-date with the developments that everybody else is making. I am sure all are improving their processes. All we are saying is that, from a thermodynamic standpoint, we are attempting to achieve a maximum recovery of energy in the form of high pressure steam while using the maximum temperature differential for the generation of steam. The only heat we lose from the system is the difference in temperature between the feed gas and the product gas, which is minimum because we have no recycle. So, we have very high recovery of steam at a minimum cost. We don't really think that methanation itself is a big, big cost in terms of the total process. If you look at other considerations, the cost of CO_2 removal is not a small cost in this whole system. So you have to look at that very, very carefully.

L. Winsor: What are the estimated potential advantages of slurry methanation over the gas recycle processes?

Dr. Blum: Our office in New York has done several economic analyses. The distinct advantage of liquid-phase methanation, other than the fact it does not have recycle cost, is that it requires only about 60% of the capital cost. For a commercial plant of 250 billion Btu per day, the capital cost is projected at about $18,000,000. Since the operating costs depend very substantially on the capital costs, there is a very big reduction in operating costs. We project at the moment an advantage in the order of four to six cents per million Btu over cold gas and hot gas recycle.

M. E. Frank: What was the inlet temperature to the hot gas recycle compressor, and what construction materials were used?

Dr. Moeller: I think to answer this question now is a bit difficult. It's just a mechanical problem of the maximum temperature the recycle compressor can handle. So, in the end, we will go to the inlet temperature to the compressor in the range of the inlet temperature to the reactor. So what we are endeavoring to attain is a simple reaction system consisting of an adiabatic reactor in series with waste heat boilers and nothing more than one recycle compressor. These compressors are used in the chemical industry with no problem in operation. So, in the end, you can go to hot recycle with an inlet compressor temperature the same as the inlet reactor temperature. All the heat from

the reaction is put into high pressure steam, with little loss to cooling water, and into feed water preheating.

H. Roberts (South African Coal, Oil, and Gas Corp.): May I say that for the pilot plant we used a reciprocating compressor which would operate only at near ambient temperature. So we simulated the operation of the hot recycle compressor by adding high pressure steam on the delivery side of the reciprocating compressor. We did not use a hot recycle compressor in the pilot plant.

G. G. Collins (Union Carbide Corp.): In the hot gas recycle system, is there an available compressor which can handle the compression of this very hot gas stream?

Dr. Moeller: There is no question that there are compressors available that have been operated in chemical plants to handle these amounts of gases at the temperature and pressure and at the pressure rise of the recycle. This is no problem any more.

Dr. Collins: Is the RMProcess basically an extension of existing refining technology with concurrent methanation, or the extension of methanation technology with concurrent reforming from the standpoint of catalyst performance requirements?

G. A. White: I should say "yes," we are extending both technologies —methanation and reforming. As you recognize, we operate over a relatively wide temperature range, and, of course, at the high temperatures similarities between methanation and reforming are quite strong. As we progress through the reactors, we get into a temperature range which most other methanation processes operate almost entirely. So, we are covering a wide range. We are not doing something with the catalyst that is quite different from what has been done before, either in reforming or methanation. We are just taking advantage of the fact that we do have a stable catalyst at high temperatures which allows us to process high carbon oxide gases. But then we must get down to the same low temperature levels as everybody else to make the same methane content. We all work in accordance with the same rules of thermodynamics.

L. Seglin: Why has Lurgi selected the hot gas recycle process for methanation rather than the isothermal reactor (ARGE) design which they used for the Fischer–Tropsch plant in SASOL's plant in South Africa?

Dr. Moeller: A methanation plant does not have a problem of selectivity. Whether you operate at low or high temperature, when using a nickel catalyst you will form only methane and no higher hydrocarbon. But with the Fischer–Tropsch synthesis, you have a wide range of possible products which can be formed. If you want to have a certain product, you must keep your temperature at a certain constant value.

This you cannot do in an adiabatic reactor unless you go to extremely high mixing ratios of fresh feed and recycle gas. In summary, it is a question of selectivity, which is the reason for using the isothermal reactor for Fischer–Tropsch. An adiabatic reactor with a waste heat boiler is cheaper than an isothermal feactor, and hence it is used for methanation.

J. Dolbear (W. R. Grace): What are the incentives for high operating temperatures, and how are the mechanical design complications met? In other words, with high temperatures and high steam concentrations, what are the problems in designing a mechanically workable reactor system?

G. A. White: Well, as members of the construction industry, we look at what are the economical ways of doing things. That's really how we got into this methanation business. We felt that if we put in a refractory-lined vessel, it would be no more expensive than more exotic materials or even carbon steel or low moly, even at the lower temperatures. The type of methanator that we use is not dissimilar to the high temperature shift catalytic reactors that have been used in many partial oxidation plants. The temperature rise even in high temperature shift can get you up over 480°C. So, we don't really think we are deviating from commercial practice in the design of the methanator itself. It is not exotic; it is very low chrome, very low quality construction material with refractory lining. So far as the catalysts are concerned, these are not exotic catalysts. I am not really prepared to discuss their manufacture. But the catalysts are not dissimilar to the reforming catalysts that have been exposed to high steam temperatures, steam pressures, and steam concentrations for many, many years in reforming operations. But we are not saying that steam does not reduce the activity of the catalyst; I think this activity reduction is probably true. But the activity of the catalyst that we need, at the temperatures at which we are operating, is so low that steam is no deterrent at all. The catalyst life that we are expecting is not different from those that have been established in the reforming industry.

S. Singh (Battelle Memorial Institute): What is the panel's opinion of compressing the synthesis gas before methanation rather than after? For example, feed the methanator at 1000 psig, the final line pressure of the pipeline gas, rather than at some lower pressure such as 400 psig at which the synthesis gases are purified?

Dr. Blum: During one stage of our development, we did a pressure optimization. The pressure optimization showed a very shallow minimum at around 300–500 psig. That is, if your syngas came under a pressure of anything less than 300 psig, it was economical to compress it up to 300–400 psig, methanate, and then compress the smaller volume of

gas. At any pressure greater than 300 psig, methanation would be run at delivered pressure from the gasifier to a subsequent pressure boosting after the reaction.

L. Seglin: Was this conclusion sensitive to the purification system you are using or did you just exclude that? Did you assume you had gas at atmospheric pressure or at some higher pressure?

Dr. Blum: We looked at the lower pressure gasifiers, and we varied utility costs, capital-related charges, and catalyst life.

G. A. White: We have looked at a case consisting of a Koppers–Totzek gas, at essentially atmospheric pressure, in combination with the COED liquefaction process. We considered the residue gas that came from gasification at atmospheric pressure, methanated it at atmospheric pressure, and took out CO_2 at atmospheric pressure before compression. That was the minimum cost for our system. It is obvious that each system will have some difference in economics, depending on what you can achieve by methanation.

Anonymous: Can such a system remove sulfur to the low levels required for present day methanation catalysts?

G. A. White: Final removal of sulfur, of course, is effected conventionally by zinc oxide which will work at atmospheric pressures as well as at any other pressure. The bulk sulfur removal can work equally well at atmospheric pressure in our system. That is, in a commercial plant we have removed sulfur to less than 1 ppm through the combination of amine and caustic. So, if we want to follow that with zinc oxide, obviously we can meet the requirements for any methanation system.

Anonymous: What are the cost differences between atmospheric and, say 300–600 psig operation?

G. A. White: I cannot give you a figure offhand. It depends on so many things, and I am sure you can appreciate that. For example, what methane content do you have in your gas? What pressure level do you really want? There are many factors involved in establishing a cost difference between atmospheric pressure and 300 lb and 600 lb. There is no way that I can give you an off-the-cuff answer. If you are serious about it, we would be very happy to give you an opinion on a specific set of conditions. But there is no generalization that I can make.

L. Seglin: Can I add a word here? If you had gas available at a given pressure, I believe it would not pay to increase the pressure of that gas just to methanate it. The savings in methanation at higher pressure would not pay for the cost of compressing the extra volume of gas. All you are really saving in methanation by increasing the pressure is maybe decreasing the volume of the bed and increasing the thickness of the wall with no significant change in cost for methanation. But at the same time you would increase significantly the compression horse-

power. I think the pressure then becomes more a function of what purification system you use, and what the trade-offs are in the system.

Dr. Moeller: I said in my paper we have done exact calculations on the economics of compressing purified syngas from Rectisol. We found that it is uneconomic to compress the syngas which has nearly three times the volume of the product gas, and so we went to SNG before final compression. We operate the SNG-to-methanation plant at that pressure which corresponds to the pressure of gasification and the pressure of off-stream plant. One other comment, I cannot see how it will work to go for gas purification at atmospheric pressure using zinc oxide. Taking these bigger plants into account, I cannot see how we can make reactors of this size that will handle such large amounts of zinc oxide. I think that will not work. Gasification may work at atmospheric pressure, but for your purification you have to operate under pressure, otherwise you cannot handle your equipment.

Dr. Blum: As a further comment on pressure optimization, and as it relates to our system, I think the response of the slurry methanation system to pressure is somewhat different from that of dry methanation. It relates to the ability of the catalyst to methanate a given amount of gas. In our system, the effective pressure is the total pressure minus the vapor pressure of the liquid phase. This doesn't hold for the standard methanation catalyst in the dry system. There is a different pressure relationship; so the optimum just might not work quite the same way.

Anonymous: When do you expect a reasonable volume, about 10% of the total demand for example, to be supplied through commercial SNG plants?

R. McClelland: As you know, we are one of many utilities faced with a gas supply problem. There are a couple of very serious problems with respect to SNG, ignoring technology. One is the long lead times required to design and construct gasification plants. Another is the extremely high cost, particularly as a result of the last six months of escalation of the cost of such facilities. Under the assumption that a way will be found to pay the cost and to acquire the investment capital required to build these kinds of facilities—and certainly the natural gas industry is looking for solutions—it is at this point unlikely that any significant number of SNG facilities will be built before the early 1980s'. The way technology looks now, those facilities would use first generation gasification processes. If there are other utility people here, this would be a good time for them to respond also. From the point of view of the utilities the kind of information which might be necessary to design and construct second generation plants is perhaps at minimum four to five years away. This would put completion and start-up of those plants into the mid- if not late 1980's.

INDEX

D

E

F

G

T

V

W

Z